

On the Impact of Sample Size in Reconstructing Noisy Graph Signals: A Theoretical Characterisation

Baskaran Sripathmanathan, Xiaowen Dong, Michael Bronstein
University of Oxford

Abstract—Reconstructing a signal on a graph from noisy observations of a subset of the vertices is a fundamental problem in the field of graph signal processing. This paper investigates how sample size affects reconstruction error in the presence of noise via an in-depth theoretical analysis of the two most common reconstruction methods in the literature, least-squares reconstruction (LS) and graph-Laplacian regularised reconstruction (GLR). Our theorems show that at sufficiently low signal-to-noise ratios (SNRs), under these reconstruction methods we may simultaneously decrease sample size and decrease average reconstruction error. We further show that at sufficiently low SNRs, for LS reconstruction we have a Λ -shaped error curve and for GLR reconstruction, a sample size of $\mathcal{O}(\sqrt{N})$, where N is the total number of vertices, results in lower reconstruction error than near full observation. We present thresholds on the SNRs, τ and τ_{GLR} , below which the error is non-monotonic, and illustrate these theoretical results with experiments across multiple random graph models, sampling schemes and SNRs. These results demonstrate that any decision in sample-size choice has to be made in light of the noise levels in the data.

Index Terms—Graph signal processing, sampling, reconstruction, least squares, graph-laplacian regularisation.

I. INTRODUCTION

REAL-world signals, such as brain fMRIs [1], urban air pollution [2], and political preferences [3], are often noisy and incomplete, making analysis of the signals harder. The reconstruction of these signals from limited observation is of practical importance, and can benefit from the fact that they can be treated as graph signals, signals defined on a network domain. Graph signal processing (GSP) generalises the highly successful tools of sampling and reconstruction in classical signal processing by extending the classical shift operator to a graph shift operator [4] such as the adjacency matrix [5] or the graph Laplacian, enabling us to extrapolate the full data across the graph from observations on a subset of vertices [6].

In the literature, the vast majority of studies on graph-based sampling focus on designing efficient sampling schemes that are approximately optimal under certain criteria [7, Chapter 6], because optimal vertex choice under noise is in general NP-hard [8], [9]. While valuable, these studies focus on the performance of sampling schemes at fixed sample sizes, while much less attention has been paid to fully understanding the impact of varying sample size on mean squared error (MSE) of reconstruction. Sample size is an important parameter in both understanding and using sampling schemes, especially in the common setting of a fixed sample budget.

The literature studies the impact of sample size both empirically and theoretically, and can be further divided by

the setting considered: whether the observations are noisy or noiseless, and by which reconstruction method. Empirical results, linked to sampling schemes, are usually obtained in the noisy setting under least squares reconstruction (LS) [10]–[12], graph-Laplacian regularised reconstruction (GLR) [12], [13], or variants of these methods [14], [15]. These results show that MSE decreases as sample size increases in a restricted range of noise level and sample size. An exception is [16, Fig. 1] which shows non-monotonicity of MSE with sample size under LS as it considers the full sample size range and a relatively high noise level. The two main theoretical results on the impact of sample size in the literature focus on slightly different settings: [17] presents sample size bounds for perfect signal reconstruction in the noiseless setting, while [8] proves that MSE decreases as sample size increases in the noisy setting and provides bounds on the impact of sample size on MSE, but assumes optimal Bayesian reconstruction. While these theoretical results provide valuable insight, the settings they are based on do not agree with those in the empirical studies above, hence a generic understanding is still lacking.

In this paper, we fill the gap in the literature by providing a theoretical characterisation of the impact of sample size on MSE in the most common settings, i.e. noisy observations and LS or GLR. More specifically, we focus on whether under sufficiently low SNRs, decreasing sample size may actually decrease MSE. Furthermore, we investigate both the full range of sample sizes and all possible levels of noise, which is important for the application of graph sampling to domains where the noise may be greater than the signal (e.g. finance [18]) or when observing more samples might not be feasible (e.g. resource-constrained settings). This breadth is only possible through our rigorous theoretical characterisation which allows us to understand behaviour at high noise levels without numeric stability issues, to characterise behaviour on arbitrarily large graphs without computational issues, and to show when certain behaviours of MSE happen and why.

Our results begin by using a Bias-Variance decomposition to explain why decreasing sample size may decrease MSE for any linear reconstruction method, and we then specialise to LS and GLR. We prove that under LS reconstruction of a k -bandlimited signal, if the samples were chosen to be optimal in the noiseless case then we can always reduce MSE under high noise by reducing sample size from k to $k - 1$. We prove that under GLR, if certain graph invariants hold on a graph with N vertices, reducing sample size from almost N vertices to $\mathcal{O}(\sqrt{N})$ vertices will reduce MSE at high noise levels, and that these invariants hold for large Erdős–Rényi

graphs with high probability. Our experiments validate this for Stochastic Blockmodel and Barabasi-Albert graphs as well. We also investigate how sensitive our results are to different kinds of noise by presenting variants of our theoretical and empirical results under both bandlimited and full-band noise.

Our paper presents four primary contributions:

- 1) A theoretical characterisation of how decreasing sample size may decrease MSE, not only under LS but also under GLR, a regularised method.
- 2) Analysis of both LS and GLR under bandlimited noise to show non-monotonicity of the MSE is not caused by just the high frequency component of the noise.
- 3) Asymptotic analysis, showing how the non-monotonicity of the MSE with sample size persists as $N \rightarrow \infty$.
- 4) Extensive experimental simulations illustrating the theoretical results under LS and GLR, and bandlimited noise.

The present work is a significant extension of a previous conference paper [19], where preliminary versions of Corollary 1.1, Proposition 1, and a weaker version of Theorem 2 were presented, corresponding to the LS part of contribution (1). Lemmas 3- 6 closely follow those in the arXiv version [19].

II. BACKGROUND & PROBLEM FORMULATION

In this section, we first introduce sampling notation. We then discuss graph signal reconstruction in three parts: what we reconstruct (graph signals), how we reconstruct them (reconstruction methods), and how the reconstruction is evaluated (optimality criteria). Finally, we present our problem setting.

A. Notation for Sampling

We use the same notation for submatrices as [20]. For any matrix \mathbf{X} and sets \mathcal{A}, \mathcal{B} , we write $[\mathbf{X}]_{\mathcal{A}, \mathcal{B}}$ to be the submatrix of \mathbf{X} with row indices in \mathcal{A} and column indices in \mathcal{B} . We define the subvector $[\mathbf{x}]_{\mathcal{A}}$ of a vector \mathbf{x} similarly. We define a specific shorthand for taking a principal submatrix:

$$[\mathbf{X}]_{\mathcal{A}} = [\mathbf{X}]_{\mathcal{A}, \mathcal{A}}.$$

We also define two pieces of notation for projections. Let $\mathcal{N} = \{1, \dots, N\}$ and $\mathcal{K} = \{1, \dots, k\}$. Then

$$\mathbf{\Pi}_{\mathcal{B}} = [\mathbf{I}]_{\mathcal{N}, \mathcal{B}} [\mathbf{I}]_{\mathcal{B}, \mathcal{N}}, \quad \mathbf{\Pi}_{bl(\mathcal{K})} = [\mathbf{U}]_{\mathcal{N}, \mathcal{K}} [\mathbf{U}]_{\mathcal{N}, \mathcal{K}}^T.$$

Finally, $\mathcal{A} \setminus \mathcal{B} = \{i \in \mathcal{A} \mid i \notin \mathcal{B}\}$ and $\mathcal{A}^c = \mathcal{N} \setminus \mathcal{A}$. In general, we adhere to standard set notation.

B. Graphs and Graph Signals

A graph \mathcal{G} consists of a set of N vertices, a set of edges between these vertices, and the associated edge weights. We assume \mathcal{G} is connected and undirected, and that the combinatorial graph Laplacian \mathbf{L} is real positive semidefinite with N distinct eigenvalues $0 = \lambda_1 < \lambda_2 < \dots < \lambda_N$ which are also called *graph frequencies* [4]¹. Write the eigendecomposition of \mathbf{L} as

$$\mathbf{L} = \mathbf{U} \begin{pmatrix} \lambda_1 & & \mathbf{0} \\ & \ddots & \\ \mathbf{0} & & \lambda_N \end{pmatrix} \mathbf{U}^T$$

¹Although we focus on the combinatorial graph Laplacian, our results on LS also hold for the normalised graph Laplacian or any graph shift operator that is positive semidefinite.

where the columns of \mathbf{U} are the eigenbasis of \mathbf{L} and form an orthonormal basis of \mathbb{R}^N . The most common signal model used in the graph signal processing literature is the bandlimited signal model, where a *k-bandlimited signal* is a linear combination of the first k columns of \mathbf{U} [5].

It is rare for observed signals to be perfectly bandlimited. While this can be modelled by considering ‘approximately bandlimited signals’ [21], [22], or other more general priors [23], [24], we take the more common approach of assuming additive observation noise. We assume we observe a corrupted signal $\mathbf{y} = \mathbf{x} + \mathbf{n}$ where

- $\mathbf{x} \sim \mathcal{N}(\mathbf{0}, \mathbf{\Pi}_{bl(\mathcal{K})})$ is a k -bandlimited Gaussian signal,
- $\mathbf{n} = \sigma \cdot \boldsymbol{\epsilon}$ is noise where $\sigma > 0$ and either
 - 1) $\boldsymbol{\epsilon} \sim \mathcal{N}(\mathbf{0}, \mathbf{I}_N)$ is an i.i.d. Gaussian, or
 - 2) $\boldsymbol{\epsilon} \sim \mathcal{N}(\mathbf{0}, \mathbf{\Pi}_{bl(\mathcal{K})})$ is a k -bandlimited Gaussian.

We refer to the $\boldsymbol{\epsilon} \sim \mathcal{N}(\mathbf{0}, \mathbf{I}_N)$ case as ‘full-band noise’ as the associated corrupted signal \mathbf{y} has high frequency components, and to the other case as ‘ k -bandlimited noise’. In the literature, noise levels are often described using the SNR = $\frac{\mathbb{E}[\|\mathbf{x}\|_2^2]}{\mathbb{E}[\|\mathbf{n}\|_2^2]}$, so $\sigma^2 = \frac{k}{N \cdot \text{SNR}}$ under full-band noise or $\frac{1}{\text{SNR}}$ under k -bandlimited noise and, as a ratio of norms, SNR is positive².

C. Reconstruction Methods

We define a *reconstruction method* (or ‘interpolation operator’ [8]) to take potentially noisy observations on a vertex sample set \mathcal{S} and reconstruct the signal across all vertices. In this paper we focus on LS and GLR, and we summarise their differences in Table I, labelling the optimisation objectives they solve, input parameters into the reconstruction, whether they are biased and whether they require computation of $[\mathbf{U}]_{\mathcal{N}, \mathcal{K}}$. Our analysis of LS also applies to the commonly used iterative reconstruction method, Projection onto Convex Sets [25], as POCS converges to LS.

TABLE I: The LS and GLR reconstruction Methods.

	Objective	Param	Bias	Needs $[\mathbf{U}]_{\mathcal{N}, \mathcal{K}}$
LS	$\arg \min_{\mathbf{x} \in \text{span}([\mathbf{U}]_{\mathcal{N}, \mathcal{K}})} \ \mathbf{x}_{\mathcal{S}} - \mathbf{y}\ _2$	k	no	yes
GLR	$\arg \min_{\mathbf{x} \in \mathbb{R}^N} \ \mathbf{x}_{\mathcal{S}} - \mathbf{y}\ _2 + \mu \mathbf{x}^T \mathbf{L} \mathbf{x}$	μ	yes	no

We call a reconstruction method *linear* if it is linear in its observations. For a fixed vertex sample set \mathcal{S} we can represent a linear reconstruction method by a matrix $\mathbf{R}_{\mathcal{S}} \in \mathbb{R}^{N \times |\mathcal{S}|}$.

Remark 1. LS and GLR are both linear:

$$\text{LS: } \mathbf{R}_{\mathcal{S}} = [\mathbf{U}]_{\mathcal{N}, \mathcal{K}} [\mathbf{U}]_{\mathcal{S}, \mathcal{K}}^{\dagger} \quad (1)$$

$$\text{GLR: } \mathbf{R}_{\mathcal{S}} = [(\mathbf{\Pi}_{\mathcal{S}} + \mu \mathbf{L})^{-1}]_{\mathcal{N}, \mathcal{S}} \quad (2)$$

where for a matrix \mathbf{A} , \mathbf{A}^{\dagger} is its Moore-Penrose pseudoinverse.

²It is common in the literature to express the SNR in decibels, which may be negative, while its ratio form remains positive. We will use the ratio form unless otherwise noted, so for example -20dB will be written as $10^{-20/10} = 10^{-2} > 0$.

Across all linear models under the noisy setting, LS leads to the minimum-variance unbiased estimator of \mathbf{x} [26], which theoretically justifies us focusing our analysis on LS. In practice GLR is often used for large graphs instead as computing $[\mathbf{U}]_{\mathcal{N},\mathcal{K}}$ is slow [12], [13].

Finally, we clarify what we mean when we consider LS with sample size less than bandwidth, which when defined as the minimisation of the objective in Table I has multiple solutions. In this case, we follow [16] and define the LS reconstruction as the unique minimum-norm solution [27, Sect. 5.5.1], hence (1) applies regardless of sample size.

D. Optimality Criteria for Sampling

To meaningfully contrast choices of vertex sample set size and selection, we need to evaluate reconstruction performance, and we do so by certain optimality criteria. In the noiseless case, the main optimality criterion for a vertex sample set \mathcal{S} is whether it is a *uniqueness set* [28], that is, if we can perfectly reconstruct any k -bandlimited signal observed on \mathcal{S} . Such a set always exists and \mathcal{S} is a uniqueness set for a bandwidth k if and only if $\text{rank}([\mathbf{U}]_{\mathcal{S},\mathcal{K}}) = k$ [16].

In the case of additive observation noise, there are multiple common optimality criteria [7, Chapter 6]:

- *MMSE criterion*: Minimise average MSE. [14], [15], [29]
- *Confidence Ellipsoid criterion*: Minimise the confidence ellipsoid around the eigenbasis co-efficients. [10], [11]
- *WMSE criterion*: Minimise worst-case MSE. [5], [13]

Under LS, these criteria have the following names and forms:

$$(MMSE) \text{ A-Optimality: minimise } \text{tr}(\mathbf{P}^{-1}) \quad (3)$$

$$(Conf. \text{ Ellips.}) \text{ D-Optimality: maximise } \det(\mathbf{P}) \quad (4)$$

$$(WMSE) \text{ E-Optimality: maximise } \lambda_{\min}(\mathbf{P}) \quad (5)$$

where \mathbf{P} is defined as

$$\mathbf{P} = \begin{cases} [\mathbf{\Pi}_{bl(\mathcal{K})}]_{\mathcal{S}} & \text{if } |\mathcal{S}| < k \\ [\mathbf{U}]_{\mathcal{S},\mathcal{K}}^T [\mathbf{U}]_{\mathcal{S},\mathcal{K}} & \text{if } |\mathcal{S}| \geq k \end{cases}$$

and we define $\text{tr}(\mathbf{P}^{-1}) = +\infty$ in (3) if \mathbf{P} is not invertible.

E. Problem Setting

In this paper, we are interested in a theoretical characterisation of the impact of sample size on MSE under all possible SNRs. For our theoretical results and experiments, we assume:

- A known graph \mathcal{G} which is connected and undirected.
- A known bandwidth k .
- A clean underlying k -bandlimited signal \mathbf{x} drawn from a known distribution.
- Observations of \mathbf{x} are corrupted by noise which is either:
 - flat-spectrum, so we observe a non-bandlimited signal.
 - k -bandlimited, so we observe a k -bandlimited signal.
- Linear reconstruction, in particular LS and GLR.

In this paper, we study the behaviour of the MMSE criterion, that is, the MSE averaged over a known signal model and known noise model, which we write as

$$\text{MSE}_{\mathcal{S}} = \mathbb{E}_{\mathbf{x},\epsilon} \left[\|\hat{\mathbf{x}} - \mathbf{x}\|_2^2 \mid \mathcal{S} \text{ observed} \right].$$

III. MAIN RESULTS

A. Overview and Proof Approaches

In this section, we prove theorems showing how the relationship between sample size and MSE changes with different levels of observation noise, with a focus on showing when reducing sample size reduces MSE. We first present a high level sketch of our approach. To study the effect of noise, we perform a Bias-Variance decomposition on the MSE:

$$\text{MSE}_{\mathcal{S}} = \underbrace{\xi_1(\mathcal{S})}_{\mathbb{E}[\text{bias}^2]} + \underbrace{\sigma^2 \cdot \xi_2(\mathcal{S})}_{\mathbb{E}[\text{variance}]}$$

where the bias term $\xi_1(\mathcal{S}) = \text{MSE}_{\mathcal{S}}$ when $\sigma^2 = 0$ is the MSE attributable to reconstruction of the clean signal, and $\xi_2(\mathcal{S})$ can be understood as a sensitivity-to-noise term (see Section III-B for derivations). With this decomposition, the relationship between sample size and MSE under different levels of noise reduces to how the bias and sensitivity-to-noise vary with respect to sample size.

The focus of the paper is not to characterise all the cases where decreasing sample size decreases MSE, but rather to clearly show that it does happen in a wide variety of cases. In service of this, we focus on certain broad cases that are more tractable, which we call ‘simplifications’. For example, we only compare a sample set \mathcal{S} to a subset of it, i.e., $\mathcal{T} \subset \mathcal{S}$.

Our general approach per reconstruction method is:

- Choose a simplification;
- Under this simplification, characterise conditions when decreasing sample size can decrease MSE;
- Show that these conditions may actually happen;
- Study these conditions as $N \rightarrow \infty$, to prove the conditions may happen on large graphs.

For LS, we simplify the problem by only considering decreasing the sample size by one at a time, which we call the ‘single vertex’ simplification. We pay particular attention to subsets sampled by sampling schemes that are optimal in the noiseless setting (Subsection III-C). For GLR, we compare observing the full graph to observing a subset of the vertices. We call this the ‘full observation’ simplification. We focus on graphs which satisfy certain graph invariants (Subsection III-E). We justify these simplifications in the relevant subsections below.

We then consider reconstruction under bandlimited noise (Subsections III-D and III-F) to show that the reduction in MSE from reducing sample size is not sensitive to our noise model, nor due to the high frequency component of the noise.

B. General Results

To understand the effect of changing the sample size on MSE at different levels of noise, we use a variant of the Bias-Variance decomposition [30] on the MSE to separate out the effect of noise. Let $\hat{\mathbf{x}}$ be a reconstruction of the signal \mathbf{x} , then

$$\text{MSE}_{\mathcal{S}} = \mathbb{E}_{\mathbf{x}} \left[\mathbb{E}_{\epsilon} \left[\|\mathbf{x} - \hat{\mathbf{x}}\|_2^2 \right] \right] \quad (6)$$

$$= \mathbb{E}_{\mathbf{x}} \left[\mathbb{E}_{\epsilon} \left[\|\mathbf{x} - \mathbb{E}_{\epsilon}[\hat{\mathbf{x}}] + \mathbb{E}_{\epsilon}[\hat{\mathbf{x}}] - \hat{\mathbf{x}}\|_2^2 \right] \right] \quad (7)$$

$$= \mathbb{E}_{\mathbf{x}} \left[2\mathbb{E}_{\epsilon} \left[(\mathbf{x} - \mathbb{E}_{\epsilon}[\hat{\mathbf{x}}])^T (\mathbb{E}_{\epsilon}[\hat{\mathbf{x}}] - \hat{\mathbf{x}}) \right] \right] \quad (8)$$

$$+ \mathbb{E}_{\mathbf{x}} \left[\|\mathbf{x} - \mathbb{E}_{\epsilon}[\hat{\mathbf{x}}]\|_2^2 + \mathbb{E}_{\epsilon} \left[\|\mathbb{E}_{\epsilon}[\hat{\mathbf{x}}] - \hat{\mathbf{x}}\|_2^2 \right] \right]. \quad (9)$$

Note that by the properties of expectation,

$$\mathbb{E}_\epsilon \left[\mathbb{E}_\epsilon [\hat{\mathbf{x}}]^T \hat{\mathbf{x}} \right] = \mathbb{E}_\epsilon [\hat{\mathbf{x}}]^T \mathbb{E}_\epsilon [\hat{\mathbf{x}}] = \mathbb{E}_\epsilon \left[\mathbb{E}_\epsilon [\hat{\mathbf{x}}]^T \mathbb{E}_\epsilon [\hat{\mathbf{x}}] \right]$$

so
$$\mathbb{E}_\epsilon \left[\mathbb{E}_\epsilon [\hat{\mathbf{x}}]^T (\mathbb{E}_\epsilon [\hat{\mathbf{x}}] - \hat{\mathbf{x}}) \right] = 0$$

and as the value of the signal \mathbf{x} is unrelated to the value of ϵ ,

$$\mathbb{E}_\epsilon \left[\mathbf{x}^T (\mathbb{E}_\epsilon [\hat{\mathbf{x}}] - \hat{\mathbf{x}}) \right] = \mathbf{x}^T \mathbb{E}_\epsilon [\mathbb{E}_\epsilon [\hat{\mathbf{x}}] - \hat{\mathbf{x}}] = 0 \quad (10)$$

$$\mathbb{E}_\epsilon \left[(\mathbf{x} - \mathbb{E}_\epsilon [\hat{\mathbf{x}}])^T (\mathbb{E}_\epsilon [\hat{\mathbf{x}}] - \hat{\mathbf{x}}) \right] = 0 \quad (11)$$

for any value of \mathbf{x} . Therefore

$$\text{MSE}_S = \mathbb{E}_\mathbf{x} \left[\underbrace{\|\mathbf{x} - \mathbb{E}_\epsilon [\hat{\mathbf{x}}]\|_2^2}_{\text{Bias}(\hat{\mathbf{x}}, \mathbf{x})^2} + \underbrace{\mathbb{E}_\epsilon \left[\|\mathbb{E}_\epsilon [\hat{\mathbf{x}}] - \hat{\mathbf{x}}\|_2^2 \right]}_{\text{Var}(\hat{\mathbf{x}})} \right] \quad (12)$$

This decomposition applies to *any* reconstruction $\hat{\mathbf{x}}$ of \mathbf{x} .

We consider reconstructing a signal with a linear reconstruction method. We first consider a generic \mathbf{R}_S . Define

$$\xi_1(S) = \|\mathbf{U}_{\mathcal{N}, \mathcal{K}} - \mathbf{R}_S \mathbf{U}_{\mathcal{S}, \mathcal{K}}\|_F^2 \quad (13)$$

$$\xi_2(S) = \begin{cases} \|\mathbf{R}_S\|_F^2 & \text{if full-band noise} \\ \|\mathbf{R}_S \mathbf{U}_{\mathcal{S}, \mathcal{K}}\|_F^2 & \text{if } k\text{-bandlimited noise} \end{cases} \quad (14)$$

For linear reconstruction, we have $\hat{\mathbf{x}} = \mathbf{R}_S[\mathbf{x} + \sigma \cdot \epsilon]_S$. By assumption, $\mathbb{E}[\epsilon] = 0$, so $\mathbb{E}_\epsilon [\hat{\mathbf{x}}] = \mathbf{R}_S[\mathbf{x}]_S$. Therefore

$$\text{Bias}(\hat{\mathbf{x}}, \mathbf{x})^2 = \mathbb{E}_\mathbf{x} \left[\|\mathbf{I} - \mathbf{R}_S[\mathbf{I}]_{\mathcal{S}, \mathcal{N}}\|_2^2 \right] \quad (15)$$

$$\text{Var}(\hat{\mathbf{x}}) = \sigma^2 \cdot \mathbb{E}_\epsilon \left[\|\mathbf{R}_S[\epsilon]_S\|_2^2 \right] \quad (16)$$

We have assumed \mathbf{x} and ϵ are Gaussian, with zero mean. For any zero-mean Gaussian random vector \mathbf{g} and compatible matrix \mathbf{A} , we know $\mathbb{E}_\mathbf{g} \left[\|\mathbf{A}\mathbf{g}\|_2^2 \right] = \text{tr}(\mathbf{A}\text{Cov}(\mathbf{g})\mathbf{A}^T)$. Writing $\text{Cov}(\mathbf{g}) = \mathbf{X}\mathbf{X}^T$, this is equal to $\|\mathbf{A}\mathbf{X}\|_F^2$. Therefore

$$\text{Bias}(\hat{\mathbf{x}}, \mathbf{x})^2 = \|\mathbf{I} - \mathbf{R}_S[\mathbf{I}]_{\mathcal{S}, \mathcal{N}}\|_F^2 = \xi_1(S) \quad (17)$$

$$\text{Var}(\hat{\mathbf{x}}) = \sigma^2 \cdot \xi_2(S) \quad (18)$$

and so

$$\text{MSE}_S = \underbrace{\xi_1(S)}_{\mathbb{E}[\text{Bias}(\hat{\mathbf{x}}, \mathbf{x})^2]} + \underbrace{\sigma^2 \cdot \xi_2(S)}_{\mathbb{E}[\text{Var}(\hat{\mathbf{x}})]}. \quad (19)$$

We will refer to $\xi_1(S)$ as the ‘bias’ of \mathbf{R}_S and $\xi_2(S)$ as the ‘sensitivity-to-noise’ of \mathbf{R}_S .

In Statistical Learning Theory, the standard Bias-Variance decomposition is used to show how increasing the complexity of a model often increases its ability to fit the data (reducing ‘bias’) while increasing its sensitivity-to-noise (increasing ‘variance’), and that the optimum model complexity minimising MSE balances these two components. In the rest of the paper, we will use our Bias-Variance decomposition to show that while decreasing the sample size for a reconstruction method might increase bias it can also decrease sensitivity-to-noise hence reducing the variance, and that the optimal sample size minimising MSE balances these two components. In one sense, this is analogous to avoiding ‘overfitting to noise’ in machine learning, where increasing the number of parameters can increase variance more than it decreases bias.

We provide the definitions and a theoretical result to quantify this. Both the ‘single vertex’ and ‘full observation’ simplifications considered in the paper compare observed set S to its subset $\mathcal{T} \subset S$ which is reflected in our definitions.

Definition III.1. Let $\mathcal{T} \subset S$. We say that

$$\begin{aligned} \mathbf{R}_\mathcal{T} \text{ is less biased than } \mathbf{R}_S & \quad \text{if } \xi_1(\mathcal{T}) < \xi_1(S) \\ \mathbf{R}_\mathcal{T} \text{ is less sensitive to noise than } \mathbf{R}_S & \quad \text{if } \xi_2(\mathcal{T}) < \xi_2(S) \end{aligned}$$

Furthermore, we say that

$$\begin{aligned} \mathcal{T} \text{ is better than } S & \quad \text{if } \text{MSE}_\mathcal{T} < \text{MSE}_S \\ \mathcal{T} \text{ is as good or better than } S & \quad \text{if } \text{MSE}_\mathcal{T} \leq \text{MSE}_S \\ \mathcal{T} \text{ is worse than } S & \quad \text{if } \text{MSE}_\mathcal{T} > \text{MSE}_S. \end{aligned}$$

For $i \in \{1, 2\}$ and $\mathcal{T} \subset S$, let

$$\Delta_i(S, \mathcal{T}) = \xi_i(S) - \xi_i(S \setminus \mathcal{T}). \quad (20)$$

$\Delta_1(S, \mathcal{T}) > 0$ means $\mathbf{R}_{S \setminus \mathcal{T}}$ is less biased than \mathbf{R}_S and $\Delta_2(S, \mathcal{T}) > 0$ means $\mathbf{R}_{S \setminus \mathcal{T}}$ is less sensitive to noise than \mathbf{R}_S . Then, by (19), the change in MSE from reducing sample size is

$$\text{MSE}_S - \text{MSE}_{S \setminus \mathcal{T}} = \Delta_1(S, \mathcal{T}) + \sigma^2 \cdot \Delta_2(S, \mathcal{T}) \quad (21)$$

so $S \setminus \mathcal{T}$ is better than S if and only if

$$\Delta_1(S, \mathcal{T}) > -\sigma^2 \cdot \Delta_2(S, \mathcal{T}). \quad (22)$$

Remark 2. If either $\Delta_1(S, \mathcal{T})$ or $\Delta_2(S, \mathcal{T})$ are positive, we can always pick σ^2 so $S \setminus \mathcal{T}$ is better than S . If both $\Delta_1(S, \mathcal{T})$ and $\Delta_2(S, \mathcal{T})$ are negative then $S \setminus \mathcal{T}$ is never better than S .

The following Theorem characterises our bias/variance trade-off by computing the noise level at which an increase in bias is outweighed by an decrease in sensitivity-to-noise (or vice-versa) on average.

Theorem 1. Assume a linear reconstruction method and consider $S \supset \mathcal{T}$. Let

$$\tau(S, \mathcal{T}) = \frac{k}{N} \cdot \frac{\Delta_2(S, \mathcal{T})}{-\Delta_1(S, \mathcal{T})}$$

then $S \setminus \mathcal{T}$ is better than S if and only if one of the following conditions is met:

$$\begin{cases} \text{SNR} < \tau(S, \mathcal{T}) & \text{and } \Delta_1(S, \mathcal{T}) < 0 & (23a) \\ \text{SNR} > \tau(S, \mathcal{T}) & \text{and } \Delta_1(S, \mathcal{T}) > 0 & (23b) \\ 0 < \Delta_2(S, \mathcal{T}) & \text{and } \Delta_1(S, \mathcal{T}) = 0. & (23c) \end{cases}$$

Proof Sketch. We first get $\frac{k}{N} \Delta_2(S, \mathcal{T}) > -\Delta_1(S, \mathcal{T}) \cdot \text{SNR}$ from (22) and then divide by $-\Delta_1(S, \mathcal{T})$, case-splitting on its different possible signs. See Appendix C for a full proof. \square

We interpret each of these conditions as follows:

- (23a) If $\mathbf{R}_{S \setminus \mathcal{T}}$ is more biased than \mathbf{R}_S , then $S \setminus \mathcal{T}$ is better than S if SNR is low enough (below a threshold τ).
- (23b) If $\mathbf{R}_{S \setminus \mathcal{T}}$ is less biased than \mathbf{R}_S , then $S \setminus \mathcal{T}$ is better than S if SNR is *high* enough (above a threshold τ).
- (23c) If $\mathbf{R}_{S \setminus \mathcal{T}}$ and \mathbf{R}_S are equally biased and $\mathbf{R}_{S \setminus \mathcal{T}}$ is less sensitive-to-noise than \mathbf{R}_S , then $S \setminus \mathcal{T}$ is better than S at every non-zero noise level.

Theorem 1 does not guarantee that any of the conditions for $S \setminus \mathcal{T}$ being better than S would happen; for example, \mathbf{R}_S

could be both less biased and less sensitive to noise than $\mathbf{R}_{\mathcal{S} \setminus \mathcal{T}}$. To show reducing sample size can reduce MSE, i.e. Δ_1 and Δ_2 are not always both non-positive, we look at specific reconstruction methods below.

We will mainly focus on showing that Δ_2 can be positive, i.e., decreasing sample size can decrease sensitivity-to-noise of the reconstruction method. The rationale behind this is that results which focus on $\Delta_2 > 0$ rather than $\Delta_1 > 0$ transfer more easily to other settings: in Appendix A we demonstrate that because we focus on when $\Delta_2 > 0$, all of our results transfer from our main setting to the case where the signal \mathbf{x} is deterministic and fixed.

To show when $\Delta_2 > 0$, we first consider a ‘single vertex’ simplification where $\mathcal{T} = \{v\}$. This is the approach we take for LS, and also motivates the ‘full observation’ simplification for GLR. For a vertex v , as shorthand we write:

$$\tau(\mathcal{S}, v) = \tau(\mathcal{S}, \{v\}), \quad \Delta_i(\mathcal{S}, v) = \Delta_i(\mathcal{S}, \{v\}).$$

We start by looking at possible combinations of signs of $\Delta_1(\mathcal{S}, v)$ and $\Delta_2(\mathcal{S}, v)$, which we present in Table II.

TABLE II: Possible signs of $\Delta_1(\mathcal{S}, v)$ and $\Delta_2(\mathcal{S}, v)$

	$\Delta_2 > 0$	$\Delta_2 \leq 0$		$\Delta_2 > 0$	$\Delta_2 \leq 0$
$\Delta_1 > 0$	×	×	$\Delta_1 > 0$	✓	✓
$\Delta_1 < 0$	✓	×	$\Delta_1 < 0$	✓	✓
$\Delta_1 = 0$	×	✓	$\Delta_1 = 0$	~	~

(a) LS Reconstruction
(b) GLR Reconstruction

In Table II, × will not happen, ✓ may happen and ~ may theoretically happen but are unlikely. A more detailed explanation of the two tables, and proofs of the ‘×’ subcases, are presented in Appendix B. We now discuss LS and GLR separately in the following sections.

C. LS with full-band noise

In this subsection we show how decreasing sample size by one can decrease MSE under LS. From Table IIa, we see that reducing sample size never reduces bias under LS, so we focus on when reducing sample size reduces sensitivity-to-noise.

Our approach in this subsection is as follows. We consider the ‘single vertex’ simplification. For a sample set \mathcal{S} and $v \in \mathcal{S}$, we first characterise under exactly what conditions $\mathcal{S} \setminus v$ is better than \mathcal{S} (Corollary 1.1). We then show that the conditions must occur under sampling schemes which are optimal in the noiseless case (Theorem 2). Finally, we comment on how the conditions persist as $N \rightarrow \infty$.

By Table IIa we can eliminate conditions (23b) and (23c) in Theorem 1 for the single-vertex simplification under LS. We simplify Theorem 1 to the following:

Corollary 1.1. Assume LS reconstruction. Then

$$\tau(\mathcal{S}, v) = \frac{k}{N} \cdot \Delta_2(\mathcal{S}, v) \quad (24)$$

and $\mathcal{S} \setminus \{v\}$ is better than \mathcal{S} if and only if

$$\text{SNR} < \tau(\mathcal{S}, v). \quad (25)$$

Proof Sketch. Under LS, $\Delta_1(\mathcal{S}, v)$ can only be -1 or 0 . This simplifies τ in Theorem 1 to (24):

1) $\Delta_1(\mathcal{S}, v) = 0$: We have $\Delta_2(\mathcal{S}, v) \leq 0$ by Table IIa. By Theorem 1, $\mathcal{S} \setminus \{v\}$ is never better than \mathcal{S} .

2) $\Delta_1(\mathcal{S}, v) = -1$: We have $\Delta_2(\mathcal{S}, v) > 0$ by Table IIa so $\tau(\mathcal{S}, v) > 0$. Theorem 1’s conditions reduce to this case. See Appendix D for a full proof. \square

This result says that if SNR is too low (below a threshold τ that depends on the bandwidth and the chosen samples), then using a smaller sample set improves the average reconstruction error. Note that we have not yet proven that condition (25) is ever satisfied, i.e., reducing sample size can reduce MSE. We outline why it is not immediately obvious that (25) can hold, and then show situations where it does hold and thus reducing sample size will reduce MSE.

Remark 3. If $\Delta_2 \leq 0$, we have $\tau(\mathcal{S}, v) \leq 0 < \text{SNR}$, so (25) cannot hold and so $\mathcal{S} \setminus \{v\}$ is never better than \mathcal{S} for any SNR.

We first note that Corollary 1.1 leaves room for a clever sampling scheme which picks \mathcal{S}_i where $\tau(\mathcal{S}_i, v)$ is always non-positive and so condition (25) never holds, and hence $\mathcal{S} \setminus \{v\}$ would never be better than \mathcal{S} for any $v \in \mathcal{S}$. Most sampling schemes in the literature construct sample sets by adding vertices one-by-one (e.g. greedy schemes, which are ‘near-optimal’ [31]). We call such schemes ‘sequential’. We now show that for any graph, a sequential sampling scheme will always eventually add a vertex where (25) can be satisfied.

Proposition 1. Consider a sequential sampling scheme that constructs sample sets $\mathcal{S}_1, \dots, \mathcal{S}_N$ where $\mathcal{S}_i = \mathcal{S}_{i-1} \cup \{v_i\}$. Then there are exactly k indices $1 \leq I_1, \dots, I_k \leq N$ where

$$\forall 1 \leq j \leq k : \tau(\mathcal{S}_{I_j}, v_{I_j}) > 0, \quad (26)$$

and so $\mathcal{S}_{I_j} \setminus \{v_{I_j}\}$ is better than \mathcal{S}_{I_j} at some SNR.

Proof Sketch. By Table IIa, $\tau \propto \Delta_2 > 0 \iff \Delta_1 < 0$. As $\Delta_1(\mathcal{S}, v) = \xi_1(\mathcal{S}) - \xi_1(\mathcal{S} \setminus \{v\}) \in \{0, -1\}$ under LS and $\xi_1(\emptyset) = k$ and $\xi_1(\mathcal{N}) = 0$, we have that $\Delta_2 > 0$ exactly k times. See Appendix E for a full proof. \square

Proposition 1 still leaves room for a hypothetical sequential sampling scheme where $\tau(\mathcal{S}, v) > 0$ only for the last k chosen vertices, and therefore if such a scheme selects $|\mathcal{S}| \leq N - k$ then $\mathcal{T} \subset \mathcal{S}$ is never better than \mathcal{S} . We now show that there is a trade-off between such a property and performance in the noiseless case, namely that any scheme which is optimal in the noiseless case, like most deterministic schemes in the literature, could not have this property. We first define optimality in the noiseless case.

Definition III.2. A sampling scheme is *noiseless-optimal* for LS reconstruction of k -bandlimited signals if the first k vertices it samples form a uniqueness set. That is, it finds the smallest possible uniqueness set [17].

Remark 4. A, D and E-optimal sampling are noiseless-optimal (see Appendix H for a proof).

We now show such schemes find $\tau(\mathcal{S}, v) > 0$ for the first k vertices they pick.

Theorem 2. Suppose we use a sequential noiseless-optimal scheme to select a vertex sample set \mathcal{S}_m of size m . For $m \leq k$:

$$\forall v \in \mathcal{S}_m : \tau(\mathcal{S}_m, v) \geq \frac{k}{N}, \quad (27)$$

i.e., for any vertex $v \in \mathcal{S}_m$, if $\text{SNR} < \tau(\mathcal{S}_m, v)$ (which always holds if $\text{SNR} < \frac{k}{N}$) then $\mathcal{S} \setminus \{v\}$ is better than \mathcal{S} . For $m > k$:

$$\forall v_+ \in \mathcal{S}_m \setminus \mathcal{S}_k : \tau(\mathcal{S}_m, v_+) \leq 0. \quad (28)$$

That is, $\mathcal{S}_m \setminus \{v_+\}$ is never better than \mathcal{S}_m for any of the vertices v_+ the sampling scheme adds beyond the first k .

Proof Sketch. For (27), $[\mathbf{I}_{bl(\mathcal{K})}]_{\mathcal{S}_m}$ and $[\mathbf{I}_{bl(\mathcal{K})}]_{\mathcal{S}_{m-1}}$ are full-rank so $\Delta_1 = -1$; we then show $\Delta_2 \geq 1$. For (28), as $m > k$, $\xi_1(\mathcal{S}_k) = \xi_1(\mathcal{S}_m)$. See Appendix G for a full proof. \square

Theorem 2 explicitly demonstrates a case where reducing sample size reduces MSE: namely if $\text{SNR} \leq \frac{k}{N}$, when the sample is picked by an A-, D- or E-optimal scheme, and $|\mathcal{S}| \leq k$, then reducing sample size will always reduce MSE.

Theorem 2 also gives us the shape of the MSE curve as sample size varies at high noise levels. In this case, $\text{MSE}_{\mathcal{S}} \approx \sigma^2 \cdot \xi_2(\mathcal{S})$ and so the change in $\text{MSE}_{\mathcal{S}}$ as sample size increases is approximately $\sigma^2 \cdot \Delta_2$. Then by Corollary 1.1, $\Delta_2 = \frac{k}{N} \tau$ under LS. Combining these with Theorem 2:

Remark 5. Using a sequential noiseless-optimal sampling scheme, such as greedy A-, D- or E- optimal sampling, under sufficiently high noise leads to the MSE being Λ -shaped with regards to sample size with a peak at $|\mathcal{S}| = k$.

The intuition behind a Λ -shaped MSE under noiseless-optimal sampling is as follows. When the sample size is below k and we increase it, we infer more about the signal—which can be seen in the noiseless case, as each of these samples improves our prediction—and inevitably incorporate some of the noise into our reconstruction. Beyond the first k , samples provide no new information about the signal in the noiseless case. These ‘additional samples’ (corresponding to (28)) are much like getting repetitive observations of already-seen vertices, which we can average to reduce the effect of noise. This is what causes the transition at $|\mathcal{S}| = k$.

Remark 6. If the MSE is Λ -shaped, then even if removing one vertex does not improve \mathcal{S} , removing multiple vertices might decrease MSE. This happens if we reduce sample size enough to transition from the right side of the peak to the left side of the peak of Λ .

We finally comment on the case of large graphs. If $\frac{k}{N}$ is fixed, the lower bound on τ in Theorem 2 is constant. Therefore, at a fixed SNR (e.g., $\frac{k}{2N}$), decreasing sample size decreases MSE on arbitrarily large graphs.

D. LS with k -bandlimited noise

We have observed that MSE can decrease when sample size decreases under LS and full band noise. This raises the question of whether the decrease is caused by some sort of interference effect between the high-frequency components of the noise and the bandlimited (low-frequency) signal. In this subsection, by showing that MSE can decrease when

sample size decreases under LS with k -bandlimited noise, we demonstrate that this is not the case.

We first show that under k -bandlimited noise the choice of sample set \mathcal{S} only influences the MSE through $\text{rank}([U]_{\mathcal{S}, \mathcal{K}})$.

Lemma 1. $\text{MSE}_{\mathcal{S}} = k + (\sigma^2 - 1)\text{rank}([U]_{\mathcal{S}, \mathcal{K}})$.

Lemma 1 makes it easy to prove the following variants of Corollary 1.1 and Theorem 2 for bandlimited noise.

Corollary 2.1. Let $v \in \mathcal{S}$ and

$$\tau_{LS_bl} = 1, \quad (29)$$

then $\mathcal{S} \setminus \{v\}$ is as good or better than \mathcal{S} if and only if

$$\text{SNR} \leq \tau_{LS_bl}.$$

The criterion in Corollary 2.1 does not depend on vertex choice, unlike Corollary 1.1. Therefore under LS and bandlimited noise, whether $\mathcal{S} \setminus \{v\}$ is as good or better than \mathcal{S} is not contingent on which vertices are in \mathcal{S} .

Next, our variant of Theorem 2 for bandlimited noise concerns when MSE changes at all, rather than when it reduces.

Corollary 2.2. Suppose we use a sequential noiseless-optimal scheme to select a vertex sample set \mathcal{S}_m of size m . For $m \leq k$:

$$\forall v \in \mathcal{S}_m : \tau(\mathcal{S}_m, v) = \tau_{LS_bl} = 1, \quad (30)$$

i.e., for any $v \in \mathcal{S}_m$, $\mathcal{S}_m \setminus \{v\}$ is better than \mathcal{S}_m if and only if $\text{SNR} < \tau_{LS_bl}$. For $m > k$:

$$\forall \text{SNR}, \forall v \in \mathcal{S}_m : \text{MSE}_{\mathcal{S}_m} = \text{MSE}_{\mathcal{S}_m \setminus \{v\}}$$

We prove Lemma 1 and Corollaries 2.1 & 2.2 in Appendix F.

As τ_{LS_bl} is not a function of the graph, we find that at a fixed $\text{SNR} < \tau_{LS_bl} = 1$, for graphs of any size (even arbitrarily large), we can reduce sample size to improve MSE.

E. GLR with full-band noise

In this subsection, we show how decreasing sample size can decrease MSE under GLR. We assume sample selection for GLR is not a function of the bandwidth k (a common setting in the literature), which means $\xi_2(\mathcal{S})$ is not a function of k .

We start by trying to simplify Theorem 1. Table IIB contains no \times scenarios and so the ‘single vertex’ simplification cannot eliminate any conditions in Theorem 1: surprisingly, $\mathbf{R}_{\mathcal{S} \setminus \{v\}}$ can be *less* biased than $\mathbf{R}_{\mathcal{S}}$ for GLR, which can be observed experimentally. Instead, as we focus on tractability and showing that it is possible to reduce sample size to reduce MSE, rather than fully characterizing all such cases, we pick a situation where $\Delta_1 \geq 0$ so we can simplify Theorem 1. Specifically, we compare the full observation set $\mathcal{S} = \mathcal{N}$ to a subset of it, which we call the ‘full observation’ simplification. As it is hard to interpret what reconstruction means under full observation [32], our results should be understood as approximately showing that reducing the sample size from nearly full observation to some smaller size may reduce MSE.

Our approach is then as follows. We first characterise under exactly which conditions a sample set $\mathcal{S} \subset \mathcal{N}$ is better than \mathcal{N} (Corollary 2.3). We then show that these conditions must occur if certain graph invariants hold (Theorem 3). Finally, we

analyse the parameters in Theorem 3 to obtain a ‘suggested sample size’ and show the conditions still occur as $N \rightarrow \infty$ (Proposition 2).

We first present the following Corollary of Theorem 1.

Corollary 2.3. Assume GLR and that $k > 1$. Consider a non-empty sample set $\mathcal{S} \subset \mathcal{N}$. Then

$$\tau(\mathcal{N}, \mathcal{S}^c) = \frac{k}{N} \cdot \frac{\Delta_2(\mathcal{N}, \mathcal{S}^c)}{-\Delta_1(\mathcal{N}, \mathcal{S}^c)} \quad (31)$$

and \mathcal{S} is better than \mathcal{N} if and only if one of the following conditions is met:

$$\begin{cases} \text{SNR} < \tau(\mathcal{N}, \mathcal{S}^c) & \text{and } [\mathbf{U}]_{\mathcal{S}^c, \{2, \dots, k\}} \neq \mathbf{0} & (32a) \\ 0 < \Delta_2(\mathcal{N}, \mathcal{S}^c) & \text{and } [\mathbf{U}]_{\mathcal{S}^c, \{2, \dots, k\}} = \mathbf{0}. & (32b) \end{cases}$$

where $[\mathbf{U}]_{\mathcal{S}^c, \{2, \dots, k\}} = \mathbf{0}$ corresponds to any k -bandlimited signal always being constant on all of \mathcal{S}^c .

Proof Sketch. We use Cauchy-Schwartz and Lemma 7 to lower bound $\xi_1(\mathcal{S})$ and show that either all k columns of $[\mathbf{U}]_{\mathcal{N}, \mathcal{K}}$ are eigenvectors of $\mathbf{\Pi}_{\mathcal{S}} + \mu \mathbf{L}$ (which is exactly when $[\mathbf{U}]_{\mathcal{S}^c, \{2, \dots, k\}} = \mathbf{0}$) and $\Delta_1(\mathcal{N}, \mathcal{S}^c) = 0$, corresponding to (32b), or $\Delta_1(\mathcal{N}, \mathcal{S}^c) < 0$, corresponding to (32a). We then apply Theorem 1. See Appendix I for a full proof. \square

We now explain the conditions in Corollary 2.3. Condition (32a) corresponds to the single case we see in Corollary 1.1. Condition (32b) is more of an edge case, e.g., if $\lambda_k < N$ and every vertex in \mathcal{S}^c has degree $N - 1$ [33, Corollary 2.3]. In (32b), $[\mathbf{U}]_{\mathcal{S}^c, \{2, \dots, k\}} = \mathbf{0}$ means any k -bandlimited signal will be constant on all of \mathcal{S}^c . Our proof shows that in the noiseless case this implies that observing \mathcal{S}^c will not improve the MSE, i.e., $\text{MSE}_{\mathcal{S} \cup \mathcal{T}_c} = \text{MSE}_{\mathcal{S}}$ for any $\mathcal{T}_c \subseteq \mathcal{S}^c$. The other condition in (32b), i.e., $0 < \Delta_2(\mathcal{N}, \mathcal{S}^c)$, corresponds to an increase in sensitivity to noise from reconstructing from those additional vertices. Therefore, condition (32b) says that if \mathcal{S}^c reveals nothing new about the underlying signal and also makes the reconstruction more sensitive to noise, one should not observe \mathcal{S}^c and only observe \mathcal{S} .

Like Corollary 1.1, Corollary 2.3 does not show that any set \mathcal{S} is ever better than \mathcal{N} , i.e., that $\tau(\mathcal{N}, \mathcal{S}^c) > 0$ ever happens. To show that τ can be positive under GLR, we bound it from below similarly to Theorem 2.

Theorem 3. Let the eigenvalues of \mathbf{L} be $0 = \lambda_1 < \lambda_2 < \dots < \lambda_N$. Let $\lceil x \rceil$ be the ceiling of x and define the vector

$$\hat{\boldsymbol{\lambda}} = (\lambda_2, \dots, \lambda_{\lceil \frac{N}{2} \rceil}, \lambda_{\lceil \frac{N}{2} \rceil}, \lambda_{\lceil \frac{N}{2} \rceil + 1}, \dots, \lambda_N) \quad (33)$$

where the middle eigenvalue $\lambda_{\lceil \frac{N}{2} \rceil}$ is repeated once. Also let

$$r_i = \frac{(\hat{\lambda}_i + \hat{\lambda}_{N-i+1})^2}{4\hat{\lambda}_i \hat{\lambda}_{N-i+1}}, \quad r = r_1 = \frac{(\lambda_N + \lambda_2)^2}{4\lambda_N \lambda_2}, \quad (34)$$

$$\rho(m) = \begin{cases} \sum_{i=1}^m r_i & \text{if } 2m \leq N \\ \rho(N - m) + (2m - N) & \text{otherwise} \end{cases}, \quad (35)$$

$$B(m) = \frac{rN}{m} + \rho(m - 1) \quad (36)$$

For any sample size $0 < m < N$, let

$$\mu_{ub}(m) = \frac{N}{\text{tr}(\mathbf{L})} \left(\sqrt{\frac{N}{B(m)}} - 1 \right) \quad (37)$$

$$\tau_{bound}(\mu, m) = \frac{\frac{1}{N} \sum_{i=1}^N (1 + \mu \lambda_i)^{-2} - \frac{B(m)}{N}}{1 + \frac{B(m)}{k} - \frac{1}{k} \sum_{i=1}^k \left(1 - \frac{1}{1 + \mu \lambda_i}\right)}. \quad (38)$$

$$\text{If } B(m) < N \quad (39)$$

$$\text{and } 0 < \mu < \mu_{ub}(m) \quad (40)$$

then, under GLR with parameter μ , for any \mathcal{S} of size m ,

$$\tau(\mathcal{N}, \mathcal{S}^c) \geq \tau_{lb}(\mu, m) > 0 \quad (41)$$

That is, if

$$\text{SNR} < \tau_{lb}(\mu, m) \quad (42)$$

then any sample set \mathcal{S} of size m is better than \mathcal{N} .

Proof Sketch. We prove that for any μ , $\xi_1(\mathcal{S}) \leq k + B(m)$ and $\xi_2(\mathcal{S}) \leq B(m)$. We also show $\xi_1(\mathcal{N}) = \sum_{i=1}^k \left(1 - \frac{1}{1 + \mu \lambda_i}\right)^2$ and $\xi_2(\mathcal{N}) = \sum_{i=1}^N (1 + \mu \lambda_i)^{-2}$. We use these to bound Δ_i , and finally apply Corollary 2.3 as our conditions mean $\Delta_2(\mathcal{N}, \mathcal{S}^c) > 0$. See Appendix J for a full proof. \square

The proof of Theorem 3 leads to an upper bound of $\text{MSE}_{\mathcal{S}}$:

Corollary 3.1. Let $B(m)$ be defined as in Theorem 3. For a sample set \mathcal{S} of size m ,

$$\text{MSE}_{\mathcal{S}} \leq k + (1 + \sigma^2) \cdot B(m). \quad (43)$$

Proof. By Lemma 8 in Appendix K, $\xi_2(\mathcal{S}) \leq B(m)$. By Lemma 9 in Appendix L, $\xi_1(\mathcal{S}) \leq k + \xi_2(\mathcal{S}) \leq k + B(m)$. Combining these using (19) gives the desired bound. \square

We contrast Theorems 2 and 3. Theorem 2 provides necessary and sufficient conditions. Theorem 3, while still useful, only provides sufficient conditions. Theorem 2 applies to any graph, but only to subsets chosen under noiseless-optimal sampling schemes, while Theorem 3 has no requirement on sampling schemes, but only applies to graphs which fulfill certain graph invariants.

Theorem 3 can be better understood by a sensitivity analysis: $r_i < r$ implies $\rho(m)$ and $B(m)$ decrease with r . Therefore for any m , as r decreases, both $\mu_{ub}(m)$ and $\tau_{lb}(m)$ increase.

The above results are for a given sample size m . We then ask what our results suggest the optimal sample size might be. Noting B may have multiple minima, we define the following:

Remark 7. Assume $N > 4$ and define

$$m_{opt} = \min_{m \in [1, N] \cap \mathbb{Z}} \arg \min B(m). \quad (44)$$

If (39) in Theorem 3 holds for some $m \in [1, N]$ then

- Condition (39) holds at a sample size of m_{opt} .
- $\mu_{ub}(m)$ and $\tau_{lb}(\mu, m)$ are both maximised at $m = m_{opt}$.
- The MSE upper bound in Corollary 3.1 is minimised at a sample size of m_{opt} .
- $m_{opt} \in \left[\left\lceil \sqrt{N} \right\rceil, \left\lceil \sqrt{rN} \right\rceil \right]$ and $m_{opt} \leq \frac{N}{2}$.

Proof. See Appendix M. \square

Based on the above, we define

$$\tau_{GLR}(\mu) = \max_m \tau_{lb}(\mu, m) = \tau_{lb}(\mu, m_{opt}). \quad (45)$$

$\tau_{GLR}(\mu)$ is the largest SNR where by Theorem 3 we know we can improve \mathcal{N} by reducing sample size. We note that *any* sample set of size m_{opt} suffices. On the other hand, even if $\text{SNR} > \tau_{GLR}$, a sample set \mathcal{S} of size m selected by an optimal sample scheme could still be better than \mathcal{N} .

Note that m_{opt} , $\mu_{ub}(m_{opt})$ and τ_{GLR} are graph invariants and they quantify amenability to signal reconstruction with low sample sizes at high noise. As r decreases, m_{opt} decreases to \sqrt{N} . This and our sensitivity analysis show that graphs with low r are more amenable to reconstruction with fewer observations via GLR³.

Finally, we consider the case of large graphs. We analyse Theorem 3 to show that $\tau_{GLR} \not\rightarrow 0$ as $N \rightarrow \infty$ and so our analysis is also relevant for large graphs. We only consider Erdős–Rényi graphs to simplify the analysis.

Proposition 2. Fix $p \in (0, 1]$. Consider graphs drawn from the distribution of random connected Erdős–Rényi graphs with N vertices and edge probability p . Then as $N \rightarrow \infty$, condition (39) in Theorem 3 holds w.h.p. both for $m = m_{opt}$ and any fixed $m > 1$. Furthermore, for any fixed $m > 1$, as $N \rightarrow \infty$,

$$r \xrightarrow{P} 1, \quad m_{opt} \cdot N^{-\frac{1}{2}} \xrightarrow{P} 1, \quad (46)$$

$$\mu_{ub}(m) \xrightarrow{P} 0, \quad \mu_{ub}(m_{opt})\lambda_2 \xrightarrow{P} +\infty. \quad (47)$$

Assume $\frac{k}{N}$ is fixed and choose $\mu = \frac{c}{\lambda_2}$, or $\frac{c}{\lambda_N}$, or $\frac{c}{\sqrt{\lambda_2\lambda_N}}$ for optimal bias-variance trade-off at $\mathcal{S} = \mathcal{N}$ [32], then

$$\tau_{GLR} \rightarrow (1 + 2c)^{-1}. \quad (48)$$

Proof Sketch. By [35, Theorem 1], $\lambda_2 \approx Np - \sqrt{2N \log N}$ and $\lambda_N \approx Np + \sqrt{2N \log N}$ as $N \rightarrow \infty$ so $\frac{\lambda_N}{\lambda_2} \xrightarrow{P} 1$ and $r \xrightarrow{P} 1$. Approximately, $B(m) \rightarrow \frac{N}{m} + m - 1$, which lets us bound μ_{ub} and τ_{GLR} . See Appendix N for a full proof. \square

F. GLR with k -bandlimited noise

Once more, one might ask whether the MSE increasing with sample size under GLR is caused by some sort of interference effect between the high-frequency components of the noise and the bandlimited (low-frequency) signal. We present a variant of Theorem 3 for k -bandlimited noise to disprove this.

We first connect the bandlimited and full-band cases:

Lemma 2. Write $\xi_{i,\text{full-band}}$ and $\xi_{i,\text{bl}}$ for ξ_i under full-band and bandlimited noises, respectively. Then $\forall \mathcal{S} \subseteq \mathcal{N}$,

$$\xi_{1,\text{bl}}(\mathcal{S}) = \xi_{1,\text{full-band}}(\mathcal{S}) \text{ and } \xi_{2,\text{bl}}(\mathcal{S}) \leq \xi_{2,\text{full-band}}(\mathcal{S}).$$

Proof. See Appendix O. \square

As ξ_1 is unchanged, Corollary 2.3 holds for bandlimited noise with $\Delta_2(\mathcal{S}, \mathcal{T}) = \xi_{2,\text{bl}}(\mathcal{S}) - \xi_{2,\text{bl}}(\mathcal{S} \setminus \mathcal{T})$. As in the full-band case, we now show conditions where $\tau > 0$ and so a subset $\mathcal{S} \subset \mathcal{N}$ is better than \mathcal{N} via a variant of Theorem 3.

³We give some intuition for r : low r , equivalent to low $\frac{\lambda_N}{\lambda_2}$, is a known condition in the Network Synchronisation literature which allows for dynamic oscillators on a network to synchronise [34].

Theorem 4. Assume k -bandlimited noise and let B be defined as in Theorem 3. For any sample size $0 < m < N$, let

$$\mu_{ub_bl}(m) = \lambda_k^{-1} \cdot \left(\sqrt{k \cdot (B(m))^{-1}} - 1 \right) \quad (49)$$

$$\tau_{lb_bl}(\mu, m) = \frac{\frac{1}{k} \sum_{i=1}^k (1 + \mu\lambda_i)^{-2} - \frac{B(m)}{k}}{1 + \frac{B(m)}{k} - \frac{1}{k} \sum_{i=1}^k \left(1 - \frac{1}{1 + \mu\lambda_i} \right)^2}. \quad (50)$$

If $B(m) < k$ (51)

and $0 < \mu < \mu_{ub}(m)$ (52)

then, for GLR with parameter μ and any set \mathcal{S} of size m ,

$$\tau(\mathcal{N}, \mathcal{S}^c) \geq \tau_{lb_bl}(\mu, m) > 0. \quad (53)$$

That is, if

$$\text{SNR} < \tau_{lb_bl}(\mu, m) \quad (54)$$

then *any* sample set \mathcal{S} of size m is better than \mathcal{N} .

Proof. See Appendix P. \square

As τ_{lb_bl} is maximised when $B(m)$ is minimised, we can define m_{opt} with the same properties as the full-band case. As we use the same bounds in the bandlimited and full-band noise cases, m_{opt} is the same in both cases. We also define

$$\tau_{GLR_bl} = \tau_{lb_bl}(m_{opt}), \quad (55)$$

with the same properties as τ_{GLR} but for bandlimited noise. As τ_{lb_bl} and μ_{ub_bl} are decreasing in $B(m)$, the sensitivity analysis also holds for τ_{lb_bl} and μ_{ub_bl} and τ_{GLR_bl} .

Finally, we consider the case of large graphs. We prove a variant of Proposition 2.

Proposition 3. As $N \rightarrow \infty$, condition (51) in Theorem 4 holds w.h.p. at a sample size of m_{opt} . Furthermore,

$$r \xrightarrow{P} 1, \quad m_{opt} \cdot N^{-\frac{1}{2}} \xrightarrow{P} 1, \quad \mu_{ub_bl}(m_{opt})\lambda_2 \xrightarrow{P} +\infty.$$

Assume $\frac{k}{N}$ is fixed and choose $\mu = \frac{c}{\lambda_2}$, or $\frac{c}{\lambda_N}$, or $\frac{c}{\sqrt{\lambda_2\lambda_N}}$ for optimal bias-variance trade-off at $\mathcal{S} = \mathcal{N}$ [32], then

$$\tau_{GLR_bl} \rightarrow (1 + 2c)^{-1}. \quad (56)$$

Proof. See Appendix Q. \square

IV. EXPERIMENTS

Our theoretical results show how the relationship between sample size and MSE changes with the level of noise, focusing on how reducing sample size will reduce MSE if the SNR is below a threshold. In this section, we demonstrate the applicability and validity of these results via empirical experiments.

We first demonstrate the applicability of our results by presenting plots of the thresholds $\tau(\mathcal{S}, v)$, τ_{GLR} and τ_{GLR_bl} against sample size (Figs. 1, 2, 3) which show concrete SNR values for $\tau(\mathcal{S}, v)$ and τ_{GLR} , giving a practical understanding of how high noise levels need to be for reducing sample size to reduce MSE for different random graph models and different parameters. In addition, we tabulate empirically the probabilities that graphs from each model satisfy the conditions of our theorems (Table III). This allows the reader to evaluate the impact of the presented theorems across different applications.

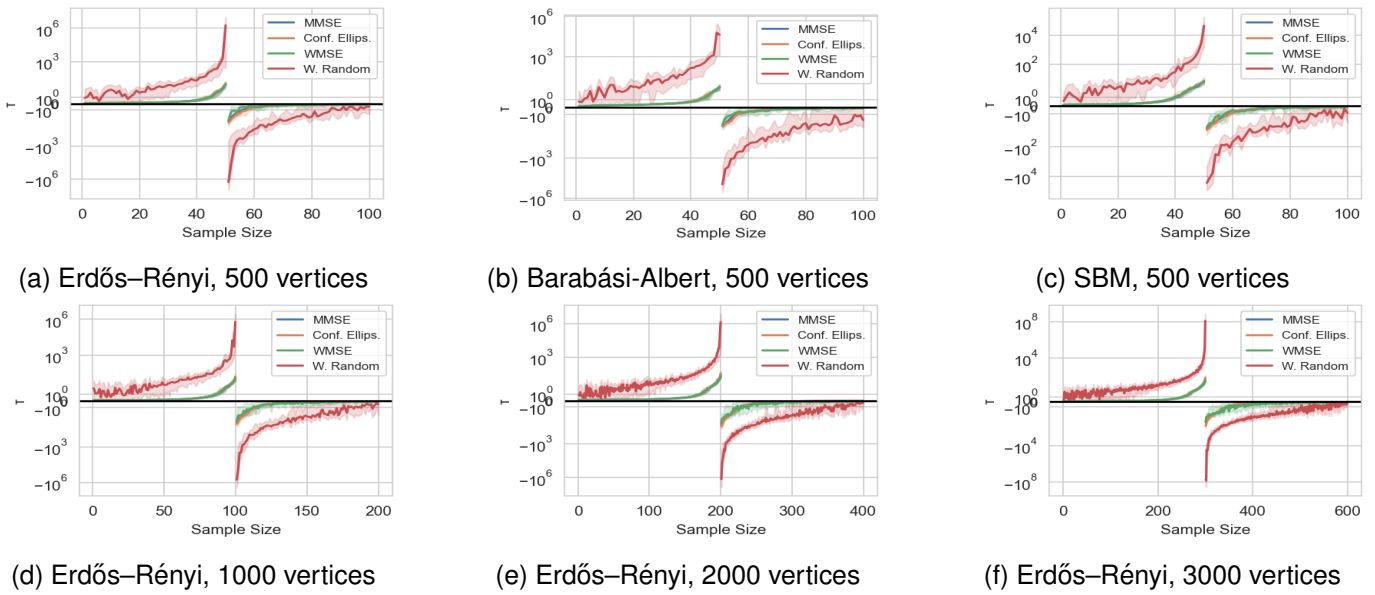


Fig. 1: $\tau(\mathcal{S}, v)$ for different random graph models and different sized graphs under LS (bandwidth = $\frac{\# \text{ vertices}}{10}$)

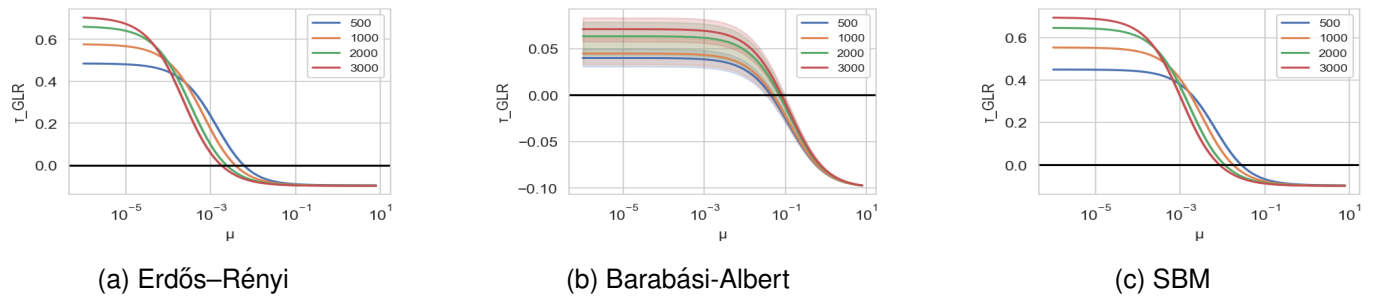


Fig. 2: τ_{GLR} for different random graph models ($\# \text{ vertices} = \text{colour}$, bandwidth = $\frac{\# \text{ vertices}}{10}$)

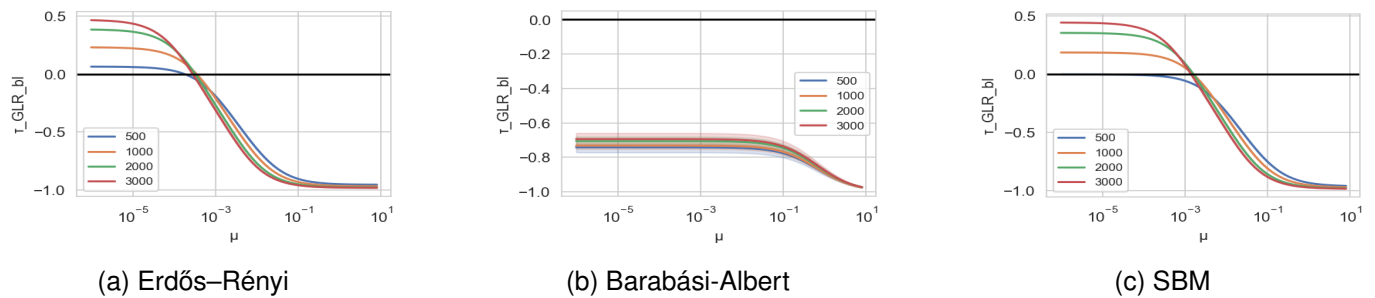


Fig. 3: τ_{GLR_bl} for different random graph models under bandlimited noise ($\# \text{ vertices} = \text{colour}$, bandwidth = $\frac{\# \text{ vertices}}{10}$)

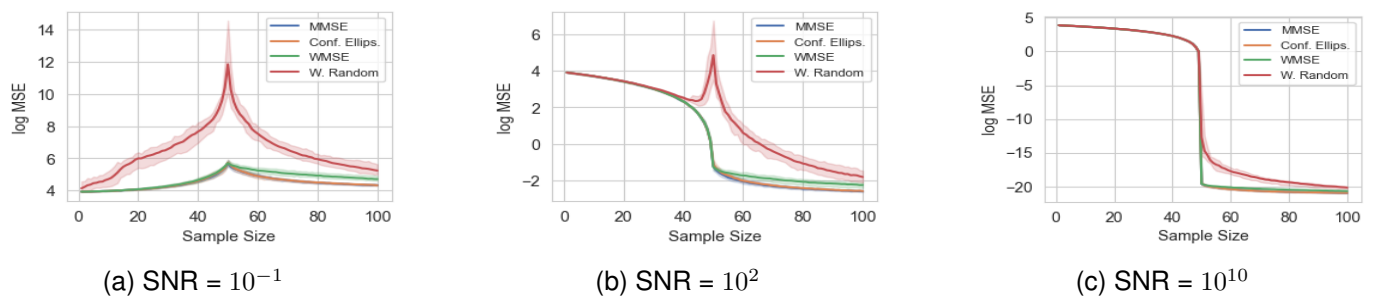


Fig. 4: Average MSE under LS on ER Graphs ($\# \text{ vertices} = 500$, bandwidth = 50)

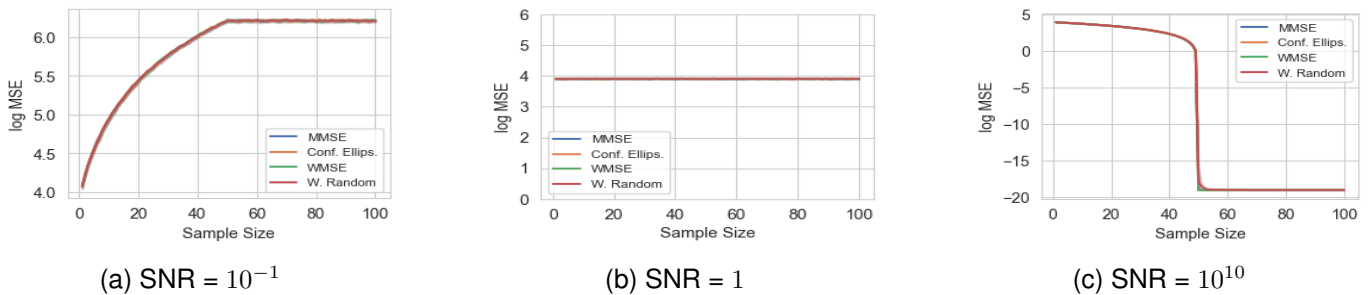


Fig. 5: Average MSE under LS on ER Graphs with bandlimited noise (#vertices=500, bandwidth = 50)

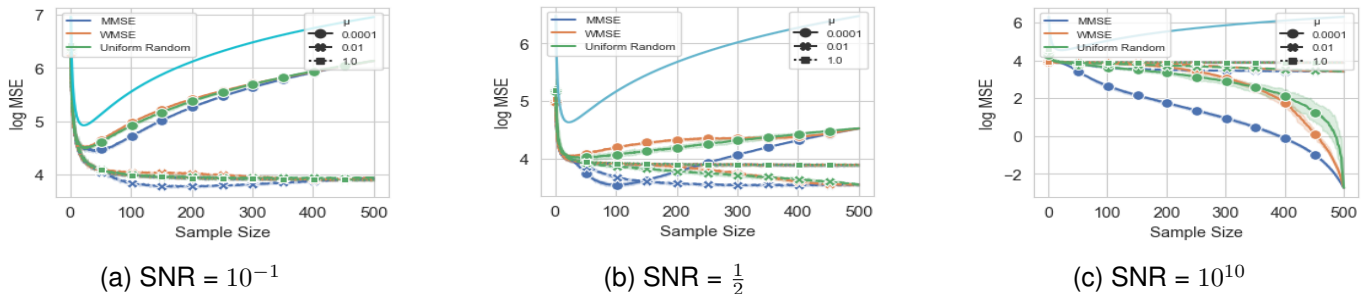


Fig. 6: Average MSE under GLR on ER Graphs (#vertices=500, bandwidth = 50), line without markers is an upper bound

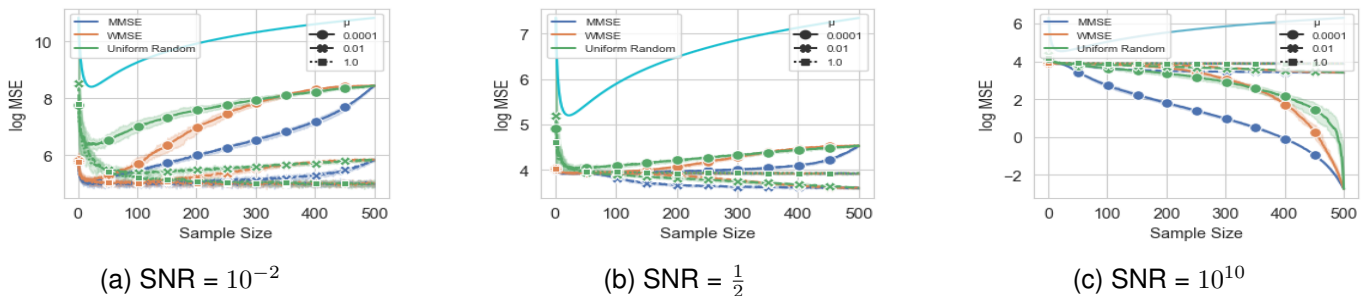


Fig. 7: Average MSE under GLR on ER Graphs under bandlimited noise (#vertices=500, bandwidth = 50), line without markers is an upper bound

We then demonstrate the validity of our results by plotting MSE_S against sample size (Figs. 4, 5, 6, 7) at SNRs below, near and above the derived thresholds, showing the behaviour of MSE_S follows our theoretical results.

A. Experimental Setup

We now present the setup of the experiments. All results are presented with 90% confidence intervals and all experiments use the combinatorial Laplacian L and its eigenbasis.

1) *Graph Generation*: We consider each of the following unweighted random graph models:

- Erdős-Rényi (ER) with edge probability $p = 0.8$ (experiments with other values of p show similar results)
- Barabási-Albert (BA) with a preferential attachment to 3 vertices at each step of its construction
- Stochastic Blockmodel (SBM) with intra- and inter-cluster edge probabilities of 0.7 and 0.1 respectively

We consider 10 instantiations of each model for plots, and 1000 instantiations of each model to assess the probability that graph invariant conditions in our Theorems are met.

We present threshold plots for graphs with 500, 1000, 2000 and 3000 vertices. We only present MSE plots for graphs with 500 vertices as they are intended as an accompaniment to our threshold plots and theorems to demonstrate their validity, and a single graph size suffices for this.

2) *Signal Generation*: We set the bandwidth $k = \lfloor \frac{N}{10} \rfloor$, as per [13]. We consider the following SNRs for full-band noise:

- LS: $10^{-1}, 10^2, 10^{10}$ (i.e. $-10dB, 20dB, 100dB$)
- GLR: $10^{-1}, 0.5, 10^{10}$ (i.e. $-10dB, -3dB, 100dB$)

and the following SNRs for bandlimited noise:

- LS: $10^{-1}, 1, 10^{10}$ (i.e. $-10dB, 0dB, 100dB$)
- GLR: $10^{-2}, 0.5, 10^{10}$ (i.e. $-20dB, -3dB, 100dB$)

These SNRs are chosen to demonstrate that there are three regimes for MSE with distinctive properties—the high noise regime, the transitional regime and the approximately noiseless regime—and that τ captures when the regimes change. Suitable values of SNRs to demonstrate this vary between reconstruction methods and noise types, hence our choices.

To test the MSE in reconstructing signals from samples, we generate 200 signals by sampling $\mathbf{y} = \mathbf{x}_{raw} + \sigma \cdot \epsilon_{raw}$ where:

1) $\mathbf{x}_{raw} \sim \mathcal{N}(\mathbf{0}, \mathbf{\Pi}_{bl(\kappa)})$

2a) If full-band noise, $\epsilon_{raw} \sim \mathcal{N}(\mathbf{0}, \mathbf{I}_N)$, $\sigma = \sqrt{\frac{k}{N \cdot \text{SNR}}}$

2b) If bandlimited noise, $\epsilon_{raw} \sim \mathcal{N}(\mathbf{0}, \mathbf{\Pi}_{bl(\kappa)})$, $\sigma = \frac{1}{\sqrt{\text{SNR}}}$

3) *Sample-Set Selection*: We generate sample sets greedily using exact analytic forms and by exactly computing $\mathbf{\Pi}_{bl(\kappa)}$.

LS: We use (3)-(5) to exactly compute the MMSE, Confidence Ellipsoid and WMSE criteria, which are deterministic and guaranteed to be noiseless-optimal. We also look at Weighted Random sampling [12], which is neither deterministic nor guaranteed to be noiseless-optimal.

GLR: We exactly compute the MMSE criterion, which is a function of SNR and noise type, and the WMSE criterion, which is not. We also consider uniform random sampling.

Note that sampling schemes in the literature tend to differ from ours mainly in that they approximate our setup for computational efficiency reasons; e.g. approximating the projection matrix $\mathbf{\Pi}_{bl(\kappa)}$ with a polynomial in \mathbf{L} [14], and approximating optimality criteria [13]. As these differences are for efficiency reasons, we do not expect them to matter in our experiments.

4) *Parameters of Reconstruction Methods*: We consider LS with bandwidth $k = \lfloor \frac{N}{10} \rfloor$ and GLR with $\mu \in \{10^{-4}, 10^{-2}, 1\}$.

B. Experimental Results

We present threshold plots for all graphs and MSE plots for ER graphs in the main body of the paper. MSE plots for BA and SBM graphs are presented in Appendix R.

1) τ and τ_{GLR} plots:

[*LS / full-band*] Figs. 1 shows $\tau(\mathcal{S}, v)$ as sample size varies for sequential sampling methods under LS, where v is the latest node added to \mathcal{S} . For ER graphs, for sample size smaller than the bandwidth, $\tau(\mathcal{S}, v) > 0$ and beyond that $\tau(\mathcal{S}, v) \leq 0$. The maximum of $\tau(\mathcal{S}, v)$ observed is approximately 10⁶ (60dB) for weighted random sampling, and approximately 10 (10dB) for the deterministic sampling methods. The confidence intervals for weighted random sampling is much wider than for the deterministic sampling methods. Next, we observe the same phenomenon as with ER for BA and SBM graphs, with maxima of approximately 10⁵ (50dB) for weighted random sampling and maxima of approximately 10 (10dB) for the deterministic sampling methods. Finally, Figs. 1d-1f show the same phenomenon as Fig. 1a happens for ER graphs at sizes of 1000, 2000 and 3000 vertices.

We now correlate our experiments and our theoretical results. As Corollary 1.1 is necessary and sufficient, the sign of $\tau(\mathcal{S}, v)$ tells us exactly when removing a vertex improves \mathcal{S} . Therefore τ being negative is an informative statement, telling us that $\mathcal{S} \setminus \{v\}$ is *never* better than \mathcal{S} . Concretely, if SNR is below the maximum $\tau(\mathcal{S}, v)$ observed, then when sample size equals bandwidth we can reduce sample size to reduce MSE.

Theorem 2 proves that noiseless-optimal methods (MMSE, Confidence Ellipsoid and WMSE in our experiments) will have $\tau(\mathcal{S}, v) > 0$ for sample sizes smaller than the bandwidth, and then $\tau(\mathcal{S}, v) \leq 0$ afterwards, and Fig. 1 validates this. Note that even though this pattern holds for Weighted Random Sampling in our experiments, Theorem 2 cannot guarantee that it will always hold for Weighted Random Sampling.

While we prove that $\tau(\mathcal{S}, v) \not\rightarrow 0$ as $N \rightarrow \infty$, we conjecture the stronger claim that at a sample size equal to bandwidth, $\tau(\mathcal{S}, v)$ might actually increase with graph size, which is supported (but not proven) by Figs. 1d-1f.

[*LS / bandlimited*] We do not provide a plot as in this case, as our theoretical results provide the magnitude of τ : by Corollary 2.2, $\tau(\mathcal{S}, v) = 1$ for $|\mathcal{S}| \leq k$ under sequential noiseless-optimal sampling. Corollary 2.2 overall says something stronger, i.e. we can always reduce MSE by reducing sample size if $\text{SNR} < 1$ at any sample size.

[*GLR / full-band*] In Fig. 2, we plot τ_{GLR} , where if $\text{SNR} < \tau_{GLR}$, then there is a sample size $m_{opt} < N$ where *any* sample set of size m_{opt} is better than \mathcal{N} . Unlike with LS, our theorems are only sufficient so $\text{SNR} > \tau_{GLR}$ is uninformative. For ER graphs, we see that τ_{GLR} is decreasing in μ , and that $\tau_{GLR} > 0$ for sufficiently small μ for all graph sizes. The maximum value in this case for τ_{GLR} ranges between 0.4 (-4dB) and 0.7 (-1.5dB). We see a similar pattern to ER graphs for BA graphs, where the main differences are that $\tau_{GLR} > 0$ for larger values of μ and that the maximum of τ_{GLR} is approximately 0.05 (-13dB). τ_{GLR} for SBM graphs behaves very similarly to ER graphs in our experiments. Note that the confidence intervals for ER and SBM graphs are so tight as to not be clearly seen in Fig. 2, while being much wider for BA graphs. As graph properties, when we sample from a random graph model, r and ρ are random variables. We observe wider confidence intervals when \mathcal{G} is sampled from the BA graph model as $\text{Var}_{\mathcal{G}}(r)$ and $\text{Var}_{\mathcal{G}}(\rho)$ are much higher than when we sample from the ER or SBM graph models.

As $\tau_{GLR} > 0$, Fig. 2 shows we can reduce sample size to reduce MSE for all examined graph models. We see τ_{GLR} is only positive for small enough μ , motivating μ_{ub} in Theorem 3. The value of μ below which $\tau_{GLR} > 0$ is at least μ_{ub} .

Finally, Proposition 2 proves that $\tau_{GLR} \not\rightarrow 0$ as $N \rightarrow \infty$ for $\mu = \frac{c}{\lambda_2}$, or $\frac{c}{\lambda_N}$, or $\frac{c}{\sqrt{\lambda_2 \lambda_N}}$ on ER graphs, i.e. for decreasing μ as N increases. We note that Fig. 2 provides empirical evidence that this might hold for all graph models tested.

[*GLR / bandlimited*] Our purpose in showing bandlimited variants is to show that reducing sample size can reduce MSE even under bandlimited noise. Figs. 3a and 3c show the same overall trend as Figs. 2a and 2c, i.e. τ_{GLR_bl} can be positive for ER and SBM graphs, giving evidence to our claim. Fig. 3b is entirely negative, and so entirely uninformative, i.e. it does not prove whether reducing sample size can or cannot reduce MSE under bandlimited noise for BA graphs, at least based on our theoretical results. As with the full-band case, Fig. 3a validates our asymptotic result for ER graphs (Proposition 3).

2) *MSE plots*: The MSE plots demonstrate the validity of our theoretical results linking MSE and sample size.

[*LS / full-band*] Fig. 4 shows log MSE against sample size for LS. For high noise (a), we see MSE increases with sample size no larger than bandwidth, and decreases afterwards. In (b), for our three deterministic noiseless-optimal sampling schemes (orange/green/blue), MSE is decreasing in sample size. For weighted random sampling, we see for sample sizes no larger than bandwidth, MSE first decreases and then increases, attaining a maximum with sample size at bandwidth, and then decreases with sample size. In (c), the almost noiseless case,

we see MSE is decreasing in sample size for all sampling schemes, with a large drop when sample size is at bandwidth.

Comparing Fig. 4 to Fig. 1a, Fig. 4a corresponds to when $\text{SNR} < \tau(\mathcal{S}, v)$, Fig. 4c corresponds to $\text{SNR} > \tau(\mathcal{S}, v)$ and Fig. 4b corresponds to when SNR lies between some values of $\tau(\mathcal{S}, v)$ for weighted random sampling. We see that MSE increases with sample size when $\text{SNR} < \tau(\mathcal{S}, v)$ and decreases otherwise, proving the validity of Corollary 1.1. Fig. 4a (green, orange, blue curves) shows that for low SNRs, optimal sampling schemes lead MSE to monotonically increase with each additional sample until the sample size reaches the bandwidth, illustrating Theorem 2 and Remark 5. We also validate Remark 6: if we are slightly above the bandwidth (50 for Fig. 4a), i.e., to the right of the peak, then reducing sample size by one does not reduce MSE; however, if we significantly reduce sample size, i.e., transitioning from just right of the peak to left of the peak, we can reduce MSE.

Interestingly, Fig. 4a shows that at a low SNR of 10^{-1} , the optimal sample size under LS is zero. This makes concrete the idea that if there is too much noise, reconstruction does not work: at this noise level letting $\hat{x} = \mathbf{0}$ rather than fitting with LS with any number of observed vertices will result in a lower MSE on average. This can also be formalised in terms of our Bias-Variance decomposition; a $\mathbf{0}$ reconstruction has high bias but zero variance, and reconstructing from a non-zero number of samples has lower bias and non-zero variance. At a sufficiently high noise level the variance term in the MSE will dominate, and the MSE from taking $\hat{x} = \mathbf{0}$ will be lower than if we reconstruct with any non-zero number of samples.

On the other hand, for high SNRs (Fig. 4c), MSE decreases monotonically as sample size increases for all sampling schemes, showing Corollary 1.1 is necessary and sufficient. Finally, Fig. 4b illustrates the situation between the two cases.

[*LS / bandlimited*] Fig. 5 shows how MSE behaves as sample size increases. Fig. 5a shows that under high noise, MSE increases with sample size when sample size is no larger than bandwidth, and is constant beyond that. Fig. 5b shows at an SNR of $\tau_{LS,bl} = 1$, MSE is constant with sample size. Finally, Fig. 5c shows that in the almost noiseless case MSE decreases with sample size. Fig. 5a demonstrates Corollary 2.1 by showing that for $\text{SNR} < \tau_{LS,bl} = 1$ the MSE is increasing with sample size. In all cases, MSE remains unchanged for sample sizes exceeding the bandlimit k , demonstrating Corollary 2.2.

[*GLR / full-band*] Fig. 6 shows how MSE changes with sample size for different values of μ , along with an upper bound (light blue) which is not dependent on μ . This bound is approximately U-shaped in all cases. For $\text{SNR} = 10^{-1}$, we see for $\mu = 10^{-4}$, under all sampling schemes, MSE is minimised at a sample size around 16 to 22. For the MMSE sampling scheme with $\mu = 0.01$, MSE is minimised at a sample size of approximately 200. In all other cases where $\text{SNR} = 10^{-1}$, MSE is minimised at full observation ($|\mathcal{S}| = 500$). For $\text{SNR} = \frac{1}{2}$ and $\mu = 10^{-4}$, MSE is minimised at a sample size a bit less than 100. For larger μ , we see MSE is minimised at full observation. In the nearly noiseless case, MSE decreases with sample size under all parameter choices. In all cases where the MSE is minimised at a sample size less than N , the MSE

is approximately U-shaped like our bound.

Fig. 6 illustrates Corollary 2.3, Theorem 3 and Corollary 3.1 in the following ways. First, the MSE upper bound corresponds to Corollary 3.1, and we can see it is greater than any observed MSE at each sample size. The sample size which minimises our upper bound is m_{opt} (Remark 7) and as $r \in (1, 1.01]$ in our Erdős–Rényi experiments, $m_{opt} \in [22, 23]$, which empirically well approximates the sample size that minimises MSE in our low μ and low SNR experiments. Second, Fig. 6 shows that MSE can decrease with increasing sample size, and Fig. 6c shows that at high SNR full observation is better than partial observation, illustrating the necessary and sufficient nature of Corollary 2.3. Finally, Fig. 6 illustrates Theorem 3 by demonstrating the dependence on SNR and μ , i.e. at low μ and SNR the optimal sample size is less than N , but at high enough μ or SNR this no longer holds.

Fig. 6 also demonstrates some limitations of the characterisation in Corollary 3.1 and Theorem 3. We see from Fig. 6b that even though the MSE at m_{opt} is lower than at N , our bound never goes below the maximum observed MSE, so is too loose to show this. This is partly because the Theorem and the Corollary bound $\xi_2(\mathcal{S})$ only as a function of $|\mathcal{S}|$, ignoring μ and the composition of \mathcal{S} . This limitation corresponds to a gap between τ_{GLR} and $\tau(\mathcal{N}, \mathcal{S}^c)$, demonstrating τ_{GLR} is a lower bound for $\tau(\mathcal{N}, \mathcal{S}^c)$ rather than an exact characterisation.

[*GLR / bandlimited*] The same observations around the subfigures of Fig. 6 and Theorem 3 also apply to the subfigures of Fig. 7 and Theorem 4; specifically, for sufficiently small μ and SNR, MSE is minimised at sample sizes well below full observation under bandlimited noise and $\tau_{GLR,bl}$ is a lower bound for $\tau(\mathcal{N}, \mathcal{S}^c)$ rather than an exact characterisation.

3) *Checking Conditions*: While our theorems for LS apply to all graphs, our theorems on GLR rely on conditions around graph invariants. We sample graphs from each random graph model to empirically show the probability the conditions of each theorem are met at a sample size of m_{opt} for some $\mu > 0$:

TABLE III: Probability theorem conditions are met

	ER	SBM	BA
Theorem 3 conditions met	100%	100%	100%
Theorem 4 conditions met	100%	45.7%	0%

Propositions 2 and 3 show the conditions in Theorems 3 and 4 hold w.h.p. for ER graphs as $N \rightarrow \infty$. However, they do not say whether they hold for a graph of a given size, or other graph models. The results in Table III show empirically that the conditions hold under full-band noise (Theorem 3) for ER, BA and SBM graphs with 500 vertices, and under bandlimited noise (Theorem 4) for ER graphs and some SBM graphs. This outlines the applicability of our theorems.

If the conditions on our Theorems are not met, they provide no information about the shape of the MSE. However, Figs. 13 and 17 in Appendix R show empirically that for BA and SBM graphs under bandlimited noise with $\text{SNR} \in \{10^{-2}, \frac{1}{2}\}$ under GLR with $\mu \in \{10^{-2}, 10^{-4}\}$, even if the conditions of Theorem 4 are not met, reducing sample size from N to below

N reduces MSE under the presented sampling schemes. We leave further investigation of this as future work.

V. DISCUSSION

In this paper we studied the impact of sample size on linear reconstruction of noisy k -bandlimited graph signals. We showed theoretically and experimentally, in the same settings as much of the sample set selection literature, that reconstruction error is not always monotonic in sample size, i.e., at sufficiently low SNRs, reconstruction error can sometimes be improved by *reducing* sample size. Our finding reveals that existing results in the literature for the noiseless setting may not necessarily generalise to the noisy case, even when considering regularised reconstruction methods. It also demonstrates the need to consider both optimal sample size selection and reconstruction methods at the same time, and motivates assessment of noise levels in datasets to do so. Future work includes extending the analysis on GLR to the normalised graph Laplacian, providing bounds on ξ_2 for LS, analysing other graph models such as Ring graphs or studying early-stopping schemes that do not use the full sample budget.

VI. ACKNOWLEDGEMENTS

This work was supported by the EPSRC Centre for Doctoral Training in Autonomous Intelligent Machines and Systems (EP/S024050/1).

REFERENCES

- [1] S. Itani and D. Thanou, "A graph signal processing framework for the classification of temporal brain data," in *2020 28th European Signal Processing Conference (EUSIPCO)*. IEEE, 2021, pp. 1180–1184.
- [2] R. K. Jain, J. M. Moura, and C. E. Kontokosta, "Big data+ big cities: Graph signals of urban air pollution [exploratory sp]," *IEEE Signal Processing Magazine*, vol. 31, no. 5, pp. 130–136, 2014.
- [3] B. Renoust, G. Cheung, and S. Satoh, "Estimating political leanings from mass media via graph-signal restoration with negative edges," in *2017 IEEE International Conference on Multimedia and Expo (ICME)*. IEEE, 2017, pp. 1009–1014.
- [4] A. Ortega, P. Frossard, J. Kovačević, J. M. Moura, and P. Vandergheynst, "Graph signal processing: Overview, challenges, and applications," *Proceedings of the IEEE*, vol. 106, no. 5, pp. 808–828, 2018.
- [5] S. Chen, R. Varma, A. Sandryhaila, and J. Kovačević, "Discrete signal processing on graphs: Sampling theory," *IEEE transactions on signal processing*, vol. 63, no. 24, pp. 6510–6523, 2015.
- [6] Y. Tanaka, Y. C. Eldar, A. Ortega, and G. Cheung, "Sampling signals on graphs: From theory to applications," *IEEE Signal Processing Magazine*, vol. 37, no. 6, pp. 14–30, 2020.
- [7] F. Pukelsheim, *Optimal design of experiments*. SIAM, 2006.
- [8] L. F. Chamon and A. Ribeiro, "Greedy sampling of graph signals," *IEEE Transactions on Signal Processing*, vol. 66, no. 1, pp. 34–47, 2017.
- [9] A. Nikolov, M. Singh, and U. Tantipongpipat, "Proportional volume sampling and approximation algorithms for a-optimal design," *Mathematics of Operations Research*, vol. 47, no. 2, pp. 847–877, 2022.
- [10] A. Jayawant and A. Ortega, "Practical graph signal sampling with log-linear size scaling," *Signal Processing*, vol. 194, p. 108436, 2022.
- [11] N. Tremblay, P.-O. Amblard, and S. Barthelmé, "Graph sampling with determinantal processes," in *2017 25th European Signal Processing Conference (EUSIPCO)*. IEEE, 2017, pp. 1674–1678.
- [12] G. Puy, N. Tremblay, R. Gribonval, and P. Vandergheynst, "Random sampling of bandlimited signals on graphs," *Applied and Computational Harmonic Analysis*, vol. 44, no. 2, pp. 446–475, 2018.
- [13] Y. Bai, F. Wang, G. Cheung, Y. Nakatsukasa, and W. Gao, "Fast graph sampling set selection using gershgorin disc alignment," *IEEE Transactions on signal processing*, vol. 68, pp. 2419–2434, 2020.
- [14] F. Wang, Y. Wang, and G. Cheung, "A-optimal sampling and robust reconstruction for graph signals via truncated neumann series," *IEEE Signal Processing Letters*, vol. 25, no. 5, pp. 680–684, 2018.
- [15] F. Wang, G. Cheung, and Y. Wang, "Low-complexity graph sampling with noise and signal reconstruction via neumann series," *IEEE Transactions on Signal Processing*, vol. 67, no. 21, pp. 5511–5526, 2019.
- [16] A. Anis, A. Gadde, and A. Ortega, "Efficient sampling set selection for bandlimited graph signals using graph spectral proxies," *IEEE Transactions on Signal Processing*, vol. 64, no. 14, pp. 3775–3789, 2016.
- [17] H. Shomorony and A. S. Avestimehr, "Sampling large data on graphs," in *2014 IEEE Global Conference on Signal and Information Processing (GlobalSIP)*. IEEE, 2014, pp. 933–936.
- [18] O. Nabar and G. Shroff, "Conservative predictions on noisy financial data," in *Proceedings of the Fourth ACM International Conference on AI in Finance*, 2023, pp. 427–435.
- [19] B. Sripathmanathan, X. Dong, and M. Bronstein, "On the impact of sample size in reconstructing graph signals," in *2023 International Conference on Sampling Theory and Applications (SampTA)*. IEEE, 2023, pp. 1–6.
- [20] F. Zhang, "Schur complements and matrix inequalities in the löwner ordering," *Linear Algebra and Its Applications*, vol. 321, no. 1-3, pp. 399–410, 2000.
- [21] S. Chen, R. Varma, A. Singh, and J. Kovačević, "Signal recovery on graphs: Fundamental limits of sampling strategies," *IEEE Transactions on Signal and Information Processing over Networks*, vol. 2, no. 4, pp. 539–554, 2016.
- [22] S. Lin, X. Xie, H. Feng, and B. Hu, "Active sampling for approximately bandlimited graph signals," in *ICASSP 2019-2019 IEEE International Conference on Acoustics, Speech and Signal Processing (ICASSP)*. IEEE, 2019, pp. 5441–5445.
- [23] Y. Tanaka and Y. C. Eldar, "Generalized sampling on graphs with subspace and smoothness priors," *IEEE Transactions on Signal Processing*, vol. 68, pp. 2272–2286, 2020.
- [24] J. Hara and Y. Tanaka, "Sampling set selection for graph signals under arbitrary signal priors," in *ICASSP 2022-2022 IEEE International Conference on Acoustics, Speech and Signal Processing (ICASSP)*. IEEE, 2022, pp. 5732–5736.
- [25] S. K. Narang, A. Gadde, E. Sanou, and A. Ortega, "Localized iterative methods for interpolation in graph structured data," in *2013 IEEE Global Conference on Signal and Information Processing*. IEEE, 2013, pp. 491–494.
- [26] C.-F. Gauss, *Theoria combinationis observationum erroribus minimis obnoxiae*. Henricus Dieterich, 1823.
- [27] G. H. Golub and C. F. Van Loan, *Matrix Computations*, 4th ed. John Hopkins University Press, 2013.
- [28] I. Pesenson, "Sampling in paley-wiener spaces on combinatorial graphs," *Transactions of the American Mathematical Society*, vol. 360, no. 10, pp. 5603–5627, 2008.
- [29] M. Tsitsvero, S. Barbarossa, and P. Di Lorenzo, "Signals on graphs: Uncertainty principle and sampling," *IEEE Transactions on Signal Processing*, vol. 64, no. 18, pp. 4845–4860, 2016.
- [30] S. Geman, E. Bienenstock, and R. Doursat, "Neural networks and the bias/variance dilemma," *Neural computation*, vol. 4, no. 1, pp. 1–58, 1992.
- [31] L. F. Chamon and A. Ribeiro, "Near-optimality of greedy set selection in the sampling of graph signals," in *2016 IEEE Global Conference on Signal and Information Processing (GlobalSIP)*. IEEE, 2016, pp. 1265–1269.
- [32] P.-Y. Chen and S. Liu, "Bias-variance tradeoff of graph laplacian regularizer," *IEEE Signal Processing Letters*, vol. 24, no. 8, pp. 1118–1122, 2017.
- [33] R. Merris, "Laplacian graph eigenvectors," *Linear algebra and its applications*, vol. 278, no. 1-3, pp. 221–236, 1998.
- [34] M. Barahona and L. M. Pecora, "Synchronization in small-world systems," *Physical review letters*, vol. 89, no. 5, p. 054101, 2002.
- [35] T. Jiang, "Low eigenvalues of laplacian matrices of large random graphs," *Probability Theory and Related Fields*, vol. 153, pp. 671–690, 2012.
- [36] R. Bhatia, *Matrix analysis*. Springer Science & Business Media, 2013, vol. 169.
- [37] A. Householder, "The kantorovich and some related inequalities," *SIAM Review*, vol. 7, no. 4, pp. 463–473, 1965.
- [38] C. Khatri and C. R. Rao, "Some extensions of the kantorovich inequality and statistical applications," *Journal of Multivariate Analysis*, vol. 11, no. 4, pp. 498–505, 1981.
- [39] K. Nordström, "Convexity of the inverse and moore–penrose inverse," *Linear algebra and its applications*, vol. 434, no. 6, pp. 1489–1512, 2011.

APPENDIX A
EXTENDING RESULTS TO OTHER SETTINGS

Our paper studies the MMSE criterion, which averages over a known distribution of signal and noise. However, as we study cases where $\Delta_2(\mathcal{S}, \mathcal{T}) > 0$, our results carry over to the setting where the signal is fixed and we average over the noise.

Firstly, we define some notation. Fix a signal \mathbf{x} , and assume have noisy observations of \mathbf{x} at \mathcal{S} . Let our reconstruction of \mathbf{x} be $\hat{\mathbf{x}}$. We write the MSE in this setting as

$$\text{MSE}_{\mathcal{S}}|_{\mathbf{x}} = \mathbb{E}_{\epsilon} \left[\|\hat{\mathbf{x}} - \mathbf{x}\|_2^2 \mid \mathcal{S} \text{ observed} \right]. \quad (57)$$

and note that $\text{MSE}_{\mathcal{S}} = \mathbb{E}_{\mathbf{x}} [\text{MSE}_{\mathcal{S}}|_{\mathbf{x}}]$.

We now provide a proposition, which shows that the results in the MMSE setting carry over to the fixed-signal setting.

Proposition 4. Suppose that $\Delta_2(\mathcal{S}, \mathcal{T}) > 0$. Then for any signal \mathbf{x} , there exists a threshold $\tau^{\mathbf{x}}(\mathcal{S}, \mathcal{T}) > 0$ such that if

$$\text{SNR} < \tau^{\mathbf{x}}(\mathcal{S}, \mathcal{T})$$

then

$$\text{MSE}_{\mathcal{S} \setminus \mathcal{T}}|_{\mathbf{x}} < \text{MSE}_{\mathcal{S}}|_{\mathbf{x}}.$$

Proof. Removing the expectation $\mathbb{E}_{\mathbf{x}}[\cdot]$ in the equations at the start of Section III-B gives that

$$\text{MSE}_{\mathcal{S}}|_{\mathbf{x}} = \|(\mathbf{I} - \mathbf{R}_{\mathcal{S}}[\mathbf{I}]_{\mathcal{S}, \mathcal{N}})[\mathbf{U}]_{\mathcal{N}, \mathcal{K}}\|_F^2 + \sigma^2 \cdot \xi_2(\mathcal{S}). \quad (58)$$

Rearrange this using $\Delta_2 > 0$ to see that $\text{MSE}_{\mathcal{S} \setminus \mathcal{T}}|_{\mathbf{x}} < \text{MSE}_{\mathcal{S}}|_{\mathbf{x}}$ if and only if

$$\sigma^2 > \frac{\left\| \left(\mathbf{I} - \mathbf{R}_{\mathcal{S} \setminus \mathcal{T}}[\mathbf{I}]_{\mathcal{S} \setminus \mathcal{T}, \mathcal{N}} \right) \mathbf{x} \right\|_2^2 - \left\| \left(\mathbf{I} - \mathbf{R}_{\mathcal{S}}[\mathbf{I}]_{\mathcal{S}, \mathcal{N}} \right) \mathbf{x} \right\|_2^2}{\Delta_2(\mathcal{S}, \mathcal{T})} \quad (59)$$

and pick $\tau^{\mathbf{x}}(\mathcal{S}, \mathcal{T})$ to be the corresponding SNR threshold (which is infinite if the LHS ≤ 0). \square

All of the proofs in the paper for specific reconstruction methods showing when reducing sample size reduces MSE do so by showing $\Delta_2(\mathcal{S}, \mathcal{T}) > 0$, and therefore Proposition 4 applies to each of them.

That is to say, in this paper we demonstrate that for both LS and GLR reconstruction, under both bandlimited and full-band noise, under certain conditions, reducing sample size reduces MSE when averaged across our signal model and noise model. By this proposition we have that for any given fixed signal $\mathbf{x} \neq 0$, under the same conditions, for both LS and GLR reconstruction, under both bandlimited and full-band noise, if SNR is below some signal-specific threshold $\tau^{\mathbf{x}}$ then reducing sample size reduces MSE.

This shows the observation that reducing sample size may reduce MSE is not fundamentally dependent on our choice of signal model.

APPENDIX B
PROOF OF TABLE II

For GLR reconstruction, Table IIb does not rule out any option. In experiments with Erdős–Rényi graphs, all options marked as \checkmark in Figure IIb can be observed at some sample size without too much difficulty under random or WMSE sampling.

The options marked \sim do not turn up in such experiments, but may happen for very specific values of μ dependent on the graph and sampling scheme.

For LS reconstruction, we decompose the pattern in Table IIa into the following statements:

- $\Delta_1 \leq 0$
- $\Delta_1 < 0$ if and only if $\Delta_2 > 0$

A. Under LS reconstruction, $\Delta_1 \leq 0$

For LS we have:

$$\mathbf{R}_{\mathcal{S}} = [\mathbf{U}]_{\mathcal{N}, \mathcal{K}} [\mathbf{U}]_{\mathcal{S}, \mathcal{K}}^{\dagger}.$$

Lemma 3. For LS,

$$\xi_1(\mathcal{S}) = k - \text{rank}([\mathbf{U}]_{\mathcal{S}, \mathcal{K}}), \quad (60)$$

$$\Delta_1(\mathcal{S}, v) \in \{0, -1\}. \quad (61)$$

Proof. As $\|[\mathbf{U}]_{\mathcal{N}, \mathcal{K}} \mathbf{A}\|_F^2 = \|\mathbf{A}\|_F^2$ for any matrix $\mathbf{A} \in \mathbb{R}^{k \times k}$,

$$\begin{aligned} \xi_1(\mathcal{S}) &= \|[\mathbf{U}]_{\mathcal{N}, \mathcal{K}} - \mathbf{R}_{\mathcal{S}}[\mathbf{U}]_{\mathcal{S}, \mathcal{K}}\|_F^2 \\ &= \|[\mathbf{U}]_{\mathcal{N}, \mathcal{K}} - [\mathbf{U}]_{\mathcal{N}, \mathcal{K}}([\mathbf{U}]_{\mathcal{S}, \mathcal{K}})^{\dagger}[\mathbf{U}]_{\mathcal{S}, \mathcal{K}}\|_F^2 \\ &= \|\mathbf{I}_k - ([\mathbf{U}]_{\mathcal{S}, \mathcal{K}})^{\dagger}[\mathbf{U}]_{\mathcal{S}, \mathcal{K}}\|_F^2 \end{aligned}$$

Let $\mathbf{\Pi} = ([\mathbf{U}]_{\mathcal{S}, \mathcal{K}})^{\dagger}[\mathbf{U}]_{\mathcal{S}, \mathcal{K}}$. $\mathbf{\Pi}$ is of the form $\mathbf{A}^{\dagger} \mathbf{A}$, so is a symmetric orthogonal projection onto the range of $([\mathbf{U}]_{\mathcal{S}, \mathcal{K}})^T$ [27, p. 290]. Orthogonal projections are idempotent ($\mathbf{\Pi} = \mathbf{\Pi}^2$) hence have eigenvalues which are 0 or 1, and therefore $\text{tr}(\mathbf{\Pi}) = \text{rank}([\mathbf{U}]_{\mathcal{S}, \mathcal{K}}) = \text{rank}([\mathbf{U}]_{\mathcal{S}, \mathcal{K}})^T$. We then have:

$$\begin{aligned} \xi_1(\mathcal{S}) &= \|\mathbf{I}_k - \mathbf{\Pi}\|_F^2 \\ &= \text{tr}((\mathbf{I}_k - \mathbf{\Pi})(\mathbf{I}_k - \mathbf{\Pi})^T) \\ &= \text{tr}((\mathbf{I}_k - \mathbf{\Pi})(\mathbf{I}_k - \mathbf{\Pi})) \\ &= \text{tr}(\mathbf{I}_k - 2\mathbf{\Pi} + \mathbf{\Pi}^2) \\ &= \text{tr}(\mathbf{I}_k - \mathbf{\Pi}) \\ &= \text{tr}(\mathbf{I}_k) - \text{tr}(\mathbf{\Pi}) \\ &= k - \text{rank}([\mathbf{U}]_{\mathcal{S}, \mathcal{K}}) \end{aligned}$$

proving (60). We now prove (61). Removing a vertex from \mathcal{S} removes a row from $[\mathbf{U}]_{\mathcal{S}, \mathcal{K}}$, reducing the rank by 0 or 1, so

$$\begin{aligned} \Delta_1(\mathcal{S}, v) &= \xi_1(\mathcal{S}) - \xi_1(\mathcal{S} \setminus \{v\}) \\ &= -\text{rank}([\mathbf{U}]_{\mathcal{S}, \mathcal{K}}) + \text{rank}([\mathbf{U}]_{\mathcal{S} \setminus \{v\}, \mathcal{K}}) \\ &\in \{0, -1\}. \end{aligned}$$

\square

Non-positivity of Δ_1 immediately follows from Lemma 3

B. Under LS reconstruction, $\Delta_1 < 0$ if and only if $\Delta_2 > 0$

We first need the following lemmas.

Lemma 4.

$$\xi_2(\mathcal{S}) = \sum_{\lambda_i^{\mathcal{S}} \neq 0} \frac{1}{\lambda_i^{\mathcal{S}}} \quad (62)$$

where $\lambda_i^{\mathcal{S}}$ is the i^{th} eigenvalue of $[\mathbf{\Pi}_{bl(\mathcal{K})}]_{\mathcal{S}}$.

Proof. As

$$\xi_2(\mathcal{S}) = \|\mathbf{R}_{\mathcal{S}}\|_F^2 = \|[\mathbf{U}]_{\mathcal{N},\mathcal{K}}[\mathbf{U}]_{\mathcal{S},\mathcal{K}}^\dagger\|_F^2 = \|[\mathbf{U}]_{\mathcal{S},\mathcal{K}}^\dagger\|_F^2 \quad (63)$$

$\xi_2(\mathcal{S})$ is the sum of the squares of the singular values of $([\mathbf{U}]_{\mathcal{S},\mathcal{K}})^\dagger$ [27, Corollary 2.4.3]. The pseudoinverse maps the singular values of $[\mathbf{U}]_{\mathcal{S},\mathcal{K}}$ onto the singular values of $([\mathbf{U}]_{\mathcal{S},\mathcal{K}})^\dagger$ in the following way [27, Section 5.5.2]:

$$\sigma_i(([\mathbf{U}]_{\mathcal{S},\mathcal{K}})^\dagger) = \begin{cases} 0 & \text{if } \sigma_i([\mathbf{U}]_{\mathcal{S},\mathcal{K}}) = 0 \\ \sigma_i([\mathbf{U}]_{\mathcal{S},\mathcal{K}})^{-1} & \text{otherwise} \end{cases} \quad (64)$$

and the squares of the singular values of $[\mathbf{U}]_{\mathcal{S},\mathcal{K}}$ are λ_i [27, Eq. (8.6.1)]. As $[\mathbf{U}]_{\mathcal{S},\mathcal{K}}[\mathbf{U}]_{\mathcal{S},\mathcal{K}}^T = [\mathbf{\Pi}_{bl(\mathcal{K})}]_{\mathcal{S}}$, summing the singular values gives the result. \square

Lemma 5.

$$\text{rank}([\mathbf{\Pi}_{bl(\mathcal{K})}]_{\mathcal{S}}) = \text{rank}([\mathbf{U}]_{\mathcal{S},\mathcal{K}}) \leq k.$$

Proof. Remember that $[\mathbf{\Pi}_{bl(\mathcal{K})}]_{\mathcal{S}} = [\mathbf{U}]_{\mathcal{S},\mathcal{K}}[\mathbf{U}]_{\mathcal{S},\mathcal{K}}^T$.

The equality: The number of strictly positive singular values of a matrix is its rank [27, Corollary 2.4.6] and both $[\mathbf{\Pi}_{bl(\mathcal{K})}]_{\mathcal{S}} = [\mathbf{U}]_{\mathcal{S},\mathcal{K}}[\mathbf{U}]_{\mathcal{S},\mathcal{K}}^T$ and $[\mathbf{U}]_{\mathcal{S},\mathcal{K}}$ have the same number of strictly positive singular values [27, Eq. (8.6.2)].

The inequality: $[\mathbf{U}]_{\mathcal{S},\mathcal{K}}$ has k columns and so column rank $([\mathbf{U}]_{\mathcal{S},\mathcal{K}}) \leq k$ and rank equals column rank. \square

We can now prove the overall result:

Lemma 6. For LS, $\Delta_1 < 0$ if and only if $\Delta_2 > 0$.

Proof. As $\Delta_1 \in \{0, 1\}$ (Lemma 3), we instead prove that $\Delta_1 = 0$ if and only if $\Delta_2 \leq 0$.

Write the eigenvalues of $[\mathbf{\Pi}_{bl(\mathcal{K})}]_{\mathcal{S}}$ as $\lambda_1, \dots, \lambda_n$ and the eigenvalues of $[\mathbf{\Pi}_{bl(\mathcal{K})}]_{\mathcal{S} \setminus \{v\}}$ as μ_1, \dots, μ_{n+1} . As $[\mathbf{\Pi}_{bl(\mathcal{K})}]_{\mathcal{S} \setminus \{v\}}$ is a principal submatrix of $[\mathbf{\Pi}_{bl(\mathcal{K})}]_{\mathcal{S}}$, by Cauchy's Interlacing Theorem [36, p. 59],

$$0 \leq \mu_1 \leq \lambda_1 \leq \dots \leq \lambda_n \leq \mu_{n+1} \leq 1 \quad (65)$$

where the outer bounds come from the fact that both matrices are principal submatrices of $\mathbf{\Pi}_{bl(\mathcal{K})}$, an orthogonal projection matrix.

1) $\Delta_1 = 0 \implies \Delta_2 \leq 0$: $\Delta_1 = 0$ implies $\text{rank}([\mathbf{U}]_{\mathcal{S},\mathcal{K}}) = \text{rank}([\mathbf{U}]_{\mathcal{S} \setminus \{v\},\mathcal{K}})$, so $\text{rank}([\mathbf{\Pi}_{bl(\mathcal{K})}]_{\mathcal{S}}) = \text{rank}([\mathbf{\Pi}_{bl(\mathcal{K})}]_{\mathcal{S} \setminus \{v\}})$. As the rank is unchanged, $[\mathbf{\Pi}_{bl(\mathcal{K})}]_{\mathcal{S}}$ has one more zero-eigenvalue than $[\mathbf{\Pi}_{bl(\mathcal{K})}]_{\mathcal{S} \setminus \{v\}}$. This means:

$$\mu_1 = 0 \quad (66)$$

$$\lambda_i = 0 \iff \mu_{i+1} = 0 \quad (67)$$

By Cauchy's Interlacing Theorem, $\lambda_i \leq \mu_{i+1}$ and so

$$\frac{1}{\lambda_i} \geq \frac{1}{\mu_{i+1}} \text{ if } \lambda_i \neq 0 \text{ and } \mu_{i+1} \neq 0. \quad (68)$$

Therefore

$$\sum_{\lambda_i^{\mathcal{S}} \neq 0} \frac{1}{\lambda_i^{\mathcal{S}}} \geq \sum_{\mu_i^{\mathcal{S}} \neq 0} \frac{1}{\mu_i^{\mathcal{S}}} \quad (69)$$

as we have the same number of non-zero terms in each of these terms by (66) and (67), and the inequality is proved by summing over the non-zero terms using (68). Equation (69) is exactly

$$\xi_2(\mathcal{S} \setminus \{v\}) \geq \xi_2(\mathcal{S}). \quad (70)$$

Rearranging gives $\Delta_2 \leq 0$.

2) $\Delta_1 = 0 \iff \Delta_2 \leq 0$: We prove the equivalent statement

$$\Delta_1 \neq 0 \implies \Delta_2 > 0. \quad (71)$$

By Lemma 3, if $\Delta_1 \neq 0$ then $\Delta_1 = -1$. This means that $\text{rank}([\mathbf{U}]_{\mathcal{S},\mathcal{K}}) - 1 = \text{rank}([\mathbf{U}]_{\mathcal{S} \setminus \{v\},\mathcal{K}})$, therefore $[\mathbf{\Pi}_{bl(\mathcal{K})}]_{\mathcal{S}}$ has one more non-zero eigenvalue than $[\mathbf{\Pi}_{bl(\mathcal{K})}]_{\mathcal{S} \setminus \{v\}}$. This means:

$$\mu_{n+1} > 0 \quad (72)$$

$$\lambda_i \neq 0 \iff \mu_i \neq 0 \quad (73)$$

By Cauchy's interlacing theorem, $\lambda_i \geq \mu_i$ and so

$$\frac{1}{\lambda_i} \leq \frac{1}{\mu_i} \text{ if } \lambda_i \neq 0 \text{ and } \mu_i \neq 0. \quad (74)$$

Let I be the number of zero eigenvalues of $[\mathbf{\Pi}_{bl(\mathcal{K})}]_{\mathcal{S}}$. Then

$$\sum_{I \leq i \leq n} \frac{1}{\lambda_i^{\mathcal{S}}} \leq \sum_{I \leq i \leq n} \frac{1}{\mu_i^{\mathcal{S}}} < \sum_{I \leq i \leq n+1} \frac{1}{\mu_i^{\mathcal{S}}}. \quad (75)$$

With the left inequality by matching terms via (73) and then summing over (74), and the right inequality because (72) means $\frac{1}{\mu_{n+1}^{\mathcal{S}}} > 0$. We then note the left and the right terms in this equality say:

$$\sum_{\lambda_i^{\mathcal{S}} \neq 0} \frac{1}{\lambda_i^{\mathcal{S}}} < \sum_{\mu_i^{\mathcal{S}} \neq 0} \frac{1}{\mu_i^{\mathcal{S}}} \quad (76)$$

or equivalently,

$$\xi_2(\mathcal{S} \setminus \{v\}) < \xi_2(\mathcal{S}). \quad (77)$$

Rearranging gives $\Delta_2 > 0$. \square

APPENDIX C PROOF OF THEOREM 1

Proof. $\mathcal{S} \setminus \mathcal{T}$ is better than \mathcal{S} if and only if $\text{MSE}_{\mathcal{S} \setminus \mathcal{T}} < \text{MSE}_{\mathcal{S}}$. By (21) this happens if and only if

$$\Delta_1(\mathcal{S}, \mathcal{T}) + \sigma^2 \cdot \Delta_2(\mathcal{S}, \mathcal{T}) > 0. \quad (78)$$

By substituting in $\sigma^2 = \frac{k}{N \cdot \text{SNR}}$ and multiplying both sides by SNR (which does not change the direction of the inequality, as $\text{SNR} > 0$), $\mathcal{S} \setminus \mathcal{T}$ is better than \mathcal{S} if and only if

$$\frac{k}{N} \Delta_2(\mathcal{S}, \mathcal{T}) > -\Delta_1(\mathcal{S}, \mathcal{T}) \cdot \text{SNR}. \quad (79)$$

We consider the conditions of (23):

(23a): $\Delta_1(\mathcal{S}, \mathcal{T}) < 0$

We can divide both sides of (79) by $-\Delta_1(\mathcal{S}, \mathcal{T})$ without changing the inequality, so (79) holds if and only if

$$\frac{k}{N} \frac{\Delta_2(\mathcal{S}, \mathcal{T})}{-\Delta_1(\mathcal{S}, \mathcal{T})} > \text{SNR}. \quad (80)$$

(23b): $\Delta_1(\mathcal{S}, \mathcal{T}) > 0$

Dividing both sides of (79) by $-\Delta_1(\mathcal{S}, \mathcal{T})$ flips the inequality, so (79) holds if and only if

$$\frac{k}{N} \frac{\Delta_2(\mathcal{S}, \mathcal{T})}{-\Delta_1(\mathcal{S}, \mathcal{T})} < \text{SNR}. \quad (81)$$

(23c): $\Delta_1(\mathcal{S}, \mathcal{T}) = 0$

$-\Delta_1(\mathcal{S}, \mathcal{T}) \cdot \text{SNR} = 0$ so (79) holds if and only if $\frac{k}{N} \Delta_2(\mathcal{S}, \mathcal{T}) > 0$, if and only if

$$\Delta_2(\mathcal{S}, \mathcal{T}) > 0. \quad (82)$$

□

APPENDIX D

PROOF OF COROLLARY 1.1

Proof. For brevity, we fix \mathcal{S} and v and write $\Delta_1 = \Delta_1(\mathcal{S}, v)$ and $\Delta_2 = \Delta_2(\mathcal{S}, v)$.

Rearranging (21) gives us that $\mathcal{S} \setminus \{v\}$ is better than \mathcal{S} if and only if

$$\Delta_1 + \sigma^2 \cdot \Delta_2 > 0 \quad (83)$$

or equivalently if and only if

$$\Delta_1 > -\sigma^2 \cdot \Delta_2. \quad (84)$$

By definition, $\sigma^2 = \frac{k}{N \cdot \text{SNR}}$, so this condition is equivalent to

$$\Delta_1 > -\frac{k}{N \cdot \text{SNR}} \Delta_2 \quad (85)$$

and as SNR is strictly positive, this is equivalent to

$$\text{SNR} \cdot \Delta_1 > -\frac{k}{N} \Delta_2. \quad (86)$$

We can now use the major lemmas from the previous appendices. By Lemma 3, we have two possible values of $\Delta_1(\mathcal{S}, v)$:

$\Delta_1 = 0$:

Lemma 6 means $\Delta_2 < 0$, so

$$\Delta_1 + \sigma^2 \cdot \Delta_2 = \sigma^2 \cdot \Delta_2 < 0 \quad (87)$$

and so $\mathcal{S} \setminus \{v\}$ is not better than \mathcal{S} .

$\Delta_1 = -1$:

Eq. (86) simplifies to:

$$-\text{SNR} > -\frac{k}{N} \Delta_2 \quad (88)$$

which is equivalent to

$$\text{SNR} < \frac{k}{N} \Delta_2. \quad (89)$$

On the one hand, v improves \mathcal{S} implies $\Delta_1 = -1$, which implies (89). On the other hand, (89) implies $\Delta_2 > 0$ which in turn implies $\Delta_1 = -1$, which means (89) implies (86), which implies $\mathcal{S} \setminus \{v\}$ is better than \mathcal{S} .

Note that the right-hand side of (89) is $\tau(\mathcal{S}, v)$; this completes the proof. □

APPENDIX E

PROOF OF PROPOSITION 1

We reframe the Proposition to the following equivalent statement:

Consider any sequence of vertices v_1, \dots, v_N with no repeated vertices, and let $\mathcal{S}_i = \{v_1, \dots, v_i\}$. Then there are exactly k indices I_1, \dots, I_k such that under LS reconstruction of a noisy k -bandlimited signal,

$$\forall 1 \leq j \leq k : \tau(\mathcal{S}_{I_j}, v_{I_j}) > 0 \quad (90)$$

and so for some $\text{SNR} > 0$, $\mathcal{S}_{I_j} \setminus \{v_{I_j}\}$ is better than \mathcal{S}_{I_j} .

Proof. By Lemma 3 in Appendix D:

$$\xi_1(\mathcal{S}_i) = k - \text{rank}([\mathbf{U}]_{\mathcal{S}_i, \mathcal{K}}), \quad (91)$$

$$\Delta_1 \in \{0, 1\} \quad (92)$$

and as $\text{rank}([\mathbf{U}]_{\mathcal{N}, \mathcal{K}}) = k$, $\xi_1(\mathcal{S}_N) = 0$. As $\xi_1(\mathcal{S}_0) = k$, we must have exactly k indices for which $\Delta_1(\mathcal{S}_i, v_i) = -1$, and by Lemma 6 in Appendix D we have exactly k indices for which $\Delta_2(\mathcal{S}_i, v_i) > 0$. As $\tau(\mathcal{S}_i, v_i) = \frac{k}{N} \Delta_2(\mathcal{S}_i, v_i)$, we're done. □

APPENDIX F

PROOFS FOR LS RECONSTRUCTION WITH BANDLIMITED NOISE

A. Proof of Lemma 1

Proof. By Appendix B, Lemma 3, under LS reconstruction,

$$\xi_1(\mathcal{S}) = k - \text{rank}([\mathbf{U}]_{\mathcal{S}, \mathcal{K}}). \quad (93)$$

Assuming LS reconstruction,

$$\xi_2(\mathcal{S}) = \|[\mathbf{U}]_{\mathcal{N}, \mathcal{K}} [\mathbf{U}]_{\mathcal{S}, \mathcal{K}}^+ [\mathbf{U}]_{\mathcal{S}, \mathcal{K}}\|_F^2 \quad (94)$$

$$= \|[\mathbf{U}]_{\mathcal{S}, \mathcal{K}}^+ [\mathbf{U}]_{\mathcal{S}, \mathcal{K}}\|_F^2. \quad (95)$$

As $\mathbf{A}^+ \mathbf{A}$ is an orthogonal projection matrix, its eigenvalues are 0 or 1. Therefore

$$\|[\mathbf{U}]_{\mathcal{S}, \mathcal{K}}^+ [\mathbf{U}]_{\mathcal{S}, \mathcal{K}}\|_F^2 = \text{rank}([\mathbf{U}]_{\mathcal{S}, \mathcal{K}}). \quad (96)$$

Add this times σ^2 to $\xi_1(\mathcal{S})$ to get the result. □

B. Proof of Corollary 2.1

Proof. As sample size increases, $\text{rank}([\mathbf{U}]_{\mathcal{S},\mathcal{K}})$ is increasing. If $\text{SNR} < 1$, then $1 < \sigma^2$ and the MSE increases with sample size by Lemma 1. \square

C. Proof of Corollary 2.2

Proof. Under a noiseless-optimal sampling scheme, after sampling k vertices we have perfect reconstruction of any clean k -bandlimited signal, and so $\xi_1(\mathcal{S}_k) = k - \text{rank}([\mathbf{U}]_{\mathcal{S}_k,\mathcal{K}}) = 0$.

Let $m \leq k$. As $[\mathbf{U}]_{\mathcal{S}_k,\mathcal{K}}$ is of full rank, for any $\mathcal{S}_m \subseteq \mathcal{S}_k$, $[\mathbf{U}]_{\mathcal{S}_m,\mathcal{K}}$ must also be full rank. Therefore

$$\text{MSE}_{\mathcal{S}_m} - \text{MSE}_{\mathcal{S}_m \setminus \{v\}} = (\sigma^2 - 1)(m - (m - 1)) \quad (97)$$

$$= \sigma^2 - 1 \quad (98)$$

so $\mathcal{S}_m \setminus \{v\}$ is better than $\mathcal{S} \iff \sigma^2 > 1 \iff \text{SNR} < 1$.

In the case where $m > k$:

$$|\mathcal{S}| \geq k \implies \text{rank}([\mathbf{U}]_{\mathcal{S},\mathcal{K}}) = k \quad (99)$$

$$\implies \text{MSE}_{\mathcal{S}} = \sigma^2 k. \quad (100)$$

which is constant as sample size increases. \square

APPENDIX G PROOF OF THEOREM 2

A. Proof of (27)

We first show that if $m \leq k$ then

$$\forall m \leq k : \forall v \in \mathcal{S}_m : \Delta_1(\mathcal{S}_m, v) = -1. \quad (101)$$

Proof. By Appendix D, Lemma 3, the noiseless error

$$\xi_1(\mathcal{S}) = k - \text{rank}([\mathbf{U}]_{\mathcal{S},\mathcal{K}}) \quad (102)$$

must be 0, as we can perfectly reconstruct any k -bandlimited signal. Therefore, $\text{rank}([\mathbf{U}]_{\mathcal{S},\mathcal{K}}) = k$.

$[\mathbf{U}]_{\mathcal{S},\mathcal{K}}$ is a $k \times k$ matrix of full rank, so its rows must be linearly independent. Any subset of linearly independent rows is linearly independent, so for any non-empty $\mathcal{R} \subset \mathcal{S}$, $[\mathbf{U}]_{\mathcal{R},\mathcal{K}}$ has linearly independent rows.

Greedy schemes pick increasing sample sets: that is, if asked to pick a vertex sample set \mathcal{S}_m of size m for $m < k$ and a sample set \mathcal{S} of size k , $\mathcal{S}_m \subset \mathcal{S}$. Therefore for any sample set \mathcal{S}_m of size $m \leq k$ picked by the scheme, $[\mathbf{U}]_{\mathcal{S}_m,\mathcal{K}}$ has independent rows.

If $[\mathbf{U}]_{\mathcal{S}_m,\mathcal{K}}$ has independent rows, then removal of any row (corresponding to removing any vertex) reduces its rank by 1; which is (101). \square

We now show that for $m \leq k$,

$$\forall m \leq k : \forall v \in \mathcal{S}_m : \Delta_2(\mathcal{S}_m, v) \geq 1. \quad (103)$$

Proof. By the previous section, we know that $[\mathbf{U}]_{\mathcal{R},\mathcal{K}}$ is full rank for $\mathcal{R} \subseteq \mathcal{S}_m$, so $[\mathbf{U}]_{\mathcal{R},\mathcal{K}}[\mathbf{U}]_{\mathcal{R},\mathcal{K}}^T = [\mathbf{\Pi}_{bl(\mathcal{K})}]_{\mathcal{R}}$ is

invertible. By Appendix B, (63), $\xi_2(\mathcal{S}_m) = \text{tr}([\mathbf{\Pi}_{bl(\mathcal{K})}]_{\mathcal{S}_m}^{-1})$. We have

$$\xi_2(\mathcal{S}_m) \quad (104)$$

$$= \text{tr}([\mathbf{\Pi}_{bl(\mathcal{K})}]_{\mathcal{S}_m}^{-1}) \quad (105)$$

$$= [\mathbf{\Pi}_{bl(\mathcal{K})}]_{\mathcal{S}_m \setminus \{v\}}^{-1} + \text{tr}([\mathbf{\Pi}_{bl(\mathcal{K})}]_{\mathcal{S}_m}^{-1}) \quad (106)$$

$$\geq [\mathbf{\Pi}_{bl(\mathcal{K})}]_{\{v\}}^{-1} + \text{tr}([\mathbf{\Pi}_{bl(\mathcal{K})}]_{\mathcal{S}_m \setminus \{v\}}^{-1}) \quad (107)$$

$$= \frac{1}{[\mathbf{\Pi}_{bl(\mathcal{K})}]_{\{v\}}} + \xi_2(\mathcal{S}_m \setminus \{v\}) \quad (108)$$

$$\geq 1 + \xi_2(\mathcal{S}_m \setminus \{v\}) \quad (109)$$

where the inequality in (107) is by [20, Eq. 5], and the final inequality is because the diagonal elements of $\mathbf{\Pi}_{bl(\mathcal{K})}$ are bounded above by its maximum eigenvalue, which is 1 as $\mathbf{\Pi}_{bl(\mathcal{K})}$ is a projection. Therefore, for all $v \in \mathcal{S}_m$,

$$\Delta_2(\mathcal{S}_m, v) = \xi_2(\mathcal{S}_m) - \xi_2(\mathcal{S}_m \setminus \{v\}) \geq 1. \quad (110)$$

\square

Finally as $\tau(\mathcal{S}_m, v) = \frac{k}{N} \Delta_2(\mathcal{S}_m, v)$,

$$\forall m \leq k : \forall v \in \mathcal{S}_m : \tau(\mathcal{S}_m, v) \geq \frac{k}{N}. \quad (111)$$

B. Proof of (28)

Proof. As $[\mathbf{U}]_{\mathcal{S}_k,\mathcal{K}}$ has k independent rows, it is of rank k . Adding further rows cannot decrease its rank, so for $m' > k$, $\text{rank}([\mathbf{U}]_{\mathcal{S}_{m'},\mathcal{K}}) \geq k$. As $[\mathbf{U}]_{\mathcal{N},\mathcal{K}}$ is of rank k , $\text{rank}([\mathbf{U}]_{\mathcal{S}_{m'},\mathcal{K}}) \leq k$. This means for all sample sizes $m' > k$, $\text{rank}([\mathbf{U}]_{\mathcal{S}_{m'},\mathcal{K}}) = k$. This says that further additions of rows do not change rank; that is:

$$\forall m' > k : \forall v \in \mathcal{S}_{m'} \setminus \mathcal{S}_k : \Delta_1(\mathcal{S}_{m'}, v) = 0 \quad (112)$$

Then, by Appendix D, Lemma 6,

$$\forall m' > k : \forall v \in \mathcal{S}_{m'} \setminus \mathcal{S}_k : \Delta_2(\mathcal{S}_{m'}, v) \leq 0 \quad (113)$$

and, like for (27, as $\tau(\mathcal{S}_m, v) = \frac{k}{N} \Delta_2(\mathcal{S}_m, v)$ and $\frac{k}{N} > 0$,

$$\forall m' > k : \forall v \in \mathcal{S}_{m'} \setminus \mathcal{S}_k : \tau(\mathcal{S}_{m'}, v) \leq 0. \quad (114)$$

\square

APPENDIX H PROOF OF REMARK 4

A-Optimality

A-optimality depends on the existence of the inverse of $[\mathbf{\Pi}_{bl(\mathcal{K})}]_{\mathcal{S}}$ existing, which requires it to be of full rank. By Appendix D, Lemma 5, if an A-optimal scheme picks a set \mathcal{S} of size k , then $\text{rank}([\mathbf{U}]_{\mathcal{S},\mathcal{K}}) = k$. Therefore, \mathcal{S} is a uniqueness set [16] and can perfectly reconstruct any k -bandlimited signal.

D- and E-optimality

We show that for sample sizes less than k we can always pick a row which keeps $[\mathbf{\Pi}_{bl(\mathcal{K})}]_{\mathcal{S}}$ full rank (of rank $|\mathcal{S}|$), and that D- and E-optimal schemes do so.

By Appendix D, Lemma 5, $\text{rank}([\mathbf{\Pi}_{bl(\mathcal{K})}]_{\mathcal{S}}) = \text{rank}([\mathbf{U}]_{\mathcal{S},\mathcal{K}})$, so we only need to ensure $\text{rank}([\mathbf{U}]_{\mathcal{S},\mathcal{K}}) = |\mathcal{S}|$.

We proceed by induction: given \mathcal{S}_1 with $|\mathcal{S}_1| = 1$, $\text{rank}([\mathbf{U}]_{\mathcal{S}_1,\mathcal{K}}) = 1$. Assume that for \mathcal{S}_i with $|\mathcal{S}_i| = i < k$, $\text{rank}([\mathbf{U}]_{\mathcal{S}_i,\mathcal{K}}) = i$. As $\text{rank}([\mathbf{U}]_{\mathcal{N},\mathcal{K}}) = k$ and $i < k$, we can find a row to add to $[\mathbf{U}]_{\mathcal{S}_i,\mathcal{K}}$ which will increase its rank (else all other rows would lie in the i -dimensional space spanned by the rows of $[\mathbf{U}]_{\mathcal{S}_i,\mathcal{K}}$, which would imply $\text{rank}([\mathbf{U}]_{\mathcal{N},\mathcal{K}}) = i$, which is a contradiction as $i < k$). Adding the vertex which corresponds to the row to \mathcal{S}_i gives \mathcal{S}_{i+1} with $\text{rank}([\mathbf{U}]_{\mathcal{S}_{i+1},\mathcal{K}}) = i + 1$.

We have shown that we can greedily choose to keep $\text{rank}([\mathbf{U}]_{\mathcal{S},\mathcal{K}}) = |\mathcal{S}|$. We now show that D- and E-optimal schemes do so. The eigenvalues of $[\mathbf{\Pi}_{bl(\mathcal{K})}]_{\mathcal{S}}$ are non-negative (see Appendix D, Eq. (65)), so any invertible $[\mathbf{\Pi}_{bl(\mathcal{K})}]_{\mathcal{S}}$ will have a strictly positive determinant and minimum eigenvalue, which are preferable under the D- and E- optimality criterion respectively to a non-invertible $[\mathbf{\Pi}_{bl(\mathcal{K})}]_{\mathcal{S}}$, which has a determinant and minimum eigenvalue of 0. Therefore, greedy D- and E- optimal sampling schemes will make sure $[\mathbf{\Pi}_{bl(\mathcal{K})}]_{\mathcal{S}}$ is invertible, and thus keep $\text{rank}([\mathbf{U}]_{\mathcal{S},\mathcal{K}}) = |\mathcal{S}|$ for $|\mathcal{S}| \leq k$. Therefore when D- and E- optimal schemes pick a set \mathcal{S} of size k , $\text{rank}([\mathbf{U}]_{\mathcal{S},\mathcal{K}}) = k$. Therefore, \mathcal{S} is a uniqueness set [16] and can perfectly reconstruct any k -bandlimited signal.

APPENDIX I PROOF OF COROLLARY 2.3

We first simplify $\xi_1(\mathcal{S})$:

$$[\mathbf{U}]_{\mathcal{N},\mathcal{K}} - \mathbf{R}_{\mathcal{S}}[\mathbf{U}]_{\mathcal{S},\mathcal{K}} \quad (115)$$

$$= \left(\mathbf{I} - (\mathbf{\Pi}_{\mathcal{S}} + \mu\mathbf{L})^{-1} \mathbf{\Pi}_{\mathcal{S}} \right) [\mathbf{U}]_{\mathcal{N},\mathcal{K}} \quad (116)$$

$$= (\mathbf{\Pi}_{\mathcal{S}} + \mu\mathbf{L})^{-1} \mu\mathbf{L}[\mathbf{U}]_{\mathcal{N},\mathcal{K}} \quad (117)$$

$$= (\mathbf{\Pi}_{\mathcal{S}} + \mu\mathbf{L})^{-1} [\mathbf{U}]_{\mathcal{N},\mathcal{K}} \mathbf{\Lambda}_k \quad (118)$$

where $\mathbf{\Lambda}_k$ is a $k \times k$ diagonal matrix with the corresponding graph frequencies to $[\mathbf{U}]_{\mathcal{N},\mathcal{K}}$ as its diagonal. Write u_i for the i^{th} column of $[\mathbf{U}]_{\mathcal{N},\mathcal{K}}$, so \mathbf{u}_i is an eigenvector of \mathbf{L} .

$$\begin{aligned} \xi_1(\mathcal{S}) &= \|[\mathbf{U}]_{\mathcal{N},\mathcal{K}} - \mathbf{R}_{\mathcal{S}}[\mathbf{U}]_{\mathcal{S},\mathcal{K}}\|_F^2 \\ &= \sum_{i=2}^k \mu\lambda_i \mathbf{u}_i^T (\mathbf{\Pi}_{\mathcal{S}} + \mu\mathbf{L})^{-2} \mathbf{u}_i \end{aligned} \quad (119)$$

Note that the condition is equivalent to the following:

$$[\mathbf{U}]_{\mathcal{S}^c, \{2, \dots, k\}} = \mathbf{0} \iff \forall i \in [2, k] : \mathbf{\Pi}_{\mathcal{S}} \mathbf{u}_i = \mathbf{u}_i \quad (120)$$

that is, the projection is idempotent on each of the $k - 1$ non-constant eigenvectors. We consider the cases where this is and is not true and correlate them to cases in Theorem 1.

A. The projection is idempotent

as $\mathbf{\Pi}_{\mathcal{S}} \mathbf{u}_i = \mathbf{u}_i$,

$$(\mathbf{\Pi}_{\mathcal{S}} + \mu\mathbf{L}) \mathbf{u}_i = (1 + \mu\lambda_i) \mathbf{u}_i \quad (121)$$

therefore \mathbf{u}_i is an eigenvector of $(\mathbf{\Pi}_{\mathcal{S}} + \mu\mathbf{L})$ with eigenvalue $1 + \mu\lambda_i$ and

$$\mathbf{u}_i^T (\mathbf{\Pi}_{\mathcal{S}} + \mu\mathbf{L})^{-2} \mathbf{u}_i = (1 + \mu\lambda_i)^{-2}. \quad (122)$$

By Lemma 7, in this case $\xi_1(\mathcal{S}) = \xi_1(\mathcal{N})$, i.e. that $\Delta_1(\mathcal{N}, \mathcal{S}^c) = 0$. This corresponds to condition (23c), and gives us condition (32b) in our Corollary.

B. The projection is not idempotent

Applying Cauchy-Schwartz to $\mathbf{x} = (\mathbf{\Pi}_{\mathcal{S}} + \mu\mathbf{L})^{-1} \mathbf{u}_i$ and $\mathbf{y} = (\mathbf{\Pi}_{\mathcal{S}} + \mu\mathbf{L}) \mathbf{u}_i$ gives, as $\mathbf{u}_i^T \mathbf{u}_i = 1$,

$$1 \leq \mathbf{u}_i^T (\mathbf{\Pi}_{\mathcal{S}} + \mu\mathbf{L})^{-2} \mathbf{u}_i \mathbf{u}_i^T (\mathbf{\Pi}_{\mathcal{S}} + \mu\mathbf{L})^2 \mathbf{u}_i. \quad (123)$$

We note that

$$\|\mathbf{\Pi}_{\mathcal{S}} \mathbf{u}_i\|_2^2 = \sum_{j \in \mathcal{S}} (\mathbf{u}_i)_j^2 < \sum_{j=1}^N (\mathbf{u}_i)_j^2 = \|\mathbf{u}_i\|_2^2 = 1 \quad (124)$$

with a strict inequality as some component of \mathbf{u}_i in \mathcal{S}^c is nonzero, by the assumption. Therefore

$$\begin{aligned} \mathbf{u}_i^T (\mathbf{\Pi}_{\mathcal{S}} + \mu\mathbf{L})^2 \mathbf{u}_i &= (\mu\lambda_i)^2 + (1 + 2\mu\lambda_i) \|\mathbf{\Pi}_{\mathcal{S}} \mathbf{u}_i\|_2^2 \\ &\leq (1 + \mu\lambda_i)^2. \end{aligned} \quad (125)$$

Therefore, by Lemma 7 and (119),

$$\xi_1(\mathcal{S}) > \xi_1(\mathcal{N}) \quad (127)$$

so $\Delta_1(\mathcal{N}, \mathcal{S}^c) < 0$

C. Simplifying Theorem 1

We see that the projection is idempotent on $(\mathbf{u}_i)_{i=2}^k$ implies $\Delta_1(\mathcal{N}, \mathcal{S}^c) = 0$, and the projection is not idempotent implies $\Delta_1(\mathcal{N}, \mathcal{S}^c) < 0$. As the projection must either be idempotent or not idempotent, these implications must be ‘if and only if’ statements. We therefore rule out (23b) in Theorem 1.

APPENDIX J PROOF OF THEOREM 3

We start by calculating $\xi_i(\mathcal{N})$.

Lemma 7. Under GLR reconstruction with parameter μ ,

$$\xi_1(\mathcal{N}) = \sum_{i=1}^k \left(1 - \frac{1}{1 + \mu\lambda_i} \right)^2 \quad (128)$$

$$\xi_2(\mathcal{N}) = \sum_{i=1}^N \left(\frac{1}{1 + \mu\lambda_i} \right)^2 \quad (129)$$

Proof. Set $\mathbf{R}_{\mathcal{N}} = (\mathbf{I} + \mu\mathbf{L})^{-1}$ in (13) and (14), noting $[\mathbf{U}]_{\mathcal{N},\mathcal{K}}$ are eigenvectors for $\mathbf{R}_{\mathcal{N}}$. \square

Let \mathcal{S} be any sample set of size m . We show that under our conditions $\Delta_2(\mathcal{S}) > 0$ and then apply Corollary 2.3. To do so, we use the following bounds:

$$\xi_2(\mathcal{S}) \leq B(m) \quad (130)$$

$$\xi_1(\mathcal{S}) \leq k + \xi_2(\mathcal{S}) \quad (131)$$

$$\xi_1(\mathcal{N}) = \sum_{i=1}^k \left(1 - \frac{1}{1 + \mu\lambda_i}\right)^2 \quad (132)$$

$$\xi_2(\mathcal{N}) = \sum_{i=1}^N \left(\frac{1}{1 + \mu\lambda_i}\right)^2 \quad (133)$$

These are proven in Appendix K Lemma 8, Appendix L Lemma 9, and Lemma 7. We therefore see that, as $\Delta_i(\mathcal{N}, \mathcal{S}^c) = \xi_i(\mathcal{N}) - \xi_i(\mathcal{S})$,

$$\Delta_2(\mathcal{N}, \mathcal{S}^c) \geq \sum_{i=1}^N \left(\frac{1}{1 + \mu\lambda_i}\right)^2 - B(m) \quad (134)$$

$$\Delta_1(\mathcal{N}, \mathcal{S}^c) \geq \sum_{i=1}^N \left(1 - \frac{1}{1 + \mu\lambda_i}\right)^2 - (k + B(m)) \quad (135)$$

We now show that $\Delta_2 > 0$. We have that $r > 0$ so $B(m) > 0$ and by assumption $B(m) < N$. Therefore $\mu_{ub}(m) > 0$ and is real and it therefore possible to pick $0 < \mu < \mu_{ub}(m)$. By assumption $0 < \mu < \mu_{ub}(m)$, so by Jensen's Inequality,

$$\sum_{i=1}^N \left(\frac{1}{1 + \mu\lambda_i}\right)^2 \geq \frac{N}{\left(1 + \mu \frac{\text{tr}(\mathbf{L})}{N}\right)^2} \quad (136)$$

$$> \frac{N}{\left(1 + \mu_{ub} \frac{\text{tr}(\mathbf{L})}{N}\right)^2} \quad (137)$$

$$= B(m) \quad (138)$$

And therefore by (134), $\Delta_2(\mathcal{N}, \mathcal{S}^c) > 0$.

We now apply Corollary 2.3. We case-split on whether $\mathbf{\Pi}_{\mathcal{S}^c} [\mathbf{U}]_{\mathcal{N}, \{2, \dots, k\}}$ is or is not $\mathbf{0}$, and show \mathcal{S} is better than \mathcal{N} in both cases.

1) (32a) - is not 0: We assume $\mathbf{\Pi}_{\mathcal{S}^c} [\mathbf{U}]_{\mathcal{N}, \{2, \dots, k\}} \neq \mathbf{0}$. By (134) and (135),

$$\tau(\mathcal{N}, \mathcal{S}^c) = \frac{k}{N} \cdot \frac{\Delta_2(\mathcal{N}, \mathcal{S}^c)}{-\Delta_1(\mathcal{N}, \mathcal{S}^c)} \geq \tau_{lb}(\mu, m) > \text{SNR} \quad (139)$$

where the last inequality is by our assumption. Therefore Corollary 2.3 (32a) holds and \mathcal{S} is better than \mathcal{N} .

2) (32b) - is 0: We assume $\mathbf{\Pi}_{\mathcal{S}^c} [\mathbf{U}]_{\mathcal{N}, \{2, \dots, k\}} = \mathbf{0}$. We have that $\Delta_2(\mathcal{N}, \mathcal{S}^c) > 0$, so Corollary 2.3 (32b) holds and \mathcal{S} is better than \mathcal{N} .

Therefore \mathcal{S} is better than \mathcal{N} regardless of whether $\mathbf{\Pi}_{\mathcal{S}^c} [\mathbf{U}]_{\mathcal{N}, \{2, \dots, k\}}$ is or is not $\mathbf{0}$ and we are done.

APPENDIX K BOUNDING $\xi_2(\mathcal{S})$ UNDER GLR

In this Appendix, we state and prove the following Lemma:

Lemma 8. Let $\hat{\lambda}, r_i, \rho, r$ and $B(m)$ be defined as in Theorem 3. Then, for any sample set \mathcal{S} of size m , and any $\mu > 0$,

$$\xi_2(\mathcal{S}) \leq B(m). \quad (140)$$

A. Preliminaries and Notation

We assume that \mathbf{L} is the combinatorial Laplacian. We write the eigenvalues of \mathbf{L} as $0 = \lambda_1 \leq \dots \leq \lambda_N$. We note, for any $\mathbf{X} \in \mathbb{R}^{x \times N}$, $\mathbf{Y} \in \mathbb{R}^{N \times y}$,

$$[\mathbf{X}]_{a,N} [\mathbf{Y}]_{N,c} = [\mathbf{X}\mathbf{Y}]_{a,c}.$$

We pick a basis suited to our proof. Let the standard basis for \mathbb{R}^N be $(\mathbf{e}_i)_{i=1}^N$. Let

$$\mathbf{v}_1 = \frac{1}{\sqrt{m}} \sum_{i \in \mathcal{S}} \mathbf{e}_i = \frac{1}{\sqrt{m}} \mathbf{\Pi}_{\mathcal{S}} \mathbf{1}_N. \quad (141)$$

so $\|\mathbf{v}_1\|_2 = 1$. Pick $\{\mathbf{v}_2, \dots, \mathbf{v}_m\}$ so that $(\mathbf{v}_i)_{i=1}^m$ is an orthonormal basis for $(\mathbf{e}_i)_{i \in \mathcal{S}}$. Finally let $(\mathbf{v}_i)_{i=m+1}^N = (\mathbf{e}_i)_{i \in \mathcal{S}^c}$. Now $(\mathbf{v}_i)_{i=1}^N$ is a basis for \mathbb{R}^N .

For the rest of this Appendix, we will write out matrices in this new basis. In our new basis, the top left entry when writing out \mathbf{L}^\dagger is

$$\mathbf{L}_{1,1} = \frac{1}{m} \mathbf{1}_m^T [\mathbf{L}^\dagger]_{\mathcal{S}} \mathbf{1}_m \in \mathbb{R} \quad (142)$$

and our frequently used projection looks like:

$$\mathbf{\Pi}_{\mathcal{S}} = \begin{pmatrix} \mathbf{I} & \mathbf{0} \\ \mathbf{0} & \mathbf{0} \end{pmatrix}.$$

We define the set $\Theta = \{2, \dots, m\}$, and note that

$$\mathbf{\Pi}_{\Theta} = \mathbf{I}_m - \frac{1}{m} \mathbf{1}_{m \times m}. \quad (143)$$

We have $\{1\} \cup \Theta = \mathcal{S}$ and $\{1\} \cup \Theta \cup \mathcal{S}^c = \mathcal{N}$. For a matrix $\mathbf{X} \in \mathbb{R}^{r \times r}$, we write

$$\mathbf{X} + \delta = \mathbf{X} + \delta \mathbf{1}_{r \times r}. \quad (144)$$

Note that for any matrix \mathbf{X} , $\forall \delta$,

$$[\mathbf{X} + \delta]_{\Theta} = [\mathbf{X}]_{\Theta} \quad (145)$$

Finally, we define a useful matrix:

$$\mathbf{P} = \mathbf{I} - \frac{1}{m} [\mathbf{I}]_{\mathcal{N}, \mathcal{S}} \mathbf{1}_{m \times N}.$$

B. Proof Overview

We decompose $\xi_2(\mathcal{S}) = \|\mathbf{R}_{\mathcal{S}}\|_F^2$ row-wise in our new basis (Subsection K-C).

$$\|\mathbf{R}_{\mathcal{S}}\|_F^2 = \|\mathbf{R}_{\mathcal{S}}\|_{\mathcal{N}, \{1\}}^2 + \left\| \mathbf{R}_{\mathcal{S}} \right\|_{\mathcal{N}, \Theta}^2 \quad (146)$$

$$= \frac{N}{m} + \left\| \mathbf{R}_{\mathcal{S}} \right\|_{\mathcal{N}, \Theta}^2 \quad (147)$$

We explicitly write out $[\mathbf{R}_{\mathcal{S}}]_{\mathcal{N}, \Theta}$ (Subsection K-D),

$$[\mathbf{R}_{\mathcal{S}}]_{\mathcal{N}, \Theta} = \mathbf{P}^T \begin{bmatrix} \frac{1}{\mu} \mathbf{L}^\dagger \\ \mu \end{bmatrix}_{\mathcal{N}, \Theta} \begin{bmatrix} \mathbf{I} + \frac{1}{\mu} \mathbf{L}^\dagger \\ \mu \end{bmatrix}_{\Theta}^{-1} \quad (148)$$

$$= \mathbf{P}^T [\mathbf{L}^\dagger]_{\mathcal{N}, \Theta} [\mu \mathbf{I} + \mathbf{L}^\dagger]_{\Theta}^{-1} \quad (149)$$

and use this to remove the dependence on μ in our bound (Subsection K-E):

$$\left\| [\mathbf{R}_{\mathcal{S}}]_{\mathcal{N}, \Theta} \right\|_F^2 \leq \left\| \mathbf{P}^T [\mathbf{L}^\dagger]_{\mathcal{N}, \Theta} [\mathbf{L}^\dagger]_{\Theta}^{-1} \right\|_F^2 \quad (150)$$

We exactly calculate the effects of \mathbf{P}^T on the Frobenius norm (which yields the $\frac{N}{m}$ term in (152))(Subsection K-F):

$$\left\| \mathbf{P}^T [\mathbf{L}^\dagger]_{\mathcal{N},\Theta} [\mathbf{L}^\dagger]_{\Theta}^{-1} \right\|_F^2 \quad (151)$$

$$= \left(\frac{N}{m} \right) \left\| [\mathbf{L}^\dagger]_{\{1\},\Theta} [\mathbf{L}^\dagger]_{\Theta}^{-1} \right\|_F^2 \quad (152)$$

$$+ \left\| [\mathbf{L}^\dagger]_{\mathcal{N},\Theta} [\mathbf{L}^\dagger]_{\Theta}^{-1} \right\|_F^2 \quad (153)$$

As

$$\left\| [\mathbf{L}^\dagger]_{\Theta} [\mathbf{L}^\dagger]_{\Theta}^{-1} \right\|_F^2 = \|\mathbf{I}_{m-1}\|_F^2 = m-1, \quad (154)$$

we get that

$$\xi_2(\mathcal{S}) = \left(\frac{N}{m} + m - 1 \right) + \text{error} \quad (155)$$

where the error term is quantified in (152) and (153).

Finally, we bound (152) and (153) using variants of the Kantorovich Inequality. We have that [37, Eq. 20-23] gives (Subsection K-G)

$$\left\| [\mathbf{L}^\dagger]_{\{1\},\Theta} [\mathbf{L}^\dagger]_{\Theta}^{-1} \right\|_F^2 \leq (r-1) \quad (156)$$

We use another variant to show that (Subsection K-H)

$$\left\| [\mathbf{L}^\dagger]_{\mathcal{N},\Theta} [\mathbf{L}^\dagger]_{\Theta}^{-1} \right\|_F^2 \leq \rho(m-1). \quad (157)$$

Combine these bounds with (150 - 153) to prove the proposition.

C. Row Decomposition

As $(\mathbf{v}_i)_{i=1}^m$ are orthogonal and span $(\mathbf{e}_i)_{i \in \mathcal{S}}$, and $\mathbf{R}_S \mathbf{1}_m = \mathbf{1}_N$,

$$\|\mathbf{R}_S\|_F^2 = \sum_{i=1}^m \|\mathbf{R}_S \mathbf{v}_i\|_2^2 \quad (158)$$

$$= \sum_{i=1}^m \left\| [\mathbf{R}_S]_{\mathcal{N},\{i\}} \right\|_2^2 \quad (159)$$

$$= \left\| \mathbf{R}_S \frac{1}{\sqrt{m}} \mathbf{1}_m \right\|_2^2 + \left\| [\mathbf{R}_S]_{\mathcal{N},\Theta} \right\|_F^2 \quad (160)$$

$$= \frac{N}{m} + \left\| [\mathbf{R}_S]_{\mathcal{N},\Theta} \right\|_F^2. \quad (161)$$

D. Explicit submatrix computation

We explicitly compute that

$$\begin{aligned} [\mathbf{R}_S]_{\mathcal{N},\Theta} &= (\mathbf{\Pi}_S + \mu \mathbf{L})^{-1} [\mathbf{I}]_{\mathcal{N},\Theta} \\ &= \mathbf{P}^T \begin{bmatrix} \mathbf{I} \\ \mu \mathbf{L}^\dagger \end{bmatrix}_{\mathcal{N},\Theta} \begin{bmatrix} \mathbf{I} + \frac{1}{\mu} \mathbf{L}^\dagger \end{bmatrix}_{\Theta}^{-1} \end{aligned} \quad (162)$$

Proof. We show the equivalent statement,

$$[\mathbf{I}]_{\mathcal{N},\Theta} \begin{bmatrix} \mathbf{I} + \frac{1}{\mu} \mathbf{L}^\dagger \end{bmatrix}_{\Theta} = (\mathbf{\Pi}_S + \mu \mathbf{L}) \mathbf{P}^T \begin{bmatrix} \mathbf{I} \\ \mu \mathbf{L}^\dagger \end{bmatrix}_{\mathcal{N},\Theta}. \quad (163)$$

We have that

$$\mu \mathbf{L} \mathbf{P}^T = \mu \mathbf{L} \quad (164)$$

$$\mathbf{\Pi}_S \mathbf{P}^T = [\mathbf{I}]_{\mathcal{N},\mathcal{S}} \left(\mathbf{I} - \frac{1}{m} \mathbf{1}_{m \times m} \right) [\mathbf{I}]_{\mathcal{S},\mathcal{N}} \quad (165)$$

$$= [\mathbf{I}]_{\mathcal{N},\mathcal{S}} [\mathbf{\Pi}_\Theta]_{\mathcal{S}} [\mathbf{I}]_{\mathcal{S},\mathcal{N}} \quad (166)$$

$$= [\mathbf{I}]_{\mathcal{N},\Theta} [\mathbf{I}]_{\Theta,\mathcal{N}} \quad (167)$$

so

$$\mu \mathbf{L} \mathbf{P}^T \begin{bmatrix} \mathbf{I} \\ \mu \mathbf{L}^\dagger \end{bmatrix}_{\mathcal{N},\Theta} = \mu \mathbf{L} \begin{bmatrix} \mathbf{I} \\ \mu \mathbf{L}^\dagger \end{bmatrix}_{\mathcal{N},\Theta} \quad (168)$$

$$= \mathbf{L} \mathbf{L}^\dagger [\mathbf{I}]_{\mathcal{N},\Theta} \quad (169)$$

$$= \left(\mathbf{I} - \frac{1}{N} \mathbf{1}_{N \times N} \right) [\mathbf{I}]_{\mathcal{N},\Theta} \quad (170)$$

$$= [\mathbf{I}]_{\mathcal{N},\Theta} \quad (171)$$

and

$$\mathbf{\Pi}_S \mathbf{P}^T \begin{bmatrix} \mathbf{I} \\ \mu \mathbf{L}^\dagger \end{bmatrix}_{\mathcal{N},\Theta} = [\mathbf{I}]_{\mathcal{N},\Theta} [\mathbf{I}]_{\Theta,\mathcal{N}} \begin{bmatrix} \mathbf{I} \\ \mu \mathbf{L}^\dagger \end{bmatrix}_{\mathcal{N},\Theta} \quad (172)$$

$$= [\mathbf{I}]_{\mathcal{N},\Theta} \begin{bmatrix} \mathbf{I} \\ \mu \mathbf{L}^\dagger \end{bmatrix}_{\Theta} \quad (173)$$

Sum these two terms for the result. \square

E. Removing the dependency on μ

By multiplying out the constant in 162, we see that

$$[\mathbf{R}_S]_{\mathcal{N},\Theta} = \mathbf{P}^T [\mathbf{L}^\dagger]_{\mathcal{N},\Theta} [\mu \mathbf{I} + \mathbf{L}^\dagger]_{\Theta}^{-1} \quad (174)$$

To prove that

$$\forall \mu > 0 : \|\mathbf{R}_S\|_F^2 \leq \left\| \mathbf{P}^T [\mathbf{L}^\dagger]_{\mathcal{N},\Theta} [\mathbf{L}^\dagger]_{\Theta}^{-1} \right\|_F^2 \quad (175)$$

we show that $\forall \mathbf{h} \in \mathbb{R}^{m-1}$

$$\forall \mu > 0 : \left\| [\mu \mathbf{I} + \mathbf{L}^\dagger]_{\Theta}^{-1} \mathbf{h} \right\|_2^2 \leq \left\| [\mathbf{L}^\dagger]_{\Theta}^{-1} \mathbf{h} \right\|_2^2 \quad (176)$$

then letting \mathbf{h} be each of the rows of $\mathbf{P}^T [\mathbf{L}^\dagger]_{\mathcal{N},\Theta}$ and summing gives (175).

Proof. Write $(\mathbf{w}_i)_{i=1}^{m-1}$ for the orthogonal eigenbasis of $[\mathbf{L}^\dagger]_{\Theta}$, $\lambda_i([\mathbf{L}^\dagger]_{\Theta})$ for its eigenvalues and let $\mathbf{h} = \sum_{i=1}^{m-1} \alpha_i \mathbf{w}_i$. As $[\mathbf{L}^\dagger]_{\Theta} = \left[\mathbf{L}^\dagger + \frac{1}{N\lambda_2} \right]_{\Theta}$ is a principal submatrix of the positive definite matrix $\mathbf{L}^\dagger + \frac{1}{N\lambda_2}$, it is positive definite, and so $\forall i : \lambda_i([\mathbf{L}^\dagger]_{\Theta}) > 0$. Therefore,

$$\left\| [\mu \mathbf{I} + \mathbf{L}^\dagger]_{\Theta}^{-1} \mathbf{h} \right\|_2^2 = \mathbf{h}^T [\mu \mathbf{I} + \mathbf{L}^\dagger]_{\Theta}^{-2} \mathbf{h} \quad (177)$$

$$= \sum_{i=1}^{m-1} \frac{\alpha_i^2}{(\mu + \lambda_i([\mathbf{L}^\dagger]_{\Theta}))^2} \quad (178)$$

$$\leq \sum_{i=1}^{m-1} \frac{\alpha_i^2}{\lambda_i([\mathbf{L}^\dagger]_{\Theta})^2} \quad (179)$$

$$= \left\| [\mathbf{L}^\dagger]_{\Theta}^{-1} \mathbf{h} \right\|_2^2 \quad (180)$$

\square

F. Column-wise decomposition

We first show that

$$\begin{aligned} \left\| \mathbf{P}^T [\mathbf{L}^\dagger]_{\mathcal{N},\Theta} [\mathbf{L}^\dagger]_{\Theta}^{-1} \right\|_F^2 &= \frac{N}{m} \left\| [\mathbf{L}^\dagger]_{\{1\},\Theta} [\mathbf{L}^\dagger]_{\Theta}^{-1} \right\|_F^2 \\ &\quad + \left\| [\mathbf{L}^\dagger]_{\mathcal{N},\Theta} [\mathbf{L}^\dagger]_{\Theta}^{-1} \right\|_F^2 \end{aligned} \quad (181)$$

Proof. Let $\mathbf{K} = [\mathbf{I}]_{\mathcal{N},\Theta} [\mathbf{L}^\dagger]_{\Theta}^{-1}$, then

$$\left\| \mathbf{P}^T [\mathbf{L}^\dagger]_{\mathcal{N},\Theta} [\mathbf{L}^\dagger]_{\Theta}^{-1} \right\|_F^2 = \text{tr}(\mathbf{K}^T \mathbf{L}^\dagger \mathbf{P} \mathbf{P}^T \mathbf{L}^\dagger \mathbf{K}) \quad (182)$$

As $\mathbf{1}_{m \times N} \mathbf{L}^\dagger = \mathbf{0}$ cross terms in $\mathbf{P} \mathbf{P}^T$ disappear in $\mathbf{L}^\dagger \mathbf{P} \mathbf{P}^T \mathbf{L}^\dagger$,

$$\mathbf{L}^\dagger \mathbf{P} \mathbf{P}^T \mathbf{L}^\dagger = \mathbf{L}^\dagger \left(\mathbf{I} + \frac{N}{m} \begin{pmatrix} \frac{1}{m} \mathbf{1}_{m \times m} & \mathbf{0} \\ \mathbf{0} & \mathbf{0} \end{pmatrix} \right) \mathbf{L}^\dagger \quad (183)$$

$$= (\mathbf{L}^\dagger)^2 + \frac{N}{m} \mathbf{L}^\dagger \mathbf{v}_1 \mathbf{v}_1^T \mathbf{L}^\dagger. \quad (184)$$

Therefore

$$\left\| \mathbf{P}^T [\mathbf{L}^\dagger]_{\mathcal{N},\Theta} [\mathbf{L}^\dagger]_{\Theta}^{-1} \right\|_F^2 \quad (185)$$

$$= \text{tr}(\mathbf{K}^T \mathbf{L}^\dagger \mathbf{L}^\dagger \mathbf{K}) + \frac{N}{m} \text{tr}(\mathbf{K}^T \mathbf{L}^\dagger \mathbf{v}_1 \mathbf{v}_1^T \mathbf{L}^\dagger \mathbf{K}) \quad (186)$$

$$= \left\| [\mathbf{L}^\dagger]_{\mathcal{N},\Theta} [\mathbf{L}^\dagger]_{\Theta}^{-1} \right\|_F^2 + \frac{N}{m} \left\| [\mathbf{L}^\dagger]_{\{1\},\Theta} [\mathbf{L}^\dagger]_{\Theta}^{-1} \right\|_F^2. \quad (187)$$

□

G. Bounding (152)

We set $\mathbf{C} = [\mathbf{L}^\dagger]_{\mathcal{S}}$, $\mathbf{U} = [\mathbf{I}]_{\Theta,\mathcal{S}}$ in [37, Eq. 20-23]. By [37, Eq. 23], we have

$$\left\| [\mathbf{L}^\dagger]_{\{1\},\Theta} [\mathbf{L}^\dagger]_{\Theta}^{-1} \right\|_F^2 \leq r - 1. \quad (188)$$

therefore,

$$\left(\frac{N}{m} \right) \left\| [\mathbf{L}^\dagger]_{\{1\},\Theta} [\mathbf{L}^\dagger]_{\Theta} \right\|_2^2 \leq \left(\frac{N}{m} \right) (r - 1). \quad (189)$$

H. Bounding (153)

We take a similar approach to K-G. Note that for all δ ,

$$\left\| [\mathbf{L}^\dagger]_{\mathcal{N},\Theta} [\mathbf{L}^\dagger]_{\Theta}^{-1} \right\|_F^2 \quad (190)$$

$$= \text{tr} \left([\mathbf{L}^\dagger]_{\Theta}^{-1} \left[(\mathbf{L}^\dagger)^2 \right]_{\Theta} [\mathbf{L}^\dagger]_{\Theta}^{-1} \right) \quad (191)$$

$$= \text{tr} \left(\left[(\mathbf{L}^\dagger)^2 \right]_{\Theta} [\mathbf{L}^\dagger]_{\Theta}^{-2} \right) \quad (192)$$

$$= \text{tr} \left(\left[(\mathbf{L}^\dagger + \delta)^2 \right]_{\Theta} [\mathbf{L}^\dagger + \delta]_{\Theta}^{-2} \right). \quad (193)$$

Let $\delta = \frac{1}{N \lceil \lambda_{N/2} \rceil}$ and let

$$\hat{\lambda} = (\lambda_2, \dots, \lambda_{\lceil \frac{N}{2} \rceil}, \lambda_{\lceil \frac{N}{2} \rceil}, \lambda_{\lceil \frac{N}{2} \rceil + 1}, \dots, \lambda_N),$$

then $\lambda_i(\mathbf{L}^\dagger + \delta) = \hat{\lambda}_{N+1-i}^{-1}$. Set $\mathbf{B} = \mathbf{I}$, $\mathbf{C} = \mathbf{L}^\dagger + \delta$, $\mathbf{X} = [\mathbf{I}]_{\mathcal{N},\Theta}$ in [38, Eq. (2.19)] to get that

$$\left\| [\mathbf{L}^\dagger]_{\mathcal{N},\Theta} [\mathbf{L}^\dagger]_{\Theta}^{-1} \right\|_F^2 \leq \rho(m - 1). \quad (194)$$

where

$$r_m = \begin{cases} \sum_{i=1}^m \frac{(\hat{\lambda}_i + \hat{\lambda}_{N-i+1})^2}{4\hat{\lambda}_i \hat{\lambda}_{N-i+1}} & \text{if } 2m \leq N \\ \left(\sum_{i=1}^{N-m} \frac{(\hat{\lambda}_i + \hat{\lambda}_{N-i+1})^2}{4\hat{\lambda}_i \hat{\lambda}_{N-i+1}} \right) + (2m - N) & \text{otherwise} \end{cases} \quad (195)$$

We can write r_m this way as it is invariant under the transformation $\hat{\lambda}_i \mapsto \hat{\lambda}_{N+1-i}^{-1}$.

APPENDIX L BOUNDING $\xi_1(\mathcal{S})$

Lemma 9. Under GLR reconstruction,

$$\xi_1(\mathcal{S}) < k + \xi_2(\mathcal{S}) \quad (196)$$

Proof. Note that

$$\begin{aligned} \mathbf{R}_S \mathbf{M}_S &= (\mathbf{\Pi}_S + \mu \mathbf{L})^{-1} \mathbf{\Pi}_S \\ &= \mathbf{I} - (\mathbf{\Pi}_S + \mu \mathbf{L})^{-1} \mu \mathbf{L} \end{aligned} \quad (197)$$

we have

$$\xi_1(\mathcal{S}) = \|\mathbf{U}\|_{\mathcal{N},\mathcal{K}} - \mathbf{R}_S [\mathbf{U}]_{\mathcal{S},\mathcal{K}} \|_F^2 \quad (198)$$

$$= \text{tr}(\mathbf{\Pi}_{bl(\mathcal{K})}) - 2[\mathbf{U}]_{\mathcal{N},\mathcal{K}}^T \mathbf{R}_S [\mathbf{U}]_{\mathcal{S},\mathcal{K}} + \|\mathbf{R}_S [\mathbf{U}]_{\mathcal{S},\mathcal{K}}\|_F^2 \quad (199)$$

$$= \text{tr}(2([\mathbf{U}]_{\mathcal{N},\mathcal{K}}^T (\mathbf{\Pi}_S + \mu \mathbf{L})^{-1} \mu \mathbf{L} [\mathbf{U}]_{\mathcal{N},\mathcal{K}}) - \mathbf{\Pi}_{bl(\mathcal{K})}) + \|\mathbf{R}_S [\mathbf{U}]_{\mathcal{S},\mathcal{K}}\|_F^2 \quad (200)$$

$$= 2 \left(\sum_{i=1}^k \mathbf{u}_i^T (\mathbf{\Pi}_S + \mu \mathbf{L})^{-1} \mathbf{u}_i \mu \lambda_i \right) - k + \|\mathbf{R}_S [\mathbf{U}]_{\mathcal{S},\mathcal{K}}\|_F^2 \quad (201)$$

By [39, Eq. (1.7)] for $i > 1$, $\mathbf{u}_i^T (\mathbf{\Pi}_S + \mu \mathbf{L})^{-1} \mathbf{u}_i \leq \mathbf{u}_i^T (\mu \mathbf{L})^{-1} \mathbf{u}_i = (\mu \lambda_i)^{-1}$, and for $i = 1$, $\lambda_1 = 0$, so

$$\left(\sum_{i=1}^k \mathbf{u}_i^T (\mathbf{\Pi}_S + \mu \mathbf{L})^{-1} \mathbf{u}_i \mu \lambda_i \right) \leq k - 1 < k \quad (202)$$

and therefore

$$\xi_1(\mathcal{S}) < k + \|\mathbf{R}_S [\mathbf{U}]_{\mathcal{S},\mathcal{K}}\|_F^2 \quad (203)$$

As $\|\mathbf{R}_S [\mathbf{U}]_{\mathcal{S},\mathcal{K}}\|_F^2 \leq \|\mathbf{R}_S [\mathbf{U}]_{\mathcal{S},\mathcal{N}}\|_F^2 = \|\mathbf{R}_S\|_F^2 = \xi_2(\mathcal{S})$, therefore

$$\xi_1(\mathcal{S}) < k + \xi_2(\mathcal{S}). \quad (204)$$

□

APPENDIX M PROOF OF REMARK 7

If condition (39) in Theorem 3 holds for some m , then $B(m) < N$ for some m . As m_{opt} minimises $B(m)$, $B(m_{opt}) < N$ and (39) holds for a sample size of m_{opt} . Furthermore, μ_{ub} is decreasing in $B(m)$ and for fixed μ , $\tau_{lb}(\mu, m)$ is decreasing in $B(m)$, so these are maximised at a sample size of m_{opt} . Our upper bound for MSE in Corollary 3.1 is decreasing in $B(m)$, so is minimised at a sample size of m_{opt} .

Finally, we bound m_{opt} assuming that $B(m) < N$ for some m . We do so in the following steps:

- 1) Show $\arg \min_{[\lfloor \frac{N}{2} \rfloor, N-1]} \rho(m)$ is either $\lfloor \frac{N}{2} \rfloor$ or $N-1$
- 2) Show $m_{opt} \in \left[1, \left\lfloor \frac{N}{2} \right\rfloor\right]$
- 3) Show $m_{opt} \in \left[\left\lfloor \sqrt{N} \right\rfloor, \left\lceil \sqrt{rN} \right\rceil\right]$

A. Bounding ρ

Let $m \in \left[\left\lfloor \frac{N}{2} \right\rfloor, N\right]$. Then $m+1 > \frac{N}{2}$. We write down $\rho(m+1) - \rho(m)$. If $m > \frac{N}{2}$, then

$$\rho(m+1) - \rho(m) = 2 - r_{N-m}. \quad (205)$$

If $m \leq \frac{N}{2}$, then $m = \lfloor \frac{N}{2} \rfloor$ and we have chosen $\hat{\lambda}$ s.t.

$$\rho(m+1) - \rho(m) = 1. \quad (206)$$

As r_i is decreasing in i , r_{N-m} is increasing in m . Either $r < 2$ and $\rho(m) < \rho(m+1)$ and $\arg \min_{[\lfloor \frac{N}{2} \rfloor, N]} \rho(m) = \{\lfloor \frac{N}{2} \rfloor\}$, or there is some z s.t. $\forall m \in \left[\left\lfloor \frac{N}{2} \right\rfloor, z\right) : r_{N-m} \leq 2$ and $\forall m \in [z, N) : r_{N-m} > 2$. Then

$$\forall m < z : \rho(m+1) > \rho(m) \quad (207)$$

$$\forall m > z : \rho(m+1) < \rho(m) \quad (208)$$

This forms a Λ shape, so the optimum is at either end of the interval, and so $\arg \min_{[\lfloor \frac{N}{2} \rfloor, N-1]} \rho(m)$ is either $\lfloor \frac{N}{2} \rfloor$ or $N-1$.

B. Proving $m_{opt} \leq \frac{N}{2}$

We case-split on $\arg \min_{[\lfloor \frac{N}{2} \rfloor, N-1]} \rho(m)$. Suppose for contradiction that

$$N-1 \in \arg \min_{[\lfloor \frac{N}{2} \rfloor, N-1]} \rho(m)$$

and $m_{opt} > \lfloor \frac{N}{2} \rfloor$. Then

$$B(m_{opt}) \geq \left(\min_m \frac{N}{m}\right) + \rho(N-1) \quad (209)$$

$$= 1 + (N-2+r) > N \quad (210)$$

This is a contradiction as $B(m_{opt})$ is the minimum of $B(m)$ and we've assumed that $B(m) < N$ for some m .

We now assume that $\arg \min_{[\lfloor \frac{N}{2} \rfloor, N-1]} \rho(m)$ is $\lfloor \frac{N}{2} \rfloor$. Then

$$\forall m \in \left[\left\lfloor \frac{N}{2} \right\rfloor + 1, N\right] : B(m) \geq 1 + \rho\left(\left\lfloor \frac{N}{2} \right\rfloor\right) \quad (211)$$

$$B\left(\left\lfloor \frac{N}{2} \right\rfloor - 1\right) = \frac{N}{\left\lfloor \frac{N}{2} \right\rfloor - 1} + \rho\left(\left\lfloor \frac{N}{2} \right\rfloor - 2\right) \quad (212)$$

$$B(m) - B\left(\left\lfloor \frac{N}{2} \right\rfloor - 1\right) = \left(1 - \frac{N}{\left\lfloor \frac{N}{2} \right\rfloor - 1}\right) \quad (213)$$

$$+ r_{\lfloor \frac{N}{2} \rfloor} + r_{\lfloor \frac{N}{2} \rfloor - 1} \quad (214)$$

$$\geq 3 - \frac{N}{\left\lfloor \frac{N}{2} \right\rfloor - 1} > 0 \quad (215)$$

as $N \geq 4$. Therefore, if $\arg \min_{[\lfloor \frac{N}{2} \rfloor, N-1]} \rho(m)$ is $\lfloor \frac{N}{2} \rfloor$ then for all $m > \frac{N}{2}$,

$$B(m) > B\left(\left\lfloor \frac{N}{2} \right\rfloor - 1\right). \quad (216)$$

and so $m_{opt} \leq \frac{N}{2}$.

C. Bounding m_{opt}

Finally, we note that if m_{opt} is a global minimum then m_{opt} is a local minimum, so $B(m_{opt}+1) \geq B(m_{opt})$ and $B(m_{opt}-1) \geq B(m_{opt})$. As $m_{opt} \leq \lfloor \frac{N}{2} \rfloor$,

$$B(m+1) - B(m) = r_m - \frac{rN}{m(m+1)} \quad (217)$$

so our inequalities can be written:

$$r_{m_{opt}} m_{opt} (m_{opt} + 1) \geq rN \quad (218)$$

$$r_{m_{opt}-1} m_{opt} (m_{opt} - 1) \leq rN \quad (219)$$

As $1 \leq r_i \leq r$ for all i , we get

$$m_{opt} (m_{opt} + 1) \geq N \quad (220)$$

$$m_{opt} (m_{opt} - 1) \leq rN \quad (221)$$

and as $(m+1)^2 > m(m+1)$ and $(m-1)^2 < m(m-1)$,

$$\sqrt{N} - 1 < m_{opt} < \sqrt{rN} + 1 \quad (222)$$

as these inequalities are strict and m_{opt} is an integer,

$$\left\lfloor \sqrt{N} \right\rfloor \leq m_{opt} \leq \left\lceil \sqrt{rN} \right\rceil. \quad (223)$$

APPENDIX N PROOF OF PROPOSITION 2

We prove the proposition by proving some bounds relating terms to r , λ_2 and λ_N , then showing that $r \rightarrow 1$.

A. Notation and Terms

While we use standard terminology in probability theory, for convenience we define some of it here.

An event E_n happens *with high probability* (abbreviated w.h.p.) if $\lim_{n \rightarrow \infty} \mathbb{P}(E_n) = 1$. A sequence of random variables X_n *converges in probability* to a random variable or constant X if $\forall \epsilon > 0 : \mathbb{P}(|X_n - X| > \epsilon) \rightarrow 0$. We write this as

$$X_n \xrightarrow{P} X.$$

Similarly, we write

$$X_n \xrightarrow{P} +\infty.$$

to mean that $\forall c > 0 : \mathbb{P}(X < c) \rightarrow 0$

B. Limits in Probability

In this section, we show $r \xrightarrow{p} 1$ in our setting. Morally our argument is that $\frac{\lambda_N}{\lambda_2} \approx \frac{Np + \sqrt{2N \log N}}{Np - \sqrt{2N \log N}} \xrightarrow{p} 1$. We now prove this formally, starting with statements including disconnected graphs, and using them to derive results about connected graphs. By [35, Theorem 1 (i) & (ii)], across all Erdős-Rényi graphs with edge probability p

$$\frac{Np - \lambda_2}{\sqrt{N \log N}} \xrightarrow{p} \sqrt{2} \quad (224)$$

$$\frac{\lambda_N - Np}{\sqrt{N \log N}} \xrightarrow{p} \sqrt{2}. \quad (225)$$

By Slutsky's Theorem, and as convergence in distribution to a constant implies convergence in probability, we add and square the ratios to get

$$\frac{(\lambda_N - \lambda_2)^2}{N \log N} \xrightarrow{p} 8. \quad (226)$$

We now bound $\frac{N \log N}{\lambda_2 \lambda_N}$. By the definition of convergence in probability, because $\frac{Np}{N \log N} \rightarrow \infty$ and by the triangle inequality,

$$\forall \epsilon > 0, \lim_{N \rightarrow \infty} \mathbb{P} \left(\left| \frac{Np - \lambda_2}{\sqrt{N \log N}} - \sqrt{2} \right| > \epsilon \right) = 0 \quad (227)$$

$$\implies \forall c > 0, \lim_{N \rightarrow \infty} \mathbb{P} \left(\left| \frac{\lambda_2}{\sqrt{N \log N}} \right| < c \right) = 0 \quad (228)$$

$$\implies \forall \epsilon > 0, \lim_{N \rightarrow \infty} \mathbb{P} \left(\left| \frac{\sqrt{N \log N}}{\lambda_2} \mathbb{1}\{\lambda_2 > 0\} \right| > \epsilon \right) = 0 \quad (229)$$

therefore

$$\frac{\sqrt{N \log N}}{\lambda_2} \mathbb{1}\{\lambda_2 > 0\} \xrightarrow{p} 0 \quad (230)$$

$$\text{As } 0 < \frac{\sqrt{N \log N}}{\lambda_N} < \frac{\sqrt{N \log N}}{\lambda_2},$$

$$\frac{N \log N}{\lambda_2 \lambda_N} \mathbb{1}\{\lambda_2 > 0\} \xrightarrow{p} 0. \quad (231)$$

we use Slutsky to multiply this with (226) to get

$$(r - 1) \mathbb{1}\{\lambda_2 > 0\} = \frac{(\lambda_N - \lambda_2)^2}{4\lambda_2 \lambda_N} \mathbb{1}\{\lambda_2 > 0\} \xrightarrow{p} 0 \quad (232)$$

By (228) we know $\lambda_2 > 0$ w.h.p. . Therefore, for any $\epsilon > 0$

$$\begin{aligned} & \mathbb{P}(|r - 1| > \epsilon \mid \lambda_2 > 0) \\ &= \frac{\mathbb{P}(|r - 1| > \epsilon \cap \lambda_2 > 0)}{\mathbb{P}(\lambda_2 > 0)} \end{aligned} \quad (233)$$

$$= \frac{\mathbb{P}(|r - 1| \mathbb{1}\{\lambda_2 > 0\} > \epsilon)}{\mathbb{P}(\lambda_2 > 0)} \rightarrow 0 \quad (234)$$

Therefore under our setting of considering only connected graphs (i.e. that $\lambda_2 > 0$), $r \xrightarrow{p} 1$.

C. Parameter Bounds

We first bound ρ and $B(m)$ in terms of r . Note that for $x \geq y$, $\frac{x}{y} + \frac{y}{x}$ is increasing in x and therefore

$$r_i = \frac{(\hat{\lambda}_i + \hat{\lambda}_{N-i+1})^2}{4\hat{\lambda}_i \hat{\lambda}_{N-i+1}} \quad (235)$$

$$= \frac{1}{4} \left(\frac{\hat{\lambda}_i}{\hat{\lambda}_{N-i+1}} + \frac{\hat{\lambda}_{N-i+1}}{\hat{\lambda}_i} + 2 \right) \quad (236)$$

$$\leq \frac{1}{4} \left(\frac{\hat{\lambda}_1}{\hat{\lambda}_N} + \frac{\hat{\lambda}_N}{\hat{\lambda}_1} + 2 \right) = r \quad (237)$$

If $x, y > 0$ then $\frac{1}{2} \left(\frac{x}{y} + \frac{y}{x} \right) \geq \sqrt{\frac{x}{y} \frac{y}{x}} = 1$ by the AM-GM inequality, and so $\forall i r_i \geq 1$. Therefore

$$1 \leq r_i \leq r \quad (238)$$

$$m \leq \rho(m) \leq rm \quad (239)$$

$$\frac{N}{m} + m - 1 \leq B(m) \leq r \left(\frac{N}{m} + m - 1 \right). \quad (240)$$

We also have that

$$\frac{1}{\lambda_N} \left(\sqrt{\frac{N}{B(m)}} - 1 \right) \leq \mu_{ub}(m) \leq \frac{1}{\lambda_2} \left(\sqrt{\frac{N}{B(m)}} - 1 \right). \quad (241)$$

D. Pulling it together

We already have that $r \xrightarrow{p} 1$. As $\sqrt{N} \leq m_{opt} \leq \lceil \sqrt{rN} \rceil$, $\frac{m_{opt}}{\sqrt{N}} \xrightarrow{p} 1$. By the squeeze theorem, for a fixed m ,

$$\frac{B(m)}{N} \xrightarrow{p} \frac{1}{m}. \quad (242)$$

Because $\frac{1}{m} < 1$ for $m > 1$, condition (39) in Theorem 3 holds w.h.p. as $N \rightarrow \infty$. As $B(m) > 0$,

$$\sqrt{\frac{N}{B(m)}} - 1 \xrightarrow{p} \sqrt{m} - 1 \quad (243)$$

Conditioning on $\lambda_2 > 0$ does not change (228), so it applies when we only consider the set of connected Erdős-Rényi graphs as well. By setting $c = \sqrt{m} - 1$ in (228), we get

$$\frac{1}{\lambda_2} \left(\sqrt{\frac{N}{B(m)}} - 1 \right) \xrightarrow{p} 0. \quad (244)$$

and therefore for fixed m , $\mu_{ub}(m) \rightarrow 0$. We now calculate $\mu_{ub}(m_{opt})$. First note that as $x \mapsto x + \frac{1}{x}$ invertible and monotone on $x \in (0, 1)$, so its inverse is continuous. Consider that $\frac{\lambda_2}{\lambda_N} \in (0, 1)$. As the inverse is continuous, we have that $\forall \epsilon > 0 \exists \delta > 0 : \left| \left(\frac{\lambda_2}{\lambda_N} + \frac{\lambda_N}{\lambda_2} \right) - 2 \right| < \epsilon \implies \left| \frac{\lambda_2}{\lambda_N} - 1 \right| < \delta$. Using this with the definition of convergence in probability and that $r \xrightarrow{p} 1$ gives

$$\frac{\lambda_2}{\lambda_N} \xrightarrow{p} 1. \quad (245)$$

Next, note that

$$\frac{\sqrt{N}}{m_{opt}} + \frac{m_{opt}}{\sqrt{N}} - \frac{1}{\sqrt{N}} \leq \frac{B(m_{opt})}{\sqrt{N}} \leq r \left(\frac{\sqrt{N}}{m_{opt}} + \frac{m_{opt}}{\sqrt{N}} \right). \quad (246)$$

so

$$\frac{m_{opt}}{\sqrt{N}} \rightarrow 1 \implies \frac{B(m_{opt})}{\sqrt{N}} \xrightarrow{p} 2. \quad (247)$$

Therefore (39) in Theorem 3 holds for m_{opt} w.h.p. as $N \rightarrow \infty$. Also

$$\frac{\mu_{ub}(m_{opt}) \lambda_2}{\sqrt[4]{N}} \geq \frac{\lambda_2}{\lambda_N} \left(\sqrt{\frac{\sqrt{N}}{B(m_{opt})}} - \frac{1}{\sqrt[4]{N}} \right) \quad (248)$$

$$\xrightarrow{p} \frac{1}{\sqrt{2}} \quad (249)$$

and therefore $\mu_{ub}(m_{opt}) \lambda_2 \xrightarrow{p} \infty$.

Finally, we bound τ_{GLR} . We first take limits of $\left(\frac{1}{1+\mu\lambda_i}\right)^2$. Note that

$$1 \leq \frac{\lambda_i}{\lambda_2} \leq \frac{N}{\lambda_2} \xrightarrow{p} 1, \quad (250)$$

$$1 \geq \frac{\lambda_i}{\lambda_N} \geq \frac{\lambda_2}{\lambda_N} \xrightarrow{p} 1 \quad (251)$$

and $\frac{\lambda_i}{\sqrt{\lambda_2 \lambda_N}} \in \left[\frac{\lambda_i}{\lambda_N}, \frac{\lambda_i}{\lambda_2}\right]$ and so $\frac{\lambda_i}{\sqrt{\lambda_2 \lambda_N}} \xrightarrow{p} 1$. Therefore, for all three choices of μ , $\mu\lambda_i \xrightarrow{p} 1$. As

$$\frac{1}{N} + \frac{N}{N-1} \left(\frac{1}{1+\mu\lambda_N}\right)^2 \leq \frac{1}{N} \sum_{i=1}^N \left(\frac{1}{1+\mu\lambda_i}\right)^2 \quad (252)$$

$$\frac{1}{N} + \frac{N}{N-1} \left(\frac{1}{1+\mu\lambda_2}\right)^2 \geq \frac{1}{N} \sum_{i=1}^N \left(\frac{1}{1+\mu\lambda_i}\right)^2 \quad (253)$$

For all three choices of μ ,

$$\frac{1}{N} \sum_{i=1}^N \left(\frac{1}{1+\mu\lambda_i}\right)^2 \rightarrow \left(\frac{1}{1+c}\right)^2. \quad (254)$$

Similarly,

$$\frac{1}{N} \sum_{i=1}^N \left(1 - \frac{1}{1+\mu\lambda_i}\right)^2 \rightarrow \left(1 - \frac{1}{1+c}\right)^2. \quad (255)$$

As $\frac{B(m_{opt})}{\sqrt{N}} \xrightarrow{p} 2$, we must have that $\frac{B(m_{opt})}{N} \xrightarrow{p} 0$ and as $\frac{k}{N}$ is constant, $\frac{B(m_{opt})}{k} \xrightarrow{p} 0$. Therefore, by Slutsky, for the three choices of optimal μ ,

$$\tau_{GLR}(\mu, m_{opt}) \rightarrow \frac{\left(\frac{1}{1+c}\right)^2}{1 - \left(1 - \frac{1}{1+c}\right)^2} = \frac{1}{1+2c}. \quad (256)$$

APPENDIX O PROOF OF LEMMA 2

Firstly, we note that ξ_1 is the MSE in the noiseless case, so is invariant to noise-type, proving $\xi_{1,\text{bandlimited}} = \xi_{1,\text{full-band}}$. We now show that $\xi_{2,\text{bandlimited}}(\mathcal{S}) \leq \xi_{2,\text{full-band}}(\mathcal{S})$.

Proof. The squared Frobenius norm is the sum of the squares of the entries of a matrix, and therefore the squared Frobenius

norm of a submatrix is less than squared Frobenius norm of the full matrix. Because of this, and as $[\mathbf{U}]_{\mathcal{S},\mathcal{N}}[\mathbf{U}]_{\mathcal{S},\mathcal{N}}^T = \mathbf{I}_{\mathcal{S}}$,

$$\xi_{2,\text{bandlimited}}(\mathcal{S}) = \|\mathbf{R}_{\mathcal{S}}[\mathbf{U}]_{\mathcal{S},\mathcal{K}}\|_F^2 \quad (257)$$

$$\leq \|\mathbf{R}_{\mathcal{S}}[\mathbf{U}]_{\mathcal{S},\mathcal{N}}\|_F^2 \quad (258)$$

$$= \|\mathbf{R}_{\mathcal{S}}\|_F^2 \quad (259)$$

$$= \xi_{2,\text{full-band}}(\mathcal{S}) \quad (260)$$

□

APPENDIX P

PROOF OF THEOREM 4

Proof. We follow the structure of Appendix J. Firstly, we note that by the same arguments as for Lemma 7,

$$\xi_2(\mathcal{N}) = \sum_{i=1}^k \left(\frac{1}{1+\mu\lambda_i}\right)^2. \quad (261)$$

By Lemma 2, we can use the bounds for $\xi_i(\mathcal{S})$ and $\xi_1(\mathcal{N})$ verbatim, therefore

$$\Delta_2(\mathcal{N}, \mathcal{S}^c) \geq \sum_{i=1}^k \left(\frac{1}{1+\mu\lambda_i}\right)^2 - B(m) \quad (262)$$

$$\Delta_1(\mathcal{N}, \mathcal{S}^c) \geq \sum_{i=1}^N \left(1 - \frac{1}{1+\mu\lambda_i}\right)^2 - (k+B(m)). \quad (263)$$

We now show that $\Delta_2 > 0$. We have that $r > 0$ so $B(m) > 0$ and by assumption $B(m) < k$. Therefore $\mu_{ub,bl}(m) > 0$ and is real and it therefore possible to pick $0 < \mu < \mu_{ub}(m)$. By assumption $0 < \mu < \mu_{ub}(m)$ and so

$$\sum_{i=1}^k \left(\frac{1}{1+\mu\lambda_i}\right)^2 \geq \frac{k}{\left(1+\mu\frac{1}{\lambda_k}\right)^2} \quad (264)$$

$$> \frac{k}{\left(1+\mu_{ub,bl}\frac{1}{\lambda_k}\right)^2} \quad (265)$$

$$= B(m) \quad (266)$$

And therefore by (262), $\Delta_2(\mathcal{N}, \mathcal{S}^c) > 0$. Note that SNR = $\frac{1}{\sigma^2}$ and apply Corollary 2.3 in the same manner as Appendix J and we are done. □

APPENDIX Q

PROOF OF PROPOSITION 3

The proof in Appendix N adapts immediately to the bandlimited case, except for proving that condition (51) in Theorem 4 holds for m_{opt} . By (247), $\frac{B(m_{opt})}{\sqrt{N}} \xrightarrow{p} 2$. As $\frac{k}{N}$ is fixed, $\frac{\sqrt{N}}{k} \rightarrow 0$, so $\frac{B(m_{opt})}{k} \xrightarrow{p} 0$ and therefore the condition holds.

APPENDIX R

ADDITIONAL RESULTS

Under LS reconstruction, we show thresholds for the ER, BA and SBM graphs with 100 vertices (Fig. ??). We also present MSE plots for the larger BA (Fig 10) and SBM (Fig. 14) graphs, and for ER plots with bandlimited noise (Fig. 5).

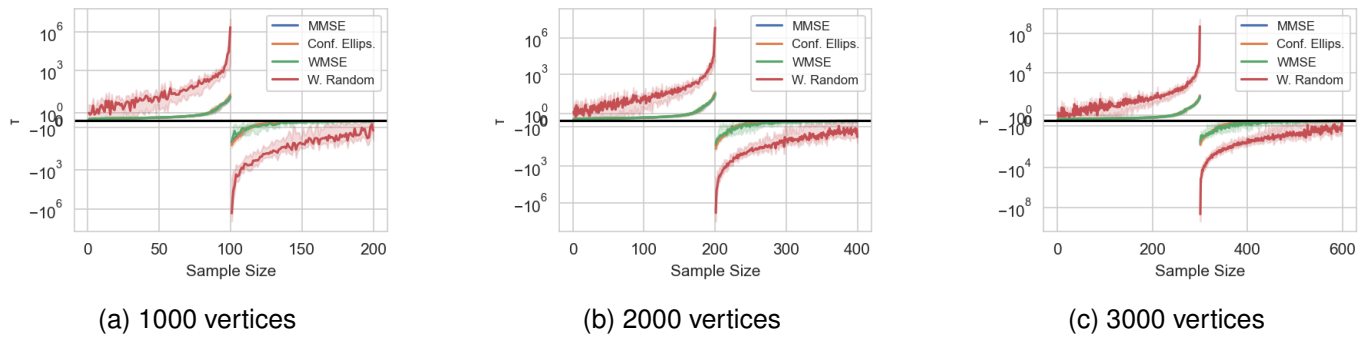


Fig. 8: $\tau(\mathcal{S}, v)$ for different sized BA graphs under LS reconstruction (bandwidth = $\frac{\# \text{ vertices}}{10}$)

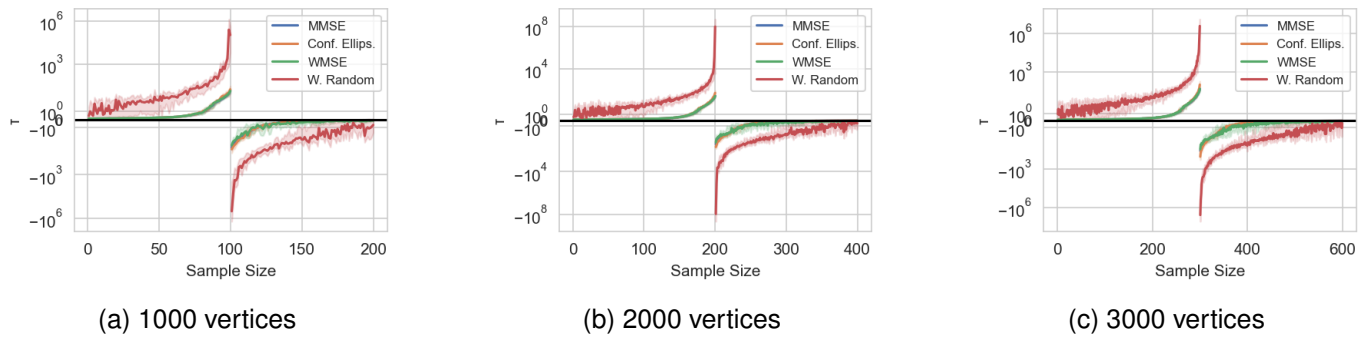


Fig. 9: $\tau(\mathcal{S}, v)$ for different sized SBM graphs under LS reconstruction (bandwidth = $\frac{\# \text{ vertices}}{10}$)

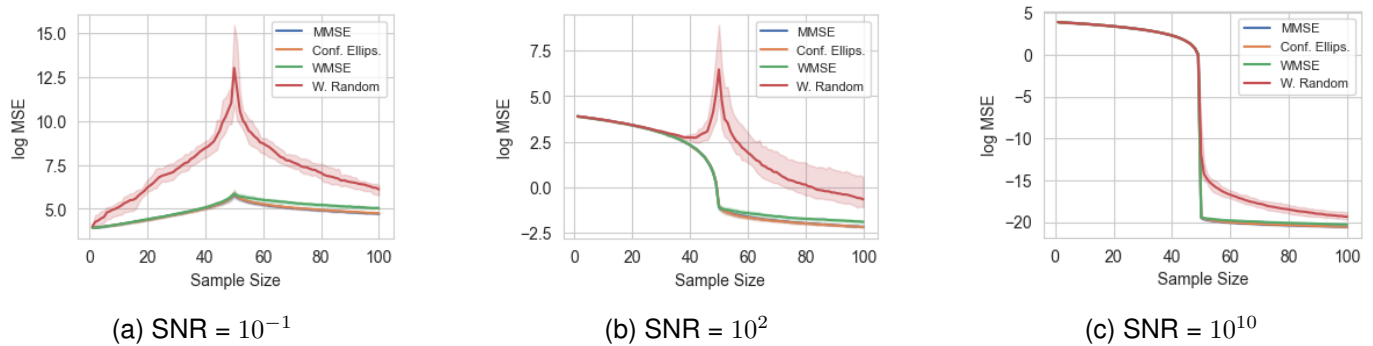


Fig. 10: Average MSE for LS reconstruction on BA Graphs ($\# \text{ vertices} = 500$, bandwidth = 50) with different SNRs

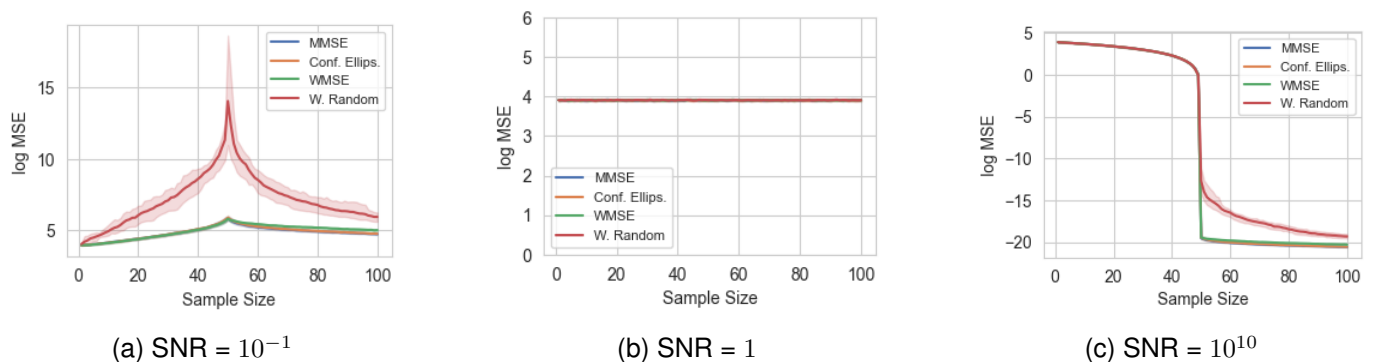


Fig. 11: Average MSE for LS reconstruction on BA Graphs with bandlimited noise ($\# \text{ vertices} = 500$, bandwidth = 50) with different SNRs

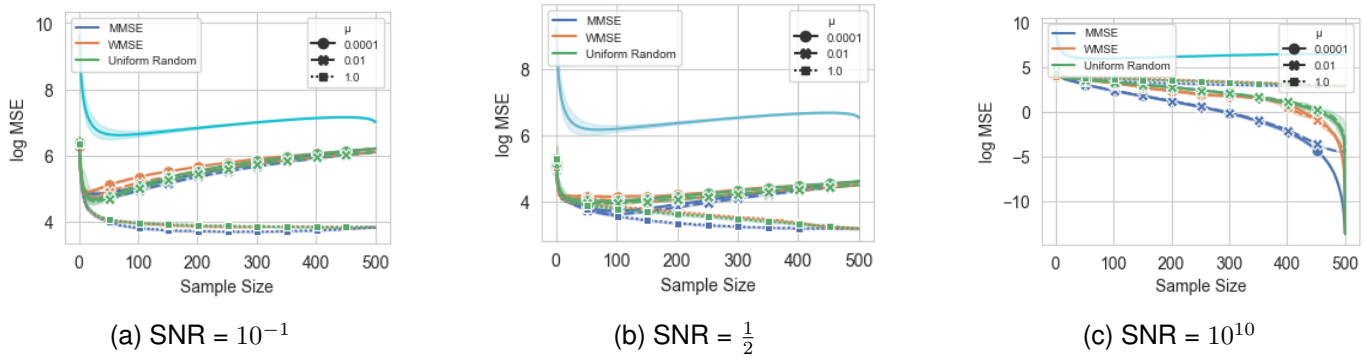


Fig. 12: Average MSE for GLR reconstruction on BA Graphs (#vertices=500, bandwidth = 50) with different SNRs, line without markers is an upper bound

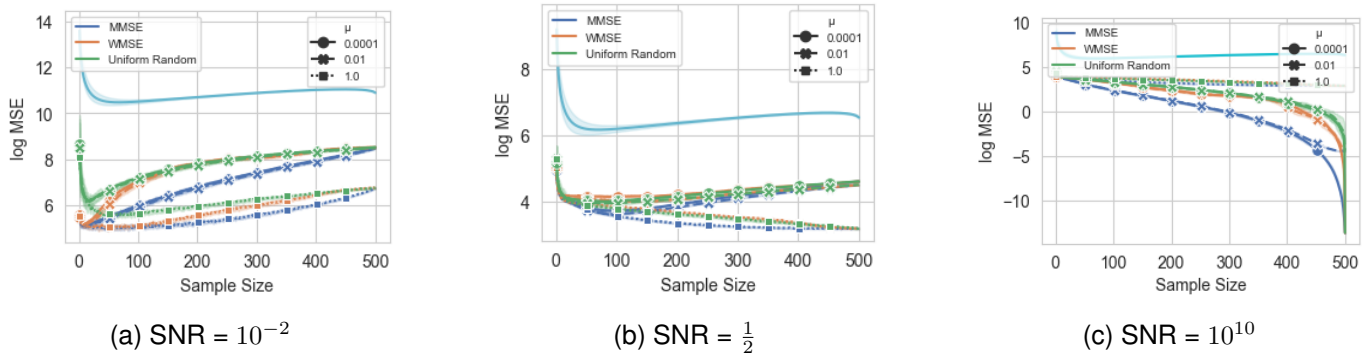


Fig. 13: Average MSE for GLR reconstruction on BA Graphs under bandlimited noise (#vertices=500, bandwidth = 50) with different SNRs, line without markers is an upper bound

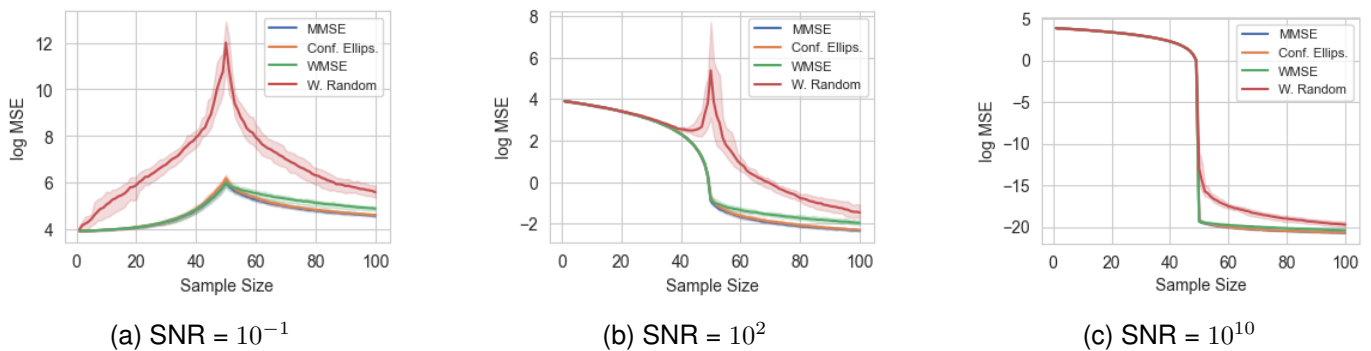


Fig. 14: Average MSE for LS reconstruction on SBM Graphs (#vertices=500, bandwidth = 50) with different SNRs

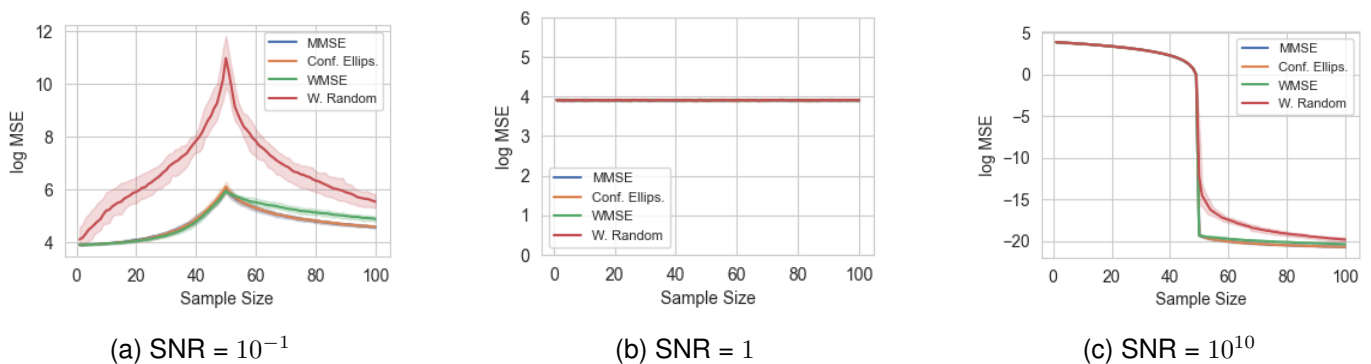


Fig. 15: Average MSE for LS reconstruction on SBM Graphs with bandlimited noise (#vertices=500, bandwidth = 50) with different SNRs

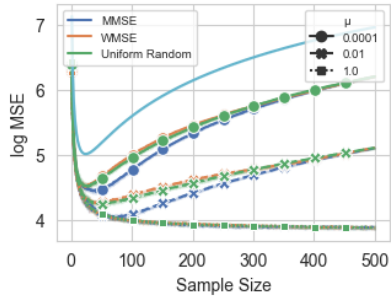
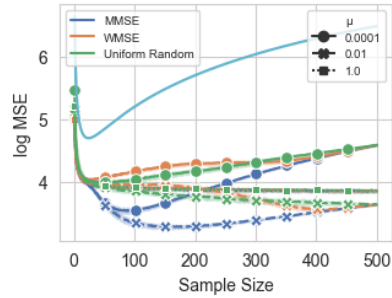
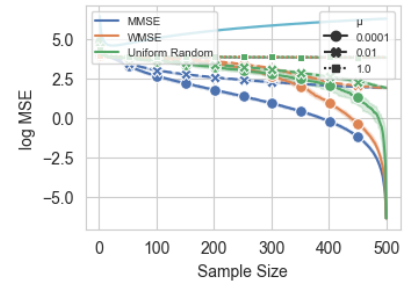
(a) $\text{SNR} = 10^{-1}$ (b) $\text{SNR} = \frac{1}{2}$ (c) $\text{SNR} = 10^{10}$

Fig. 16: Average MSE for GLR reconstruction on SBM Graphs ($\#$ vertices=500, bandwidth = 50) with different SNRs, line without markers is an upper bound

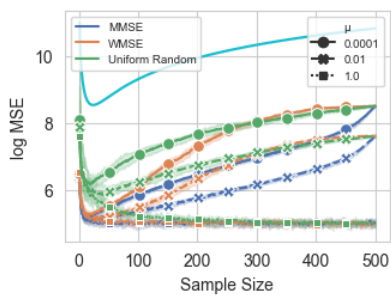
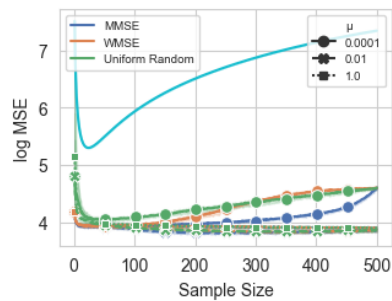
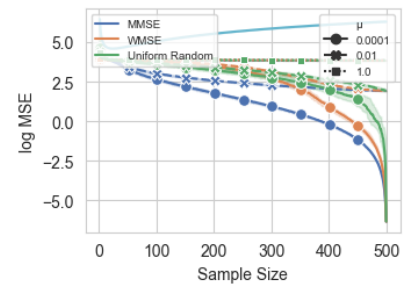
(a) $\text{SNR} = 10^{-2}$ (b) $\text{SNR} = \frac{1}{2}$ (c) $\text{SNR} = 10^{10}$

Fig. 17: Average MSE for GLR reconstruction on SBM Graphs under bandlimited noise ($\#$ vertices=500, bandwidth = 50) with different SNRs, line without markers is an upper bound